

Network formation and
reorganization in the olfactory
system of *Xenopus laevis*

Dissertation

for the award of the degree

“Doctor of Philosophy (Ph.D.)”

Division of Mathematics and Natural Sciences

of the Georg-August-Universität Göttingen

within the doctoral program Cellular and Molecular Physiology of the Brain (CMPB)

of the Georg-August University School of Science (GAUSS)

submitted by

Sara Joy Hawkins

from Warsaw, Indiana, USA

Göttingen, 2021

Thesis Committee

Prof. Dr. Ivan Manzini (Reviewer)

Department of Animal Physiology and Molecular Biomedicine, Institute of Animal Physiology, Justus-Liebig University, Gießen

Prof. Dr. Jochen Staiger (Reviewer)

Department of Neuroanatomy, Institute of Neuroanatomy, University Medical Center, Georg-August-University, Göttingen

Dr. Camin Dean

Principal Investigator, Synaptic Dysfunction Group, Deutsches Zentrum für Neurodegenerative Erkrankungen (DZNE), Berlin

Members of the Examination Board

Prof. Dr. Ivan Manzini (Reviewer)

Department of Animal Physiology and Molecular Biomedicine, Institute of Animal Physiology, Justus-Liebig University, Gießen

Prof. Dr. Jochen Staiger (Reviewer)

Department of Neuroanatomy, Institute of Neuroanatomy, University Medical Center, Georg-August-University, Göttingen

Further members of the Examination Board:

Dr. Camin Dean

Principal Investigator, Synaptic Dysfunction Group, Deutsches Zentrum für Neurodegenerative Erkrankungen (DZNE), Berlin

Prof. Dr. Ralf Heinrich

Department of Cellular Neurobiology, Schwann-Schleiden Research Center, Georg-August-University, Göttingen

Prof. Dr. André Fiala

Department of Molecular Neurobiology of Behavior, Schwann-Schleiden Research Center, Georg-August University, Göttingen

Prof. Dr. Martin Göpfert

Department of Cellular Neurobiology, Faculty of Biology and Psychology, Georg-August University, Göttingen

Date of oral examination: 09.02.2022

Contents

Chapter 1: Introduction	1
The sense of smell.....	1
Common features of the vertebrate olfactory system	2
Odorants and odorant receptors	3
Olfactory receptor neurons and transduction mechanisms	4
cAMP-dependent cell signaling	5
cAMP-independent cell signaling.....	5
Structure and wiring in the vertebrate olfactory bulb	6
Cell maintenance in the vertebrate olfactory system	8
The olfactory system of larval <i>Xenopus laevis</i>	11
Life cycle and olfactory subsystems	12
Odorants, odorant receptors and transduction mechanisms	12
Structuring and wiring in the olfactory bulb	15
Behavior	15
Aim of this thesis.....	17
Chapter 2:	18
Functional reintegration of sensory neurons and transitional dendritic reduction of mitral/tufted cells during injury-induced recovery of the larval <i>Xenopus laevis</i> olfactory circuit	18
Abstract	19
Introduction	19
Material and methods	22
Animal care, olfactory nerve transection and sensory neuron labeling	22
Immunohistochemistry	23
Whole mount preparation of the olfactory bulb	24
Visualization of axonal debris in the olfactory bulb	24
Olfactory receptor neuron labeling via electroporation.....	24
Labeling of the olfactory bulb for volume quantification	25
Sparse cell electroporation to label individual mitral/tufted cells	25
Calcium imaging experiments.....	26
Image and data processing	27
Solutions	29

Results.....	29
Structural and functional consequences after olfactory nerve transection in the main olfactory epithelium	29
Relative changes in olfactory bulb volume – axon degradation and reinnervation by newly formed olfactory sensory neurons.....	33
Increased cell death in the olfactory bulb following olfactory nerve transection .	36
Dynamic changes of dendritic tuft complexity in mitral/tufted cells following olfactory nerve transection.....	38
Recovery of odorant-induced responses in the glomerular layer and mitral/tufted cells of the olfactory bulb	40
Discussion	42
Timeline for regeneration in the olfactory system of larval <i>Xenopus laevis</i> after olfactory nerve transection.....	42
Olfactory map recovery and injury-induced dendritic reshaping of second-order neurons.....	44
Conclusion	47
Chapter 3:	48
Restoration of distinct odor processing streams in the olfactory bulb underlies the recovery of odor-guided behavior after injury in larval <i>Xenopus laevis</i>	48
Abstract	49
Introduction.....	50
Material and methods	53
Animal care.....	53
Bulk electroporation of olfactory receptor neurons and olfactory nerve transection	54
Functional calcium imaging and image data processing.....	54
Odor-guided behavior assay.....	57
Analyses of behavioral responses to odor stimuli in non-transected <i>Xenopus</i> larvae.....	58
Analyses of behavioral responses to odor stimuli in transected <i>Xenopus</i> larvae	59
Statistical analyses	59
Results.....	60
Odorant-induced receptor neuron axon terminal activity within glomerular clusters in the olfactory bulb of larval <i>Xenopus laevis</i>	60
Reintegrating olfactory receptor neurons reestablish distinct odor processing streams in the olfactory bulb after olfactory nerve transection	62

Reintegrating olfactory receptor neurons reestablish multi-stimulus response tuning profiles throughout the olfactory bulb after olfactory nerve transection ...	65
Odorant-guided behavioral responses in unlesioned larval <i>Xenopus laevis</i>	67
Neural rewiring of the olfactory bulb after olfactory nerve transection re-establishes odorant-guided behaviour in larval <i>Xenopus laevis</i>	72
Discussion	74
Distinct subsets of olfactory receptor neurons show odorant and forskolin-induced activity in the olfactory bulb 3 weeks after olfactory nerve transection .	74
Accurate neural rewiring in the olfactory bulb after olfactory nerve transection leads to the reformation of two segregated odor processing streams.....	75
Odorant-guided behavior is reestablished 7-9 weeks after recovery from olfactory nerve transection.....	77
Chapter 4: General discussion	80
Regulation of stem cell proliferation in the olfactory epithelium	80
Injury-induced regeneration of the olfactory system of larval <i>Xenopus laevis</i>	84
Cell death, neurogenesis and network rewiring in the olfactory system of <i>Xenopus laevis</i> during metamorphosis	89
Injury induced regeneration of the mammalian olfactory system	90
Olfactory dysfunction and odor representations in the olfactory bulb	92
Summary	95
Acknowledgements	96
List of abbreviations	97
List of figures and tables	99
References	101

Chapter 1: Introduction

The sense of smell

Every organism is made up of, and surrounded by, a myriad of molecular structures with varying features. Unsurprisingly, the ability to “sense” chemical features from the surrounding environment arose early on during the process of evolution, and is now one of the most widespread sensory modalities across species (Ache and Young, 2005). The sense of smell, or olfaction, is a form of chemosensation, in which molecular features from the external environment, called odorants, are detected and interpreted by the olfactory system (Farbman, 1992). The olfactory system is responsible for recognizing an almost infinite number of odorants that do not vary across any single parameter (Manzini et al., 2022). A range of what is visible or audible, for example, can be defined by the frequency and intensity of wavelengths (Bushdid et al., 2014), whereas a range of what can be perceived as an odor is much more difficult to define (Manzini et al., 2022).

During the course of evolution olfactory systems have shown an incredible capacity for adaptation across all types of environmental niches, existing in both fully aquatic and terrestrial species, in vertebrates and invertebrates alike, providing countless adaptive advantages (Ache and Young, 2005; Weiss et al., 2021). Although the input is hugely varied, across different environments and species, olfactory systems across phyla are highly conserved in regards to anatomy, organization and function (Hildebrand and Shepherd, 1997; Gelperin, 1999; Eisthen, 2002; Ache and Young, 2005). They are composed of a neuronal network made up of neuroepithelial regions that reside within the peripheral nervous system, that connect with olfactory processing and relay centers in the central nervous system (Manzini et al., 2022). The processing of odorants lead to the regulation of physiological and behavioral changes essential for survival and reproduction (Ache and Young, 2005; Manzini et al., 2022). When we smell an odor, our brain is actively transforming specific molecular features of our environment, i.e. odorants, into physiologically relevant outcomes. Odors can be attractive or repulsive, can lead us to recall pleasant or unpleasant memories, make us hungry or sexually aroused, anxious or calm, etc. We share this olfactory process, to some degree, with all other species.

Common features of the vertebrate olfactory system

Olfaction begins with the detection of odorants by odorant receptor proteins. Odorant receptor proteins are expressed on the apical dendritic appendages of olfactory receptor neurons (ORNs; Glezer and Malnic, 2019). Olfactory receptor neurons reside in the olfactory epithelium (OE), that lines peripheral sensory organs (Farbman, 1992). The peripheral location of the OE allows ORNs, and their odorant receptors, to easily interact with odorants in the environment. Olfactory receptor neurons extend their axons, via the olfactory nerve (ON), into the central nervous system (Farbman, 1992). When odorants successfully bind to receptor proteins, ORN depolarization ensues, leading to the transmission of olfactory information to a brain region called the olfactory bulb (OB; Farbman, 1992). In the OB, ORN axon terminals form synaptic connections with dendrites of 2nd order neurons and interneurons in densely packed neuropil structures called glomeruli (Nishizumi and Sakano, 2015). Olfactory information is then modulated and relayed to higher brain centers via the axonal projections of 2nd order neurons (Farbman, 1992). Higher olfactory processing centers mediate odorant induced physiological and behavioral changes. These changes naturally vary across species and are involved in orientation, in the location of food sources, in the avoidance of predators and other potential threats, in the identification of conspecifics and the attraction of mates, and in care-giving to offspring (Bartoshuk, 1989; Ache and Young, 2005; Hart and Chao, 2010; Hansson and Stensmyr, 2011; Chamero et al., 2012; Manzini et al., 2014; Li and Liberles, 2015; Manoel et al., 2019; Boesveldt and Parma, 2021; Tirindelli, 2021).

An animal's fitness relies heavily on its behavioral response to environmental stimuli. The functional stability of the olfactory system, and the maintenance of odor representations in the brain, are thus likely to be of substantial importance. Interestingly, the olfactory circuit is capable of maintaining function while exhibiting lifelong neuronal turnover – a feature common to all olfactory systems (Eisthen, 2002; Schwob, 2002). This neuronal turnover has been shown to promote network adaptation to sensory experience and learning (Lepousez et al., 2013; Lledo and Valley, 2016), and allows for extensive recovery from injury (Brann and Firestein, 2014; Cummings et al., 2014). This exceptional feature of the olfactory system has

made it a commonly used system to study the cellular and molecular processes involved in neuroregeneration (Schwob, 2002; Sokpor et al., 2018).

Odorants and odorant receptors

Odorants are made up of highly varied molecular features, or sets of features, that can be perceived as an odor. These “inputs”, unlike with other sensory systems (like the auditory and visual system), do not vary along any single parameter (Manzini et al., 2022). They are detected by highly specialized odorant receptor proteins that have varying affinities to specific molecular properties (Manzini et al., 2022). The olfactory system’s ability to detect this wide variation of odorants is achieved by maintaining a large number of genes that encode odorant receptor proteins in the genome (Buck and Axel, 1991). This vast array of olfactory receptor proteins is what ultimately provides each species with their ethologically-relevant odor space.

Modern olfactory neuroscience arose with the discovery of the so called odorant receptor (OR) gene family, a multigene family of G protein-coupled receptors (GPCRs) (Buck and Axel, 1991). G protein-coupled receptors are cell surface proteins, with substantial amino acid sequence variability, that detect molecules outside the cell and activate transduction pathways within the cell (Fredriksson et al., 2003), such as cAMP-dependent and phosphatidylinositol-dependent signal transduction pathways. Odorant receptor proteins are made up of seven membrane-spanning hydrophobic domains, including odorant binding sites located in extracellular domain and a carboxyl terminal region, that interacts with G-proteins, located in the cytoplasmic domain (Buck and Axel, 1991). The family of OR-type odorant receptors were first discovered in the rat genome (Buck and Axel, 1991), but we now know that they are found in all major vertebrate lineages and are the largest family of olfactory receptors in the olfactory system (Buck and Axel, 1991; Zhang and Firestein, 2002; Zhang et al., 2004). Alongside the OR-type of olfactory receptors, a variety of other families of olfactory receptors have been discovered, that differ mainly based on gene sequence and molecular structure. These odorant receptors include vomeronasal type 1 receptors (V1Rs)(Dulac and Axel, 1995), vomeronasal type 2 receptors (V2Rs)(Herrada and Dulac, 1997; Matsunami and Buck, 1997; Ryba and Tirindelli, 1997), trace amine associated receptors (TAARs)(Liberles and Buck, 2006), formyl-peptide receptors (FPRs) (Liberles et al., 2009; Rivière et al., 2009), and MS4A receptors (Greer et al.,

2016). The OR-type of receptor proteins generally binds with small volatile airborne molecules (Matsumoto et al., 2010), whereas the VR-type of receptor proteins generally binds with water-soluble, non-volatile, macromolecules such as peptides and proteins (Leinders-Zufall et al., 2004). The TAAR-type of receptor protein has been found to bind with amines (Shi and Javitch, 2002).

Although odorant receptors were first discovered in rodents, the most common ancestral odorant receptor is thought to have arisen before the divergence of jawed/jawless fish (Freitag et al., 1999). In fish, ORNs have been found to express ORA-type receptor proteins that are homologous to the mammalian V1Rs (Pfister and Rodriguez, 2005; Saraiva and Korsching, 2007; Shi and Zhang, 2007), and OlfC-type receptor proteins, homologous to ancestral mammalian V2Rs. Most fish species studied have also been found to express a high number of TAAR-type receptor proteins (Hashiguchi and Nishida, 2007), suggesting that this type of receptor protein plays an essential role in the detection of relevant waterborne odorants.

Olfactory receptor neurons and transduction mechanisms

Olfactory receptor neurons reside in the OE and express olfactory receptor proteins (Glezer and Malnic, 2019). These proteins interact with odorant ligands and translate odor binding energy into changes in membrane potential. Olfactory receptor neurons can be distinguished based on their morphological subtype, the type of receptor protein they express (and therefore the odorants with which they bind), and the transduction cascade they employ to send odorant information to the OB. In general, ORNs have a bipolar morphology (Schild and Restrepo, 1998; Ache and Young, 2005). At the apical end of their cell body they possess an outward facing dendritic knob that can be ciliated or microvillar (Menco, 1984; Schild and Restrepo, 1998; Falk et al., 2015), where odorant receptors are expressed (Glezer and Malnic, 2019). At the basal end of their soma they project a branched or unbranched axon toward the OB that terminates in one or multiple glomeruli (Klenoff and Greer, 1998; Nezlin and Schild, 2000; Del Punta et al., 2002; Larriva-Sahd, 2008; Hassenklover and Manzini, 2013; Weiss et al., 2020).

In certain species and in some specific olfactory subsystems ORNs have been found to express multiple odorant receptors, however, as a general rule, ORNs typically express only one type of olfactory receptor that will define its sensitivity to chemical

stimuli, and therefore its odorant tuning profile (Katada, 2005). Some ORNs express olfactory receptor proteins that are very broadly tuned and can be activated by many different odorant molecules whereas others are highly selective. Olfactory receptor neurons, again depending on the olfactory receptor they express, can also vary in terms of thresholding for a particular odorant – some being active at lower concentrations of an odorant, and others only at higher concentrations (Meister and Bonhoeffer, 2001; Fried et al., 2002).

The most well characterized types of intracellular signaling cascades include – a cAMP-dependent transduction mechanism (Nakamura and Gold, 1987; Firestein et al., 1991), that has been found to be associated to OR- and TAAR-type receptor proteins, generally expressed in ciliated ORNs; and a cAMP-independent transduction mechanisms, associated to V1R/ORR- and V2R/OlfC-type receptor proteins, generally expressed in microvillous ORNs.

cAMP-dependent cell signaling

When an odorant successfully binds to a GPCRs, such as an OR, or a TAAR, generally expressed on ciliated ORNs, this triggers the exchange of GDP to GTP within the coupled heterotrimeric G-protein. This exchange results in the release of the G protein's α subunit, bound with GTP, from the heterotrimeric G-protein. The G protein's α subunit and bound with GTP, together activate membrane-bound adenylylase III (ACIII) (Pace et al., 1985). Adenylylase III, in turn, converts ATP to cAMP (Pace et al., 1985; Bakalyar and Reed, 1990). This intracellular second messenger, cAMP, opens cyclic nucleotide gated ion channels, which results in the influx of Na^+ and Ca^{2+} (Nakamura and Gold, 1987; Firestein et al., 1991; Lowe and Gold, 1993a). The influx of Ca^{2+} leads release of Cl^- through calcium activated chloride channels (Kleene and Gesteland, 1991; Kurahashi and Yau, 1993; Lowe and Gold, 1993b). The resulting cAMP-dependent net depolarization triggers action potentials, leading to the relay of odorant related information to cells in the OB.

cAMP-independent cell signaling

The main components involved in cAMP-independent transduction mechanisms include – diacylglycerol (DAG), inositol-1,4,5-trisphosphate (IP3) and the transient receptor potential channel type 2 (TRPC2). The conformational change of the G protein upon odorant ligand binding activates membrane-bound phospholipase C,

which leads to the release of DAG and IP3 (Rünnenburger et al., 2002). These second messengers, DAG and IP3, trigger the influx of Ca^{2+} via two pathways. After IP3 is released, it dissipates from the membrane and to an increase in cytosolic Ca^{2+} calcium levels released from intracellular compartments (Yang and Delay, 2010; Kim et al., 2011), whereas DAG moves laterally through the plasma-membrane and activates TRPC2 (Liman et al., 1999; Lucas et al., 2003; Spehr and Munger, 2009). Transient receptor potential channel type 2 activation leads to further increase of intracellular Ca^{2+} levels and to the efflux of Cl^- through calcium activated anoctamine chloride channels (Lucas et al., 2003; Yang and Delay, 2010; Kim et al., 2011; Dibattista et al., 2012; Amjad et al., 2015; Münch et al., 2018; Manzini et al., 2022). Again, the resulting net depolarization triggers action potentials leading to the relay of odorant related information to cells in the OB.

Structure and wiring in the vertebrate olfactory bulb

Olfactory receptor neurons expressing the same olfactory receptor are intermingled and dispersed throughout the OE in a mosaic-like distribution (Strotmann et al., 1992, 1994; Ressler et al., 1993; Vassar et al., 1993; Mombaerts et al., 1996; Zapiec and Mombaerts, 2020; Kurian et al., 2021), but project their axons to specific subsets of glomeruli in the OB (Figure 1.1; Ressler et al., 1994; Vassar et al., 1994; Mombaerts et al., 1996; Feinstein and Mombaerts, 2004; Mombaerts, 2006). Therefore, each glomerulus is generally innervated by ORNs that express the same odorant receptor (Ressler et al., 1994; Vassar et al., 1994; Feinstein and Mombaerts, 2004). These clusters of synaptic connections, i.e. glomeruli, can be seen as functional units of odor coding. Projection neurons (PNs), the second order neurons with which ORN axons form synaptic connection in the OB, relay odor coding information to higher olfactory brain centers (Nagayama et al., 2014; Bear et al., 2016). Consequently, different higher brain centers are activated based on the specific subsets of glomeruli activated, and glomerular activation is based on the combinatorial activity of ORNs expressing different receptor proteins.

The general structure of the OB is highly conserved across vertebrates (Hildebrand and Shepherd, 1997; Rossler, 2002; Lledo et al., 2005). From the surface to the center of the OB several layers can be distinguished – the nerve layer, the glomerular layer, the external plexiform layer, the mitral cell layer, the internal plexiform layer and the

granule cell layer (Figure 1.1; Manzini et al., 2022). All axons of ORNs enter the OB through the nerve layer, and terminate in the glomerular layer, where they synapse with dendritic terminals of PNs, – mitral and tufted cells, – and interneurons, – several types of juxtglomerular cells (Figure 1.1; Pinching and Powell, 1971a, 1971b; White, 1972; Klenoff and Greer, 1998; Rodriguez-Gil et al., 2015; Manzini et al., 2022). Projection neurons are generally divided into two populations of cells, the mitral and tufted cells, both of which project primary dendrites into glomeruli and secondary dendrites into the granule cell layer of the OB, where they form dendrodendritic synapses with granule cells (Figure 1.1, Rall et al., 1966; Pinching and Powell, 1971a, 1971b). Mitral and tufted cells make up a heterogenous population of glutamatergic neurons that can be distinguished based on their location in the OB, the size of their soma, and how their dendrites and axons wire within the brain. Mitral/tufted cell (MTC) axons converge in the lateral olfactory tract and transmit information to higher brain centers (Figure 1.1; Von Campenhausen and Mori, 2000; Larriva-Sahd, 2008).

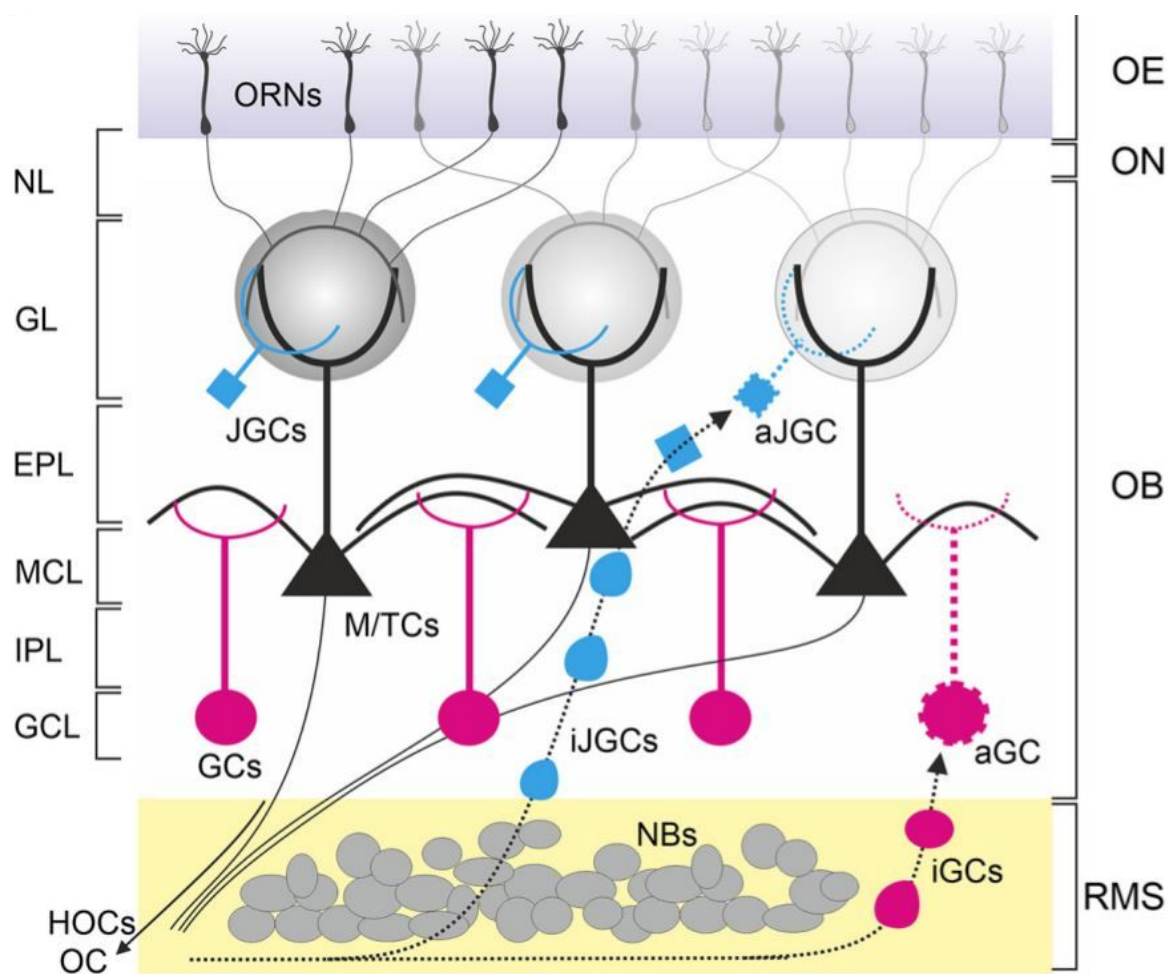


Figure 1.1 *General wiring structure of the vertebrate olfactory system and proliferative activity in the olfactory bulb (adapted from Manzini et al., 2022).* Olfactory receptor neurons (ORNs) reside in the olfactory epithelium (OE) and project their axons, via the olfactory nerve (ON), into the olfactory bulb (OB). Olfactory receptor neuron axons terminate in the glomerular layer (GL) where they form synaptic connections with mitral/tufted cells (M/TCs) and juxtglomerular cells (JGCs) within glomeruli (gray circles). Mitral/tufted cells form dendrodendritic connection with granule cells (GCs) in the external plexiform layer (EPL), and project their axons to olfactory cortices (OC) and higher olfactory centers (HOCs). A central stem cell niche provides neuroblasts (NBs) that migrate through the rostral migratory stream (RMS) to the OB, where they differentiate and form new interneurons (JGCs and GCs) throughout life. NL, nerve layer; MCL, mitral cell layer; IPL, internal plexiform layer; GCL, granule cell layer; a, apoptotic; i, immature.

Cell maintenance in the vertebrate olfactory system

Alongside ORNs and PNs there are other cells that reside in the OE and OB that play an important role in supporting and maintaining functional stability in the olfactory system (Manzini et al., 2022). The vertebrate OE has a pseudostratified layering structure, where each layer, from apical to basal, contains different cell populations (Figure 1.2). The most apical layer of the OE faces the external environment and is made up of tightly packed somata of supporting cells (SCs) as well as the dendrites of ORNs (Figure 1.2). The peripheral location of the OE allows ORNs, and their corresponding odorant receptors, to easily interact with odorants but puts these neurons in a vulnerable position in relation to the external world (Moulton, 1974). Supporting cells form tight junction connections between each other, creating an impermeable barrier in order to protect ORNs, and their end feet transverse the OE and make contact with the basal lamina (Graziadei and Graziadei, 1979; Monti Graziadei and Graziadei, 1979; Miragall et al., 1994; Nomura et al., 2004). Supporting cells are also involved in eliminating cell debris and noxious substances, regulating the extracellular environment, activating intraepithelial cell signaling and modulating signal transduction (Ding and Coon, 1988; Chen et al., 1992; Suzuki et al., 1995; Hassenklöver et al., 2008). The intermediate layer of the OE houses several layers of ORN somata, at varying degrees of maturity (Figure 1.2). Olfactory receptor neurons have been found to have a lifespan between several weeks to a few months (Mackay-Sim and Kittel, 1991; Holl, 2018), continuously requiring renewal. The most basal layer of the OE houses a heterogeneous group of cells called basal cells (BCs). Basal cells include stem cells and progenitor cells that give rise to new olfactory epithelial cells

throughout life (Figure 1.2). These stem cells provide the regenerative capacity associated to the OE (Graziadei and Graziadei, 1979; Monti Graziadei and Graziadei, 1979; Schwob, 2002; Schnittke et al., 2015; Suzuki et al., 2015; Schwob et al., 2017). In the rodent OE, two types of BCs, globose and horizontal BCs, can be distinguished morphologically and functionally. Horizontal BCs are for the most part quiescent but have been found to give rise to new globose basal cells and become active after lesion-induced loss of ORNs (Carter, 2004; Leung et al., 2007; Iwai et al., 2008; Suzuki et al., 2013, 2015; Joiner et al., 2015). Globose BCs are considered the putative progenitor cells that give rise to neurons and non-neuronal cells in the OE. From the asymmetric division of globose BCs, progenitor cells arise and eventually become immature ORNs (Figure 1.2). As they integrate in the OE and reconnect their axon in glomeruli they become fully mature ORNs.

Another cell type associate to the OE is the olfactory ensheathing cells (OECs; Figure 1.2). These cells form a group of heterogenous cells with similar properties to Schwann cells and astrocytes. They reside in the lamina propria, along the ON and in the apical portion of the OB. As their name suggests, OECs ensheath ORN axons, and have been found to promote axonal regeneration and wound healing, as well as participate in the regulation of the extracellular matrix (Manzini et al., 2022).

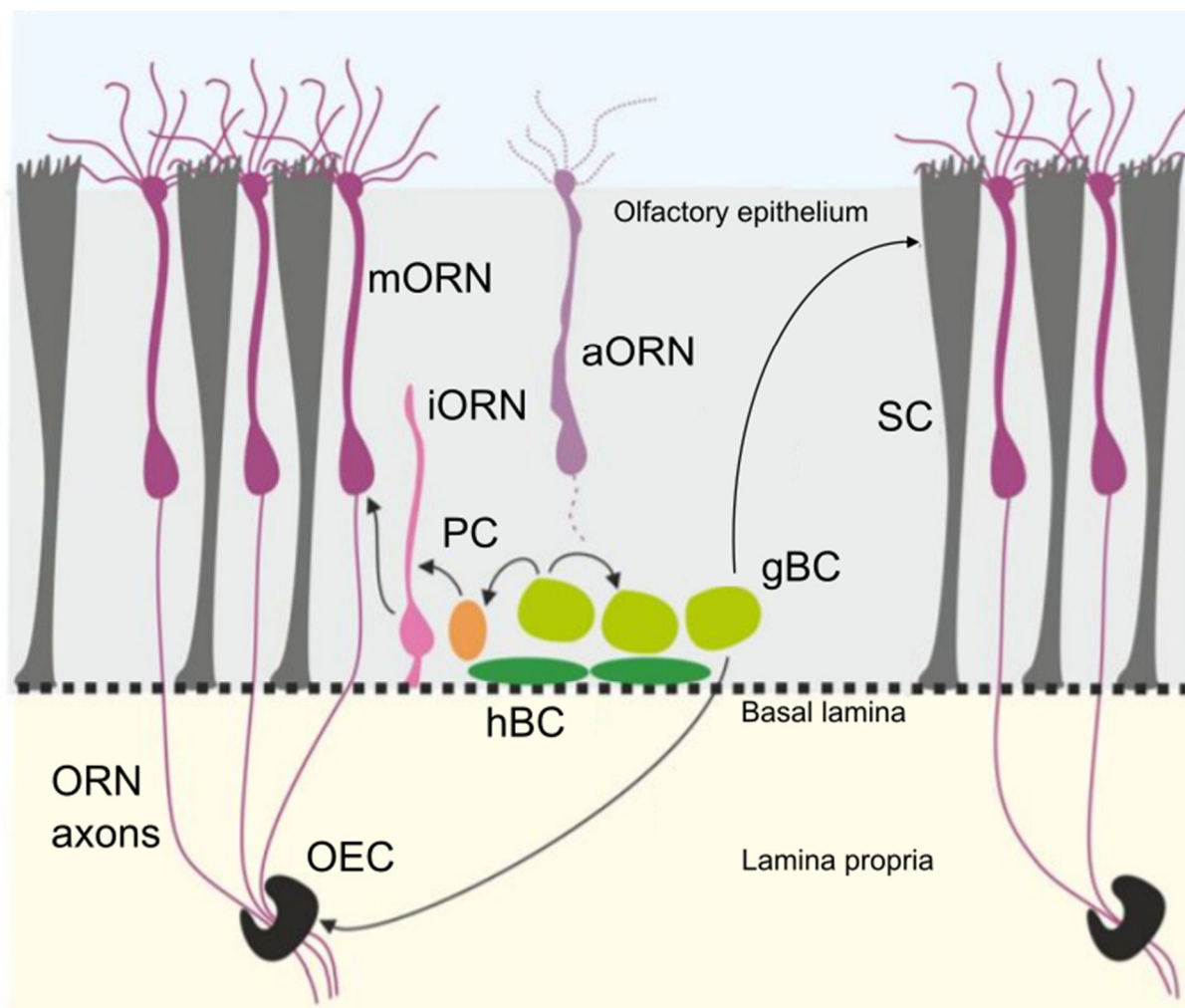


Figure 1.2 General structure of the vertebrate olfactory epithelium and proliferative activity (adapted from Manzini et al., 2022). The olfactory epithelium has a multilayered cell structure that includes supporting cells (SC), mature olfactory receptor neurons (mORN), immature olfactory receptor neurons (iORN), progenitor cells (PC), globose basal cells (gBC) and horizontal basal cells (hBC). The olfactory epithelia terminates at the basal lamina, through which olfactory receptor neuron (ORN) axons project to the olfactory bulb, via the olfactory nerve, ensheathed by olfactory ensheathing cells (OEC). a, apoptotic

As mentioned, in the peripheral olfactory system a stem cell niche, housing the different types of basal cells, replenish ORN and non-neuronal cell types of the OE that integrate into the central nervous system (Graziadei and Monti Graziadei, 1978; Graziadei and Graziadei, 1979; Monti Graziadei and Graziadei, 1979; Huard et al., 1998; Schwob, 2002; Moulton et al., 2008). The central nervous system, however, also retains a stem cell niche that provides a constant supply of interneurons to the OB (Figure 1.1; Altman, 1969; Lim and Alvarez-Buylla, 2016). Although adult neurogenesis is notoriously rare in the central nervous system, it has been found to

occur in certain regions of the brain – in the subventricular zone and in the subgranular zone (Altman and Das, 1965; Altman, 1969; Gage, 2002). It is along the lateral ventricle of the subventricular zone that new interneurons, juxtglomerular and granule cells are formed (Figure 1.1; Lois and Alvarez-Buylla, 1994; Figueres-Oñate et al., 2019).

The continuous turnover of neurons and interneurons in the olfactory system has made this system an interesting model to study stem cell proliferation, differentiation, maturation and survival as well as axon and dendrite wiring mechanisms. The regulation of constitutive and regenerative processes involved in lifelong cell maintenance versus repair after damage has been found to involve differing cellular activity and molecular signaling (Schwob et al., 2017; Calvo-Ochoa et al., 2021). Disrupting the olfactory system can, therefore, provide information on regulatory processes that influence the maintenance of neuronal network function. Olfactory dysfunction generally arises from damage to the main functional structures of the olfactory system and the higher olfactory centers. This damage can be caused by the process of aging, viral infections, exposure to noxious substances, neurodegenerative diseases and head trauma (for a review see Doty, 2009). Different forms of damage to each of these functional portions of the olfactory system can be performed on animal models in laboratory settings allowing for the study of particular features that enhance or hinder recovery from lesion.

The olfactory system of larval *Xenopus laevis*

The *Xenopus* olfactory system is an interesting model to study olfactory evolution and adaptability to different lifestyles (Bear et al., 2016; Silva and Antunes, 2017; Weiss et al., 2021) as they spend early development in a completely aquatic environment, and during metamorphosis they develop a secondarily aquatic lifestyle in which they can detect both water and airborne odorants (Altner, 1962; Hansen et al., 1998; Dittrich et al., 2016). During the course of vertebrate evolution, olfactory systems have shown a tendency towards segregation into various subsystems. Amphibians are the first in the vertebrate lineage to have evolved an anatomically distinct accessory olfactory system that exists alongside the main olfactory system (Eisthen, 1997).

Life cycle and olfactory subsystems

Xenopus laevis develops from a fertilized egg into a free swimming tadpole, that goes through metamorphosis before becoming a juvenile froglet. The larval *Xenopus* olfactory system includes two anatomically segregated peripheral olfactory organs in the nose, the principal cavity and the vomeronasal organ. These peripheral organs house ORNs that detect waterborne odorants during the process of buccal pumping, a mechanisms that also allows for gill irrigation and filter feeding (Gradwell, 1971; Wassersug and Hoff, 1979). During buccal pumping water flows into the olfactory organs, lined with olfactory epithelia. The water then flows through the choana and reaches the buccal cavity from where it is expelled again. Olfactory receptor neurons from these anatomically distinct peripheral organs project their axons, which coalesce in the ON, towards the main and accessory OB, respectively (Jungblut et al., 2012; Weiss et al., 2020). The accessory OB is situated lateroventrally to the main OB and in both areas, ORNs synapse with PNs and interneurons in glomeruli (Manzini et al., 2022).

After a period of larval development, *Xenopus* goes through different stages of metamorphosis. During these stages a complete restructuring of the olfactory system takes place as tadpoles develop into juvenile froglets. During metamorphosis, a vast amount of ORN cell death and neurogenesis occurs, along with extensive rewiring of the OB. At the end of the metamorphic process juvenile froglets possess two fully formed nasal cavities, a principal and a middle cavity, as well as the adult vomeronasal organ, all lined with olfactory epithelia. The adult principal cavity is filled with air, and is commonly referred as the adult air nose, and the newly formed adult middle cavity is filled with water, and is referred to as the adult water nose (Altner, 1962; Hansen et al., 1998; Dittrich et al., 2016). The vomeronasal organ is filled with water throughout the entire life cycle. Juvenile froglets mature into adult frogs and maintain an almost exclusively aquatic lifestyle. Odorant receptor expression patterns change across development and metamorphosis in *Xenopus*, as the entire olfactory system is rearranged (Mezler et al., 1999; Gliem et al., 2013; Syed et al., 2013, 2017).

Odorants, odorant receptors and transduction mechanisms

In larval *Xenopus*, the OE that lines the principal cavity in the nose possesses both ciliated and microvillous ORNs dispersed throughout the OE (Figure 1.3; Taniguchi et

al., 1996; Hansen et al., 1998; Nakamuta et al., 2011; Benzekri and Reiss, 2012; Gliem et al., 2013). These ORNs project their axons to the main OB (Figure 1.3; Taniguchi et al., 1996; Hansen et al., 1998; Benzekri and Reiss, 2012). The OE of the *Xenopus* vomeronasal organ houses microvillous ORNs (Eisthen, 1992; Benzekri and Reiss, 2012) that project their axons to the accessory OB (Figure 1.3). Although these two epithelial regions are anatomically segregated they have similar molecular features, specifically in relation to odorant receptor gene expression (Mezler et al., 1999; Hagino-Yamagishi et al., 2004; Date-Ito et al., 2008; Amano and Gascuel, 2012; Gliem et al., 2013; Syed et al., 2013).

In the main OE of larval *Xenopus*, OR- and TAAR-type receptors are presumed to be expressed in ciliated ORNs (Figure 1.3). These ORs can be either type I ORs (most commonly found in fish) and type II ORs (most commonly found in mammals; (Freitag et al., 1995; Mezler et al., 1999; Niimura and Nei, 2005; Saraiva and Korsching, 2007; Shi and Zhang, 2007). Of the five known *Xenopus* TAAR genes, only two are expressed in the main OE, TAAR4a and TAAR4b (Hussain et al., 2009; Syed et al., 2015). These TAARs have been proposed to detect amines (Syed et al., 2015) as they have been associated to amine detection in teleost fish olfactory systems (Shi and Javitch, 2002).

Subtypes of VRs are differentially expressed in the olfactory epithelia of *Xenopus* (Hagino-Yamagishi et al., 2004; Date-Ito et al., 2008; Syed et al., 2013), and have been found to be more numerous than what has been found in rodent olfactory systems (Figure 1.3; Niimura and Nei, 2005). Microvillous ORNs in the main OE presumably express V1Rs (Freitag et al., 1995; Mezler et al., 1999) or V2Rs (Hagino-Yamagishi et al., 2004; Syed et al., 2013, 2017). In the vomeronasal organ, only microvillous ORNs are found, expressing V2R-type receptors (Figure 1.3; Mezler et al., 1999; Gliem et al., 2013, 2013; Syed et al., 2017). Vomeronasal type 2 receptors have been found to show responses to amino acid odorants in aquatic vertebrates (Alioto and Ngai, 2006; DeMaria et al., 2013; Syed et al., 2013) and are therefore assumed to be expressed in amino acid sensitive ORNs in the *Xenopus* main OE (Gliem et al., 2013; Syed et al., 2013).

When odorants bind to the odorant receptors of microvillous ORNs transduction of olfactory information to the brain is presumed to occur through cAMP-independent

transduction mechanisms (Figure 1.3). A subset of ORNs in the main OE has been found to respond to amino acid odorants and exhibit a cAMP-independent transduction mechanism (Manzini et al., 2002; Manzini and Schild, 2003; Czesnik et al., 2006) and are therefore presumed to be microvillous. Another subset of ORNs in the main OE has been found to respond to pharmacological agents that activate cAMP-dependent transduction mechanisms, e.g., forskolin, and are presumed to be ciliated (Figure 1.3). These ciliated ORNs have been proposed to be activated by bile acids and amines (Weiss et al., 2021).

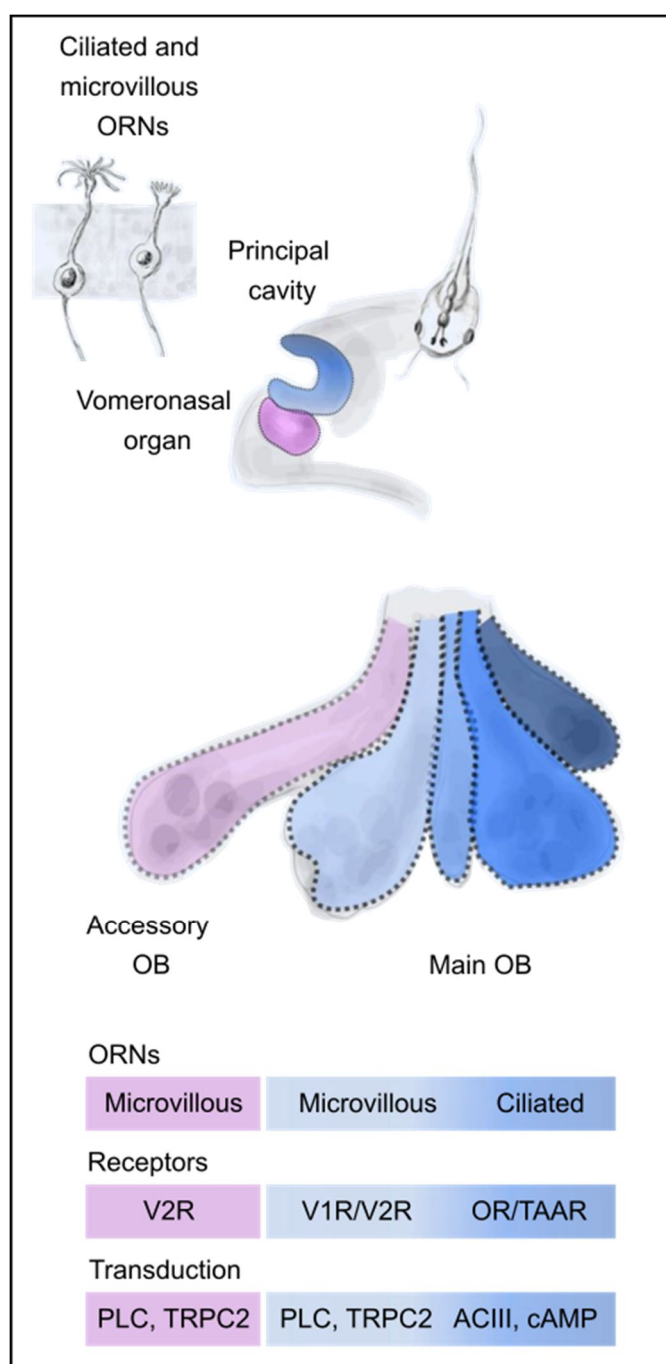


Figure 1.3 *Features and wiring characteristics in the olfactory system of larval *Xenopus laevis* (adapted from Weiss et al., 2021).* Morphological types of olfactory receptor neurons (ORNs) that lie in the olfactory epithelium of the principal cavity and the vomeronasal organ. Olfactory receptor neuron axons project from the vomeronasal organ and synapse in glomeruli in the accessory olfactory bulb (OB). These olfactory vomeronasal neurons are presumed to be microvillous, express V2R-type receptor proteins, and transduce signals to the brain through cAMP-independent transduction mechanisms. Olfactory receptor neurons that project their axons from the principal cavity to the main olfactory bulb can be either ciliated or microvillous. The microvillous receptor neurons are presumed to express V1R- or V2R-type receptor proteins and transduce signals to the brain through cAMP-independent transduction mechanisms. The ciliated ORNs are presumed to express OR- or TAAR-type receptor proteins, and transduce information to the brain via cAMP-dependent transduction mechanism. Note that the olfactory bulb is divided into multiple varying glomerular clusters.

Structuring and wiring in the olfactory bulb

Olfactory receptor neurons, intermingled throughout the main OE, project their axons via the ON into the main OB, where they segregate into streams and innervate different glomerular clusters that can be distinguished based on the subtype of ORNs with which they are innervated. Two coarsely segregated odor processing streams can be distinguished in the main OB of larval *Xenopus* (Manzini et al., 2007; Gliem et al., 2013). A more laterally located glomerular cluster is innervated by ORNs that respond mainly to amino acid odorants, and transmit information to the brain via cAMP-independent transduction mechanisms (Manzini and Schild, 2003; Gliem et al., 2013; Syed et al., 2017). These ORNs are presumably microvillous, expressing V1Rs or V2Rs (Manzini et al., 2007; Nakamuta et al., 2011; Gliem et al., 2013; Syed et al., 2017). A more medially located glomerular cluster is innervated by ORNs that transmit information to the brain via cAMP-dependent transduction mechanisms ((Manzini et al., 2007; Nakamuta et al., 2011; Gliem et al., 2013). These ORNs are presumably ciliated, and express ORs (Manzini et al., 2007; Gliem et al., 2013).

A characteristic feature of ORNs in larval *Xenopus* is that almost all axons bifurcate into multiple axonal branches and synapse within more than one glomerulus (Nezlin and Schild, 2005). The PNs that are innervated by ORNs and that project their axons into higher olfactory brain centers are made up of a heterogeneous population of second order neurons, that are called MTCs, and these also often project multiple primary dendrites into multiple distinct glomeruli (Nezlin and Schild, 2005). Interneurons in larval *Xenopus* brain include juxtglomerular cells that reside around glomeruli, and granule cells, that reside in the granule cell layer (Nezlin and Schild, 2000; Hassenklover and Manzini, 2013; Weiss et al., 2020).

Behavior

Larval anuran amphibians have a fully developed olfactory system that permits them to detect waterborne odorants. Odor perception plays an important role in regulating tadpole behavior, ex. – locating food sources (Veeranagoudar et al., 2004; Heerema et al., 2020), recognizing con- or heterospecifics, as well as kin (Blaustein and O'hara, 1982; Waldman, 1986), detecting predators or alarm signals (Mirza et al., 2006; Supekar and Gramapurohit, 2018; Raices, 2020), etc. For a comprehensive review of

how olfaction plays an important role in behavior in anuran amphibians see (Weiss et al., 2021).

Aim of this thesis

My goal with the following work was to examine specific structural and functional features of the olfactory system of larval *Xenopus laevis*, in order to compare these features with possible changes that occur after a lesion of the system. For my investigations I severed the connection between the OE and the OB, by transecting the olfactory nerve, causing the complete loss of olfactory function. I then investigated aspects of regeneration within the olfactory system that could potentially lead to recovery of olfactory function:

- Anatomical and functional changes in the cellular components that make up the OE, specifically SCs, ORNs and BCs, the stem/progenitor cells that give rise to new neurons and non-neuronal components of the OE;
- Apoptotic events in the OE and OB and structural changes of the OB after denervation;
- Morphological changes in PNs after the loss of synaptic input;
- Anatomical and functional changes in ORN axon wiring and odorant induced signaling in the OB;
- Functional changes in odorant induced responses of PNs in the OB;
- Odor induced behavioral changes during degeneration and recovery of the olfactory system.

Chapter 2:

Functional reintegration of sensory neurons and transitional dendritic reduction of mitral/tufted cells during injury-induced recovery of the larval *Xenopus laevis* olfactory circuit

Published as Original Research article in Frontiers in Cellular Neuroscience and available under <https://doi.org/10.3389/fncel.2017.00380>

Authors and affiliations:

Sara J. Hawkins^{1,2}, Lukas Weiss^{1,2}, Thomas Offner^{1,3}, Katarina Dittrich^{1,2}, Thomas Hassenklöver^{1,2,3*} and Ivan Manzini^{1,2,3*}

¹ Institute of Neurophysiology and Cellular Biophysics, University of Göttingen, Göttingen, Germany

² Institute of Animal Physiology, Department of Animal Physiology and Molecular Biomedicine, Justus Liebig University Giessen, Giessen, Germany

³ Center for Nanoscale Microscopy and Molecular Physiology of the Brain (CNMPB), Göttingen, Germany

Keywords:

Xenopus laevis, olfactory receptor neurons, neuronal stem cells, degeneration, regeneration, glomerulus, network reconstruction

Author contributions:

The experiments were conceived and designed by TH and IM. The experiments were performed by SJH, LW, TO and KD. SJH, LW, TO and TH analyzed the data. SJH, TH and IM wrote the article. All authors participated in the discussion of the data and in production of the final version of the manuscript.

Abstract

Understanding the mechanisms involved in maintaining lifelong neurogenesis has a clear biological and clinical interest. In the present study, we performed olfactory nerve transection on larval *Xenopus* to induce severe damage to the olfactory circuitry. We surveyed the timing of the degeneration, subsequent rewiring and functional regeneration of the olfactory system following injury. A range of structural labeling techniques and functional calcium imaging were performed on both tissue slices and whole brain preparations. Cell death of olfactory receptor neurons and proliferation of stem cells in the olfactory epithelium were immediately increased following lesion. New olfactory receptor neurons repopulated the olfactory epithelium and once again showed functional responses to natural odorants within 1 week after transection. Reinnervation of the olfactory bulb (OB) by newly formed olfactory receptor neuron axons also began at this time. Additionally, we observed a temporary increase in cell death in the OB and a subsequent loss in OB volume. Mitral/tufted cells, the second order neurons of the olfactory system, largely survived, but transiently lost dendritic tuft complexity. The first odorant-induced responses in the OB were observed 3 weeks after nerve transection and the olfactory network showed signs of major recovery, both structurally and functionally, after 7 weeks.

Introduction

While many mammalian species appear to have lost regenerative capacity of neuronal tissue during evolution, early diverging vertebrates exhibit elevated neuroregenerative potential and have been shown to be capable of restoring entire brain regions after lesion (for review (Ferretti, 2011)). This ability is not only variable among species but also has a strong developmental component. After development is complete, most stem cells of the central nervous system undergo terminal differentiation and lose their ability to divide (Kauffman, 1968; Caviness et al., 1995). Even in cases where neurogenesis is still possible, the system often no longer possesses the mechanisms that once allowed newly formed neurons to successfully integrate into a neural circuit (Christie and Turnley, 2013). The vertebrate olfactory system is an exceptional case and has become increasingly more relevant as a model to study neuroregenerative

processes, as it is known for its lifelong capacity to replenish cells lost during natural turnover (Graziadei and Metcalf, 1971; Graziadei, 1973), as well as to regenerate after severe lesion (Schwob, 2002). Olfactory receptor neurons (ORNs) of the olfactory epithelium reside in an exposed location, prone to external stress factors, and thus have a limited lifespan. Eventually they undergo caspase-mediated programmed cell death and multipotent stem cells of the basal layers of the olfactory epithelium compensate for this loss in order to sustain the sense of smell (Cowan and Roskams, 2002; Leung et al., 2007). Newly generated sensory neurons extend their axons toward the olfactory bulb (OB) in search of synaptic targets, eventually forming functional connections with second order neurons, mitral and tufted cells, in functional structures called glomeruli (Nezlin et al., 2003; Manzini, 2015; Kosaka and Kosaka, 2016). A correct integration is essential to allow the successful propagation of olfactory information from second order neurons to higher brain centers. Not only input neurons of the olfactory network, but also neurons of the odor processing brain circuitry, are constantly replaced (Kaplan and Hinds, 1977). The stem cell population located in the subventricular zone is mainly responsible for supplying the OB with new interneurons (Lim and Alvarez-Buylla, 2016), which has been shown to be essential in adjusting olfactory performance (Mouret et al., 2009). The turnover of neurons that occurs both in the olfactory epithelium and OB is not restricted to developmental stages, but continues throughout life, allowing network adaptations to sensory experience, learning, and even recovery after extensive injury (Schwob, 2002; Brann and Firestein, 2014; Cummings et al., 2014). Although the regenerative capacity of the olfactory system has been illustrated numerous times in various organisms, the way in which this system is capable of withstanding massive lesion and recovering functionally is still not fully understood (Yu and Wu, 2017). It is crucial to understand the processes that hinder an efficient recovery, and to find perspectives to facilitate correct network reconstitution. Olfactory dysfunction following head trauma is common, and is frequently due to shearing injuries at the cribriform plate that lacerate the olfactory nerves (ONs)(Coelho and Costanzo, 2016). Recovery is variable and highly dependent on the severity and location of the injury (Doty et al., 1997; Gudziol et al., 2014; Coelho and Costanzo, 2016). Increased inflammation and glial scar formation that occur in the mammalian system pose a major challenge for ON recovery and successful reinnervation of the bulbar network by axons of newly generated ORNs (Kobayashi and Costanzo, 2009). After loss of olfactory sensory input in mammals, it

has been shown that mitral cell dendritic tufts persistently degrade (Murai et al., 2016). In humans, only approximately 1/3 of patients show at least a partial recovery of their sense of smell (Doty et al., 1997; Gudziol et al., 2014) and no effective treatment is available yet to treat post-traumatic neuronal damage or to assist in the recovery of the olfactory system (Coelho and Costanzo, 2016).

We performed ON transection on larval *Xenopus laevis* in order to disrupt the neuronal network of a highly regenerative vertebrate olfactory system (Figure 2.1). The aim was to further understand aspects of degeneration and recovery of neural circuits after injury, and to investigate how neural disruption and the potential for circuit restoration in this system differs from that found in the mammalian system. We show that ON transection targets ORNs for cell death, leaving other components of this system involved in the process of regeneration largely unperturbed. We have established a timeline of post-transection events, up until the point of recovery of the olfactory system, revealing a transient decline of dendritic arborizations of postsynaptic mitral/tufted cells (MTCs) during the period of denervation. Our results are a clear illustration of how the maintenance of a permissive environment in a highly regenerative system can allow neuronal regeneration and subsequent formation of correct axonal and dendritic connections, creating a reliable foundation for future research on the topic of neuroregeneration.

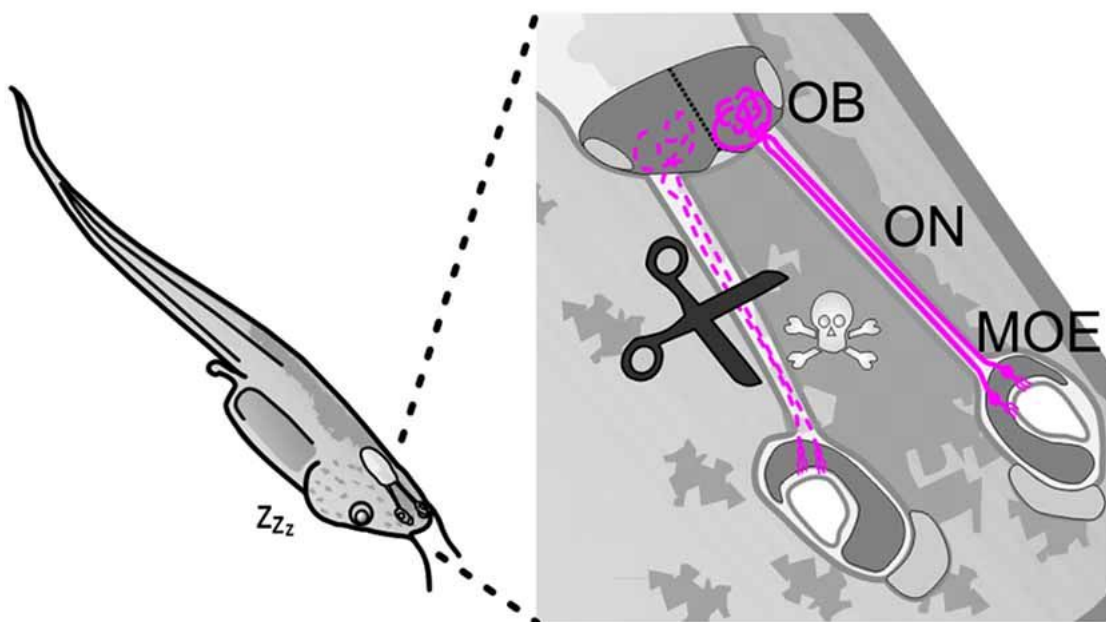


Figure 2.1 *Olfactory nerve transection as a model injury to induce neuronal damage in the olfactory system of larval *Xenopus laevis*.* Schematic depiction of a tadpole with a close up of its olfactory system. Bipolar olfactory receptor neurons (magenta) of the MOE extend their axons via the ON into the OB. Fine scissors can be used to transect the ON, leading to axon degeneration and olfactory receptor neuron cell death. MOE, main olfactory epithelium; OB, olfactory bulb; ON, olfactory nerve.

Material and methods

Animal care, olfactory nerve transection and sensory neuron labeling

All *Xenopus laevis* larvae used in this study were raised in our breeding colony at the University of Göttingen. They were kept in water tanks (50 l) at a water temperature of 19–22°C and fed with algae (Dose Aquaristik). All procedures for animal handling were approved by the governmental animal care and use office (Niedersächsisches Landesamt für Verbraucherschutz und Lebensmittelsicherheit, Oldenburg, Germany, Az.16/2136) and were in accordance with the German Animal Welfare Act as well as with the guidelines of the Göttingen University Committee for Ethics in Animal Experimentation. As an injury model for substantial damage in the olfactory system, we transected the ONs of *Xenopus laevis* tadpoles to disrupt the neuronal population in the olfactory organ. For ON transection, we used freely swimming, premetamorphic larvae with an already well developed olfactory system, ranging from developmental stage 48 (ca. 7 days after fertilization at 22–24°C) to stage 51 (ca. 17 days after fertilization at 22–24°C; Nieuwkoop and Faber, 1994). We surveyed the extent of recovery only in animals that did not exceed developmental stage 56, when major metamorphic remodeling of the olfactory system started to occur. Pigmented and albino *Xenopus laevis* larvae were anesthetized in 0.02% MS-222 (ethyl 3-aminobenzoate methanesulfonate; Sigma-Aldrich), and their ONs were transected with very fine scissors without damaging surrounding tissue (Figure 2.1). To label sensory neurons, Biocytin (ϵ -biotinoyl-L-lysine, Molecular Probes, ThermoFisher Scientific) or microRuby crystals (tetramethylrhodamine/biotin linked dextran, 3 mM; Molecular Probes, Thermo Fisher Scientific) were placed into the lesioned nerve in immunohistochemistry experiments and in experiments to visualize axonal degradation in the OB (see below), respectively. The wound was closed with tissue adhesive (Histoacryl L; Braun). After transection, animals were transferred to a beaker filled with fresh tap water for recovery. In a subset of experiments, this transection

procedure was repeated every week to survey the volumetric changes in the OB (see below). At different time intervals after injury, animals were chilled in ice water until paralyzed and killed by severing the brain and spinal cord with a scalpel. Subsequent experiments were performed on an excised block of tissue containing the olfactory epithelia, ONs and the OB.

Immunohistochemistry

To visualize changes in the olfactory epithelium and OB after bilateral ON transection we performed immunolabeling on slices of the olfactory system. For 5-bromo-20 - deoxyuridine (BrdU, Sigma-Aldrich) labeling experiments, animals were kept in normal tap water with 100 μ M BrdU for 24 h before dissection. BrdU exposure with this concentration was shown to not induce negative side effects, such as increased apoptosis, alterations of cell marker expression patterns or foraging behavior (Pozzi, 2015). Animals were killed (as described above) 1,2,3,7 and 21 days after ON transection (as described above). Seven and 21 days post-transection, newly generated ORNs were labeled via an additional ON transection 1 h before killing the animals. Excised tissue blocks were fixed in 4% formaldehyde, washed in PBS, embedded in 5% lowmelting-point agarose (Sigma-Aldrich), glued onto the stage of a vibratome (VT 1200S, Leica) and cut horizontally into slices. Tissue blocks used to label the olfactory epithelium were sliced at 75 μ m thickness, whereas tissue used to label the OB was cut at 95 μ m thickness. Nonspecific binding was blocked with 2% normal goat serum (NGS; MP Biomedicals) in PBS containing 0.2% Triton X-100 (PBST, Carl Roth) for 1 h. Slices of BrdU treated animals were incubated in 1 N HCl at 37°C for 45 min to denature DNA and subjected to multiple changes of PBS. Slices were incubated overnight at 4°C with one of the following primary antibodies—anti-*Xenopus laevis* cytokeratin II (1h5, monoclonal, derived from mouse, obtained from the Developmental Studies Hybridoma Bank developed under the auspices of the National Institute of Child Health and Human Development and maintained by the University of Iowa, Department of Biological Sciences (Iowa City, IA)); anti-active caspase-3 (polyclonal anti-active caspase-3, ab13847, derived from rabbit using a synthetic peptide corresponding to human active + procaspase 3 aa 150–250 conjugated to keyhole limpet hemocyanin (KLH), RRID:AB_443014; Abcam; characterized by (Thompson and Brenowitz, 2010) and previously used in *Xenopus laevis* tissue by (Dittrich et al., 2016)); or anti-BrdU (B2531, monoclonal, derived from

mouse, Sigma-Aldrich). Primary antibodies were diluted in 2% NGS/PBST (1:1000, 1:600, 1:100 respectively) and washed off with PBS after the incubation period. Alexa 488-conjugated goat anti-mouse or anti-rabbit secondary antibody (Invitrogen, Thermo Fisher Scientific) was applied at a dilution of 1:250 in 1% NGS/PBS for 1 h. The secondary antibodies were washed off in several changes of PBS. To visualize biocytin-backfilled ORNs, slices were incubated in Alexa 568- or 647-conjugated streptavidin (Molecular Probes, Thermo Fisher Scientific) at a final concentration of 5 µg/ml in PBST for 1 h and repeatedly rinsed in PBS. In active caspase-3 immunostaining experiments, cell nuclei were labeled with 10 µg/ml propidium iodide (Molecular Probes, Thermo Fischer Scientific) for 15 min. After repeated washing steps with PBS, slices were mounted on glass slides using mounting medium (Dako). Images stacks were acquired using upright confocal laser-scanning microscope (LSM 780/Axio Examiner, Zeiss) with an axial resolution of 1 µm.

Whole mount preparation of the olfactory bulb

After excising a tissue block containing the olfactory system as described above, the ventral palatial tissue was removed to expose the ventral side of the OB and the caudal portion of the ONs. This whole mount preparation was transferred into an imaging chamber containing standard bath solution (see “Solutions” section) and stabilized by a small platinum grid with nylon threads.

Visualization of axonal debris in the olfactory bulb

Animals were killed and whole mount preparations of the OB were made from excised tissue blocks 1, 2, 3 and 7 days after unilateral ON transection (as described above). Microruby labeled, degenerating ORN axons were visualized from the ventral side of the OB using an upright multi-photon microscope (A1R-MP, Nikon).

Olfactory receptor neuron labeling via electroporation

To visualize axonal reinnervation of the OB, fluorophorecoupled dextran (Alexa 594, Alexa 488, Cascade Blue, 10,000 MW, Molecular Probes, Thermo Fisher Scientific) was introduced into sensory neurons via electroporation (for details, see (Haas et al., 2002; Hassenklöver and Manzini, 2014). Albino *Xenopus laevis* were anesthetized, dye crystals were introduced into both nasal cavities and dissolved in the residual moisture. Two thin, platinum electrodes were carefully placed in the nasal cavities.

The electrodes were connected to a voltage pulse generator (ELP-01D; npi Electronics), and 12 pulses (20–25 V, 25 ms duration at 2 Hz) with alternating polarity were applied. After electroporation, animals were transferred into a beaker filled with fresh tap water for recovery and killed 1 or 2 days later. Whole mount preparations of the OB were made from excised tissue blocks 1, 2, 3 and 7 weeks after unilateral ON transection (as described above). Image stacks of the whole intact OB were acquired from the ventral side (for details see (Hassenklöver and Manzini, 2014)) using an upright multi-photon microscope (A1R-MP, Nikon).

Labeling of the olfactory bulb for volume quantification

Animals were killed (see above) 1, 2, 3 and 7 days after unilateral nerve transection and a whole mount preparation of the OB was prepared from excised tissue blocks (as described above). The preparation was incubated in bath solution (see “Solutions” section) containing 100 μ M Calcein green/AM (Molecular Probes, Thermo Fisher Scientific), 30 μ M Alexa 594 dextran (10,000 MW, Molecular Probes, Thermo Fisher Scientific), and 50 μ M MK571 (Sigma-Aldrich), an inhibitor of multidrug resistance transporters. Calcein green/AM was initially dissolved in DMSO (Sigma-Aldrich) and Pluronic F-127 (Molecular Probes, Thermo Fisher Scientific). After an incubation time of 2 h, a series of image stacks of the whole ventral OB was obtained using multiphoton microscopy. Relative changes of the OB volume of the transected side to the non-transected side were compared.

Sparse cell electroporation to label individual mitral/tufted cells

Individual MTCs were investigated for morphological changes after the loss of ORN axon innervation. Animals were killed 1, 3 and 7 weeks after unilateral nerve transection and whole mount preparations were produced from tissue blocks containing the olfactory system (as described above). MTCs were labeled via sparse cell electroporation in the ventrolateral OB using a stereomicroscope with epifluorescence illumination. Electroporation micropipettes (Warner instruments, resistance 10–15 M Ω) were filled with Alexa 488 or Alexa 594 dextran solution (1–5 μ l, 3 mM dissolved in bath solution) and mounted on a pipette holder containing a silver wire electrode covered with silver chloride. A train of square voltage pulses (50 V, 300 μ s, 500 ms at 200–300 Hz) was triggered by an Axoprotector 800A (Molecular devices) single cell electroporator to transfer dye into neurons (for more details, see

(Hassenklöver and Manzini, 2014)). Image stacks of MTCs were acquired with a z-resolution of 1–2 μm using multiphoton microscopy from the ventral side of the OB. MTCs labeled in the non-transected side of the OB were used as controls.

Calcium imaging experiments

To analyze functional changes in the various cell populations of the main olfactory epithelium (MOE) after ON transection, functional calcium imaging experiments were performed on acute slices of the olfactory organ. Tissue blocks containing the olfactory system were glued to the stage of a vibratome. Two horizontal cuts were made to produce a slice with cells of the MOE exposed on both the dorsal and ventral side. Depending on angular position of the tissue block and size of the olfactory organ, the final slice thickness was between 120 μm and 140 μm . Calcium indicator mixture consisted of 50 μM Fluo-4/AM (Molecular Probes, Thermo Fisher Scientific), 100 μM MK571 (Sigma-Aldrich) in bath solution. Fluo-4/AM was initially dissolved in DMSO and Pluronic F-127 with final concentrations not exceeding 0.5% and 0.1%, respectively. Slices were incubated for 35 min with calcium indicator mixture on a shaker. Changes of intracellular calcium concentration of individual cells of the MOE were monitored using a laser-scanning confocal microscope (LSM 510/Axiovert 100 M, Zeiss, Jena, Germany). A time series of one focal plane was acquired. Virtual slice thickness excluded fluorescence from more than one cell layer and the field of view covered a square with an edge length of 360 μm . We performed calcium imaging in whole mount olfactory system explants to investigate the extent of functional recovery of the olfactory network after ON transection. Calcium indicator mixture consisted of 1000 μM Fluo-4/AM (Molecular Probes, Thermo Fisher Scientific), 600 μM MK571 (Sigma-Aldrich), 18 μM Cascade Blue (10,000 MW dextran; Molecular Probes, Thermo Fisher Scientific) in bath solution and the supernatant dye solution was collected after a centrifugation step (1 min, 16.1 rcf). A whole mount preparation was made from a tissue block containing the olfactory system (as described above). A micropipette (Warner Instruments, resistance 10–15 $\text{M}\Omega$) filled with dye solution was penetrated into the ventro-lateral part of the OB using a micromanipulator. Dye solution was pressureinjected into the MTC layer at up to three different locations under visual control using epifluorescent illumination. After 35 min of incubation, calcium responses of postsynaptic MTCs in an OB volume were recorded using an upright multiphoton microscope (A1R-MP, Nikon, excitation wavelength: 800 nm). Via

fast volumetric resonant scanning, we measured time series of cubic volumes of the amino acid-sensitive, ventrolateral OB (lateral dimensions: 170 μm , 512 \times 512 pixel; axial dimension: 120–180 μm ; step size: 3–5 μm) at 0.5–1 Hz per image stack. Preparations were stabilized using a stringed platinum grid in a recording chamber, which was constantly perfused with bath solution applied by gravity feed from a storage syringe through an applicator placed directly above the MOE. The stimuli were applied without stopping the flow and bath solution was constantly removed from the recording chamber through a syringe needle positioned caudally to the preparation. Before application of stimuli, baseline fluorescence was recorded for at least 10 s. After stimulation, fluorescence changes were monitored for at least 50 s. The reproducibility of the responses was verified by regularly repeating the application at least twice. The minimum interstimulus interval was at least 2 min in all of the experiments. All experiments were conducted at room temperature.

Image and data processing

The brightness and contrast of some image stacks from structural measurements were adjusted in the image processing software Fiji (Schindelin et al., 2012). Spectral imaging and linear unmixing (Zen software, Zeiss) were used to separate overlapping fluorescent signals in slices with active caspase-3 labeling. To quantify cell death and proliferation, active caspase3-positive and BrdU-positive cells were manually counted. 3D image stacks were visualized in the image processing software Fiji to utilize the volumetric information for the quantification. The average diameter of counted cell profiles was 9 μm , and labeled structures with a diameter smaller than 4 μm or without identifiable nucleus (stained with propidium iodide in active caspase-3 labeled slices) were omitted from the quantification. Multiple sections of each OB were used for quantification. In olfactory organ slices, a randomly chosen 5 μm thick partial sub-volume of the whole acquired image stack was manually quantified. For the quantification of OB volume, multiple image stacks were stitched together using image processing software Fiji (Preibisch et al., 2009). Cross sectional areas of the transected and non-transected side of the OB were measured at five different levels on the z-axis of the image stack. The sum of these areas was used as an estimate of the OB volume, and the relative change of OB volume between the transected side and the non-transected side was determined for each animal. These changes were calculated for animals killed at different time-points after transection. The relative

difference in volume of the left and right hemibulbs of non-transected animals was used as control. To identify changes in dendritic morphology of individual MTCs after ON transection, a region of interest was cropped out and digitally isolated by restricting the field of view in x-y axis to a single tuft and by making a sub-stack to include only planes containing the tuft. As a last pre-processing step, the image stacks were rendered binary using Otsu's thresholding method implemented in Fiji (Otsu, 1979). Blunt dendritic terminals were not used in statistical analysis. Tuft morphology was examined using Sholl's technique for quantitative analysis of complex dendritic branching structures in Fiji (Sholl, 1953; Ferreira et al., 2014). The starting point was centered on the main apical dendrite of MTCs at $\sim 40 \mu\text{m}$ from the tuft. From there, the dendritic intersections for concentric 3D spheres with stepwise increasing radii of $1 \mu\text{m}$ were calculated. For the calculation of the average linear tuft-complexity curves, the maxima of intersections of the single tufts of each group were aligned and the curves averaged at each radius of the Sholl analysis. Data visualization and statistical analyses were conducted using custom written Matlab scripts (Mathworks, Natwick). Changes in calcium indicator fluorescence are given as $\Delta F/F$ values in percent. The values were calculated for each pixel according to the following equation: $\Delta F/F = (F - F_0)/F_0$. F_0 represents an averaged pixel fluorescence value derived from the time interval prior to the stimulus and F is the actual pixel fluorescence value at each recorded time point. A response was assumed if the following criteria were met: (i) the maximum amplitude of the calcium transient had to be higher than the maximum of the pre-stimulus intensities; (ii) the onset of the response had to be within ten frames after stimulus application. To facilitate selection of responsive regions of interest, a "pixel correlation map" was obtained by calculating the cross-correlation between the fluorescence signals of a pixel to that of its immediate neighbors (Junek et al., 2009). Analyzed regions of interest in each olfactory epithelium were counted and the number of cells responsive to each stimulus was calculated for each time point. For OB measurements, difference images were calculated for each recorded plane by averaging the fluorescence value of the interval prior to stimulation, and subtracting this value from the mean peak response of the odor induced fluorescence peak (2–3 points for mean peak calculation). Functional imaging data were analyzed using custom written programs in Matlab. Averaged data are presented as mean \pm standard deviation. Statistical significance was determined by Kruskal-Wallis rank sum test

followed by Dunn's multiple comparison post hoc test. To control familywise error rate for multiple comparisons a Holm-Bonferroni correction was applied.

Solutions

Standard bath solution consisted of (in millimolar): 98 NaCl, 2 KCl, 1 CaCl₂, 2 MgCl₂, 5 glucose, 5 Napyruvate, 10 hydroxyethyl piperazineethanesulfonic (HEPES), 230 mOsmol/l, pH 7.8. High K⁺ bath solution consisted of (in millimolar): 17 NaCl, 80 KCl, 1 CaCl₂, 2 MgCl₂, 5 glucose, 5 Napyruvate, 10 HEPES, 230 mOsmol/l, and pH 7.8. Adenosine-50 - triphosphate (ATP), 2-methylthio-ATP (2-MeSATP), and bath solution chemicals were purchased from Sigma-Aldrich. Amino acids and purinergic receptor agonists were dissolved in bath solution (10 mM stock) and applied at a final concentration of 100 μM, either individually or as a component in a mixture. All pharmacologic agents were dissolved as concentrated stock solutions, aliquoted and frozen. Aliquots were thawed only once and the working solutions (see specific experiments) were freshly prepared before performing each experiment.

Results

Structural and functional consequences after olfactory nerve transection in the main olfactory epithelium

To observe structural changes occurring in the MOE after bilateral ON transection, we visualized major cell populations of the MOE, namely supporting cells (SCs), proliferative basal cells (BCs) and ORNs. We found no changes in the morphological structure of the SC layer of the MOE post-transection in comparison to non-transected animals. The apical layer of the MOE exhibited typical cytokeratin II-like immunoreactivity and labeled SCs were clearly visible in control animals, as well as in all analyzed time points post-transection (Figure 2.2A). Cytokeratin II-positive cells always formed an undisrupted, tightly packed columnar monolayer on the apical surface of the MOE, and spanned their basal processes across the entire epithelium terminating in endfeet-like structures (Hassenklöver et al., 2008). To assess the proliferative activity in the MOE, we conducted BrdU-labeling experiments to visualize cells in the S-phase of mitosis. In healthy control animals, 8 ± 4 BrdU positive cells ($n = 5$) were visible in the BC layer of the MOE, restricted mainly to the area adjacent to

the basal lamina (Figure 2.2B,G). The number of BrdU-positive cells in the MOE was significantly increased 1, 2 and 3 days after transection to 111 ± 76 ($p = 0.044$, $n = 5$), 119 ± 27 ($p = 0.025$, $n = 5$) and 136 ± 37 ($p = 0.0054$, $n = 5$), respectively (Figure 2.2B,G). The area occupied by proliferating cells was expanded more deeply into the MOE and several labeled cells were also found in intermediate and apical layers (Figure 2.2B). One week after injury, proliferative activity returned to a level indistinguishable from healthy controls with 19 ± 10 BrdU-positive cells ($n = 5$). To assess the extent of apoptosis in the MOE, we investigated immunoreactivity to a protein involved in programmed cell death, active caspase-3. In the control situation, 4 ± 2 active caspase-3 positive cells ($n = 5$) were visible in the MOE (Figure 2.2C,G), showing a constricted, bleb-like appearance typical for apoptotic cells (Dittrich et al., 2016). The number of active caspase-3 positive cells was enormously increased 1 and 2 days after ON transection, with 122 ± 48 ($n = 5$) and 333 ± 107 ($p = 0.0044$, $n = 5$), respectively (Figure 2.2C,G). Labeled cells were found in all layers of the MOE, but the majority was located in the intermediate ORN layer. Three and 7 days post-transection, the number of apoptotic cells decreased back to control levels with 8 ± 3 ($n = 5$), and 3 ± 2 ($n = 5$) labeled cells, respectively (Figure 2.2C,G). The population of ORNs, labeled via the ON during transection, was severely affected with rapidly decreasing numbers of ORNs during the first 2 days, and virtually none 3 days post-transection (Figure 2. 2A–C).

We analyzed functional changes in the various cell populations of the MOE after ON transection. As stimulations, we applied a solution containing either a purinergic receptor agonist, ATP or 2-MeSATP, to induce responses in non-neuronal cells or a mixture of amino acids to activate amino acid-sensitive ORNs. ATP has been shown to activate cells in both the SC and BC layers, whereas 2-MeSATP activates only cells in the BC layer, thus allowing us to make a distinction between the two cell populations based on the different response profiles (Hassenklöver et al., 2008, 2009). A high K^+ bath solution was used to generally activate all ORNs. All stimulations were applied to every slice preparation. A total of 19 slices that included the lateral portion of the OE, and that exhibited responsive cells were used in statistical analysis. Slices were obtained from non-transected control animals ($n = 3$) and from animals killed 1, 2, 3 and 7 days post-transection ($n = 4, 5, 4$ and 3 , respectively). We found that not only were ATP and 2-MeSATP responsive cells still present in the SC and BC layer of the

MOE after nerve transection, but the number of responsive cells was increased in the BC layer, where the proliferative stem cell population resides (Figure 2.2D,E,H). The average number of cells per slice with stable responses exclusively to ATP, located in the SC layer, showed no significant increase at any of the time-points observed when compared to control (12 ± 13). No significant difference from the control situation was observed 1, 2, 3 or 7 days after ON transection (15 ± 5 ; 14 ± 9 ; 11 ± 9 ; 14 ± 11 ; Figure 2.2H). All slices analyzed showed cells responsive to ATP. Representative example traces of ATP responsive cells are depicted in Figure 2.2D (five cells from one MOE slice per time-point). The average number of cells per slice with stable responses to 2-MeSATP showed a slight increase from 10 ± 6 in the control situation to 34 ± 16 , 38 ± 21 , 58 ± 21 and 41 ± 14 , 1,2,3 and 7 days after transection, respectively (Figure 2.2H). All slices analyzed showed cells responsive to 2-MeSATP, and responsive cells were found to be located in the BC layer of the MOE. Example traces of 2-MeSATP responsive cells can be seen in Figure 2.2E (five cells from one MOE slice per time-point). We found that the average number of high K^+ responsive cells in the MOE decreased progressively from 94 ± 45 in the control situation, to 51 ± 27 1 day after transection, and 28 ± 16 2 days after transection (Figure 2.2H). It began to increase 3 days after nerve transection (34 ± 31), and was progressively higher 1 week after transection (66 ± 20). To further analyze functional changes in the ORN population we applied $100 \mu\text{M}$ amino acid mix, natural water born odorants indicative of the presence of food in the environment, to the MOE. A sub-population of ORNs has been shown to respond to amino acids and has been found to be predominantly located in the lateral portion of the MOE (Gliem et al., 2013). In the normal MOE, 7 ± 2 ORNs were responsive to the amino acid mixture. No significant difference in the number of amino acid responsive cells was found 1 day post-transection (2 ± 3). We found no amino acid responsive cells in the MOE 2, and 3 days post-transection (Figure 2.2F,H), a significant decrease from the control situation ($p = 0.021$ and $p = 0.029$, respectively). Responses were again observable 1 week after nerve transection (3 ± 3), showing no significant difference when compared to the control situation. Example traces of amino acid responsive ORNs can be seen in Figure 2.2F (five cells from one MOE slice per time-point).

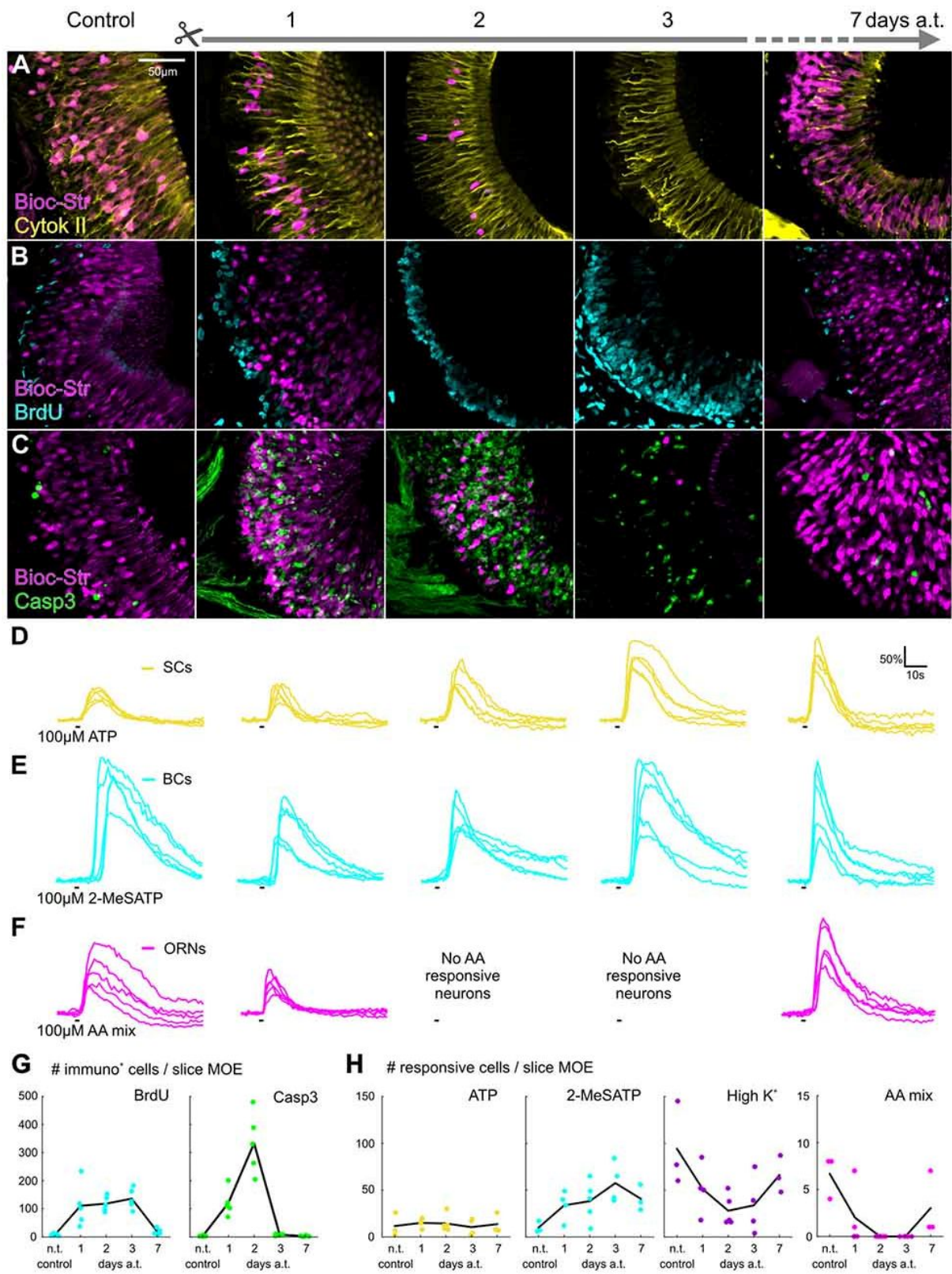


Figure 2.2 Timeline of structural and functional changes in the main olfactory epithelium after olfactory nerve transection. (A–C) Maximum projections of image stacks from representative slices of the MOE before and after ON transection (1, 2, 3 and 7 days). ORNs (Bioc-Str, magenta), Supporting cells (SCs; A, yellow), dividing cells (B, cyan), apoptotic cells (C, green) were labeled and investigated for structural

changes post-transection. (D–F) Representative calcium transients of five individual cells of one acute slice preparation after stimulation with adenosine-50 -triphosphate (ATP) (D, yellow), 2-MeSATP (E, cyan) and an amino acid mixture (F, magenta). Depicted are a non-transected control and specimens 1, 2, 3 and 7 days post-transection. (G) Graphs depicting changes in the number of BrdU positive cells (filled cyan circles), and active caspase-3 positive cells (filled green circles), per slice of the MOE for each time-point analyzed (black lines connect the mean values for each time-point). (H) Graphs depicting changes in the number of responsive cells per acute slice of the MOE for each time-point analyzed (black lines connect the mean values for each time-point): ATP-responsive cells located in the SC layer (yellow filled circles), 2-MeSATP-responsive cells (cyan filled circles) and cells activated by high K⁺ bath solution (purple filled circles) and amino acids (magenta filled circles). AA, amino acid; a.t., after transection; BC, basal cell; Bioc-Str, Biocytin-Streptavidin; BrdU, 5-bromo-20 -deoxyuridine; Casp3, active-Caspase3; Cytok II, Cytokeratin type II; MOE, main olfactory epithelium; n.t., non-transected; ON, olfactory nerve; ORN, olfactory receptor neuron; SC, supporting cell.

Relative changes in olfactory bulb volume – axon degradation and reinnervation by newly formed olfactory sensory neurons

Experiments performed on the olfactory organ (described above) have shown that extensive cell death occurs in the population of ORNs in the first days following ON transection. We compared the relative change in volume between the hemibulb on the transected side with that on the non-transected side for each animal killed at different timepoints after transection. The hemibulbs of non-transected control animals were almost of identical volume ($2 \pm 3\%$, $n = 4$). We found that the hemibulb on the transected side decreased significantly by $13 \pm 6\%$ in relation to the non-transected side within 1 week post-transection ($p = 0.048$, $n = 5$), and was still decreased after 3 weeks with a volume reduction of $15 \pm 1\%$ ($p = 0.048$, $n = 4$, Figure 2.3A, filled circles). Seven weeks after ON transection, the hemibulb on the lesioned side showed a tendency towards recovery and the volume was only $11 \pm 6\%$ ($n = 5$) smaller than the intact control side. We hypothesize that the observed OB volume changes are due to the loss of axonal input and subsequent reinnervation by axons of newly generated ORNs during recovery. Weekly ON transections effectively impedes ORNs from reconnecting to the OB, and allows us to observe how the OB is affected by this lack of input over a longer period. Repeatedly transected animals showed a significant decrease in OB volume of $25 \pm 7\%$ after 3 weeks ($p = 0.015$, $n = 6$) and of $36 \pm 7\%$ 7 weeks after initial ON transection ($p = 0.00027$, $n = 5$). The decrease in OB volume was significantly larger 7 weeks after weekly transection in comparison to recovering

animals ($p = 0.027$, Figure 2.3A, open circles). To observe the cause of these volume reductions after ON transection, we investigated the fate of injured receptor neurons in the OB and their axonal degeneration. The axonal projection of ORNs into the OB in healthy *Xenopus laevis* larvae is depicted in Figure 2.3B highlighting the characteristic organization into lateral, intermediate (including small cluster), and medial glomerular cluster. We found that the onset of axon fragmentation does not begin until after the first day post-transection, as seen in the first left hand panel of Figure 2.3C, where the glomerular clusters are still clearly discernible and the ON is mostly intact ($n = 5$). Two days after transection we found that the axon terminals and clusters start to disassemble and the dye used to label the ORNs accumulated throughout the glomerular layer (open arrowheads, $n = 6$). Three days post-transection most axon fibers were degraded, dye accumulations were more dispersed across the OB, and were eventually found in more caudal layers of the OB, towards the ventricular system ($n = 5$). One week post-transection none of the original axon fibers or cluster organization was identifiable anymore and the dye from former axonal staining was highly dispersed ($n = 7$). Our experiments performed on the olfactory organ have shown that already 1 week post-transection functional, odorant sensitive ORNs reappear in the olfactory epithelium (Figure 2.2). This indicates that also in this time window a reinnervation of the OB could potentially occur. To verify this hypothesis, we stained ORNs to determine when axons of newly formed ORNs reach the OB and begin the process of reinnervation (Figure 2.3D). We found that already 1 week post-transection some newly formed ORN axons reach the OB via the reestablished ON ($n = 6$). However, the axon terminals were restricted to a small area close to the ON and did not show glomerular arborizations. After 2 weeks, the number of labeled axons and the covered area in the OB was increased ($n = 4$). Nevertheless, many axons exhibited long branches without being correctly connected and a proper organization into glomerular clusters was still missing (Figure 2.3D, filled arrowheads). Reinnervation progressed in the following weeks as pioneering axons began to form organized structures resembling normal glomerular clustering around 3 weeks after ON transection ($n = 6$). Although the progress of reinnervation varied between animals, at 7 weeks post-transection most OBs exhibited a glomerular cluster organization similar to the non-transected controls ($n = 5$).

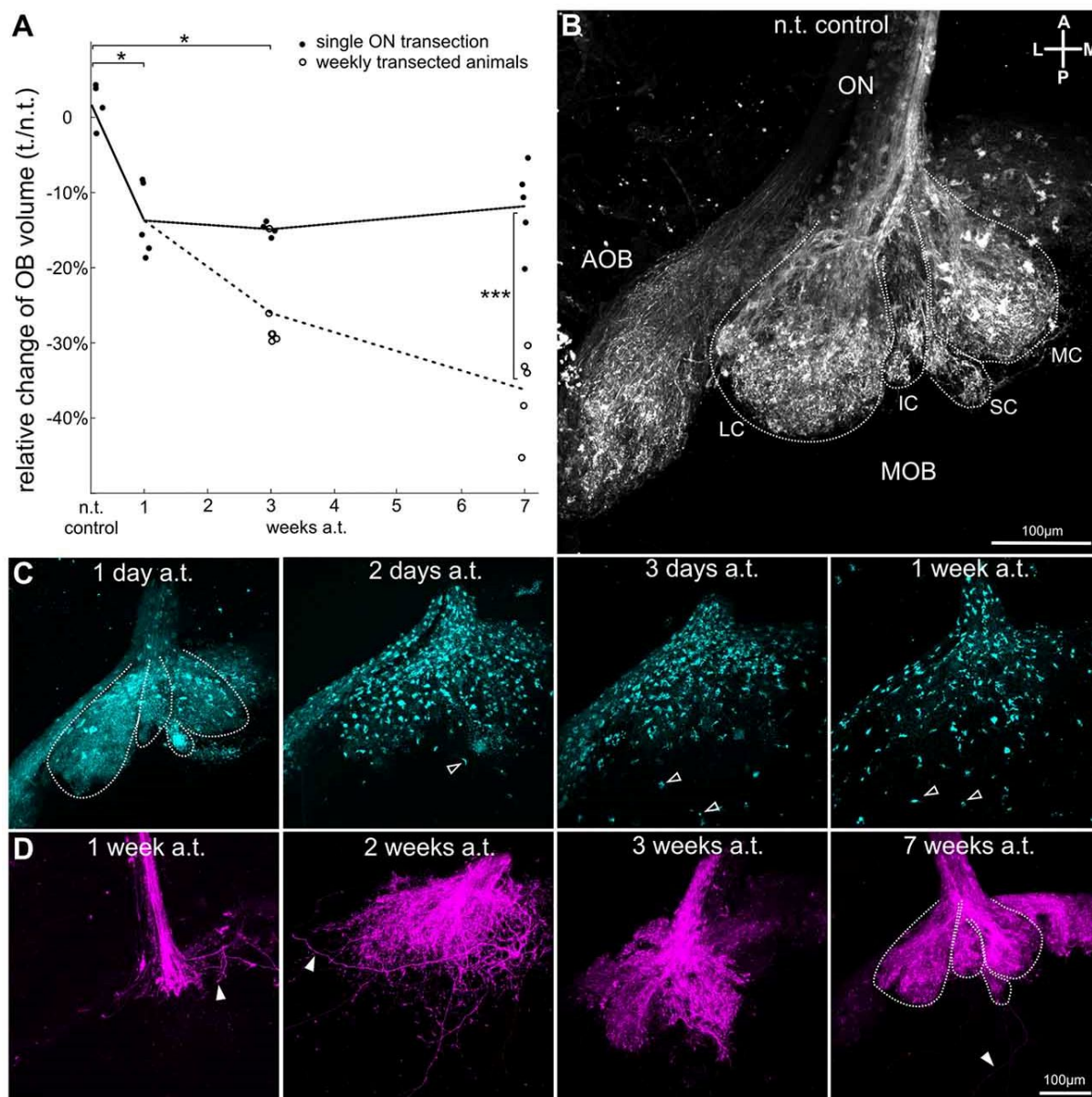


Figure 2.3 Olfactory nerve transection induces transitional olfactory bulb volume reduction due to axonal degradation of olfactory receptor neurons and subsequent reinnervation by new neurons. (A) Graph shows relative changes in OB volume recovering after ON transection (filled black circles, black line connects mean values for each time-point analyzed) and of animals subjected to weekly ON transection to hinder reconnection of ORN axons to the OB (empty circles, dotted line connects mean values for each time-point analyzed). Animals were transected unilaterally, and changes in OB volume are shown as the percentage of decrease in volume of the transected side in relation to the non-transected side. (B) Non-transected OB with ORN axons (white) stained by nasal electroporation of fluorescent dextrans. Typical ventral glomerular clusters are outlined with a dotted white line: lateral (LC), intermediate (IC), small cluster (SC) and medial cluster (MC). The ORN axons of the accessory olfactory bulb (AOB) are also visible on the lateral side of the OB. (C) ON transection induces gradual axonal degradation in the OB. Axons (cyan) were labeled by microRuby via the ON, which is anterogradely transported along the axons. Two days post-transection degeneration of axonal fibers became apparent and fluorescent dye began to accumulate in aggregates that gradually dispersed

through the OB over time (posterior agglomerates highlighted by open arrowheads, glomerular clusters are outlined with a dotted white line). (D) Representative images of the OB showing reconnecting ORN axons (magenta) stained by nasal electroporation at different time-points after ON transection (1, 2, 3 and 7 weeks). Examples of individual axons are highlighted by filled arrowheads and glomerular clusters are outlined with a dotted white line. A, anterior; AOB, accessory olfactory bulb; a.t., after transection; IC, intermediate cluster; L, lateral; LC, lateral cluster; M, medial; MC, medial cluster; MOB, main olfactory bulb; n.t., non-transected; OB, olfactory bulb; ON, olfactory nerve; ORN, olfactory receptor neuron; P, posterior; SC, small cluster. Statistical significance was tested using Kruskal-Wallis test followed by Dunn's multiple comparison post hoc test with Holm-Bonferroni correction (*p < 0.05, ***p < 0.001).

Increased cell death in the olfactory bulb following olfactory nerve transection

Being that ON transection had a clear impact on the OB volume, we investigated if postsynaptic neurons of the OB network were also affected as a next step. To assess potential cell loss in the OB we performed active caspase-3 immunostainings on slices of the OB. We found that caspase-3 mediated cell death also occurred in cells located in the OB rapidly after ON transection (Figure 2.4). Apoptotic cells were located predominantly in the ON layer and in the glomerular layer of the OB (Figure 2.4C). The number of apoptotic cells counted in each slice of the OB increased significantly from 5 ± 5 in the control situation (n = 25), to 51 ± 37 just 1 day after ON transection (p = 0.00034, n = 8) and to 58 ± 22 3 days post-transection (p = 0.000016, n = 9; Figure 2.4A). After 1 and 3 weeks there is no significant difference when compared to the control situation with 10 ± 7 (n = 5), and 3 ± 1 (n = 7) labeled apoptotic cells, respectively (Figure 2.4A,B,D).

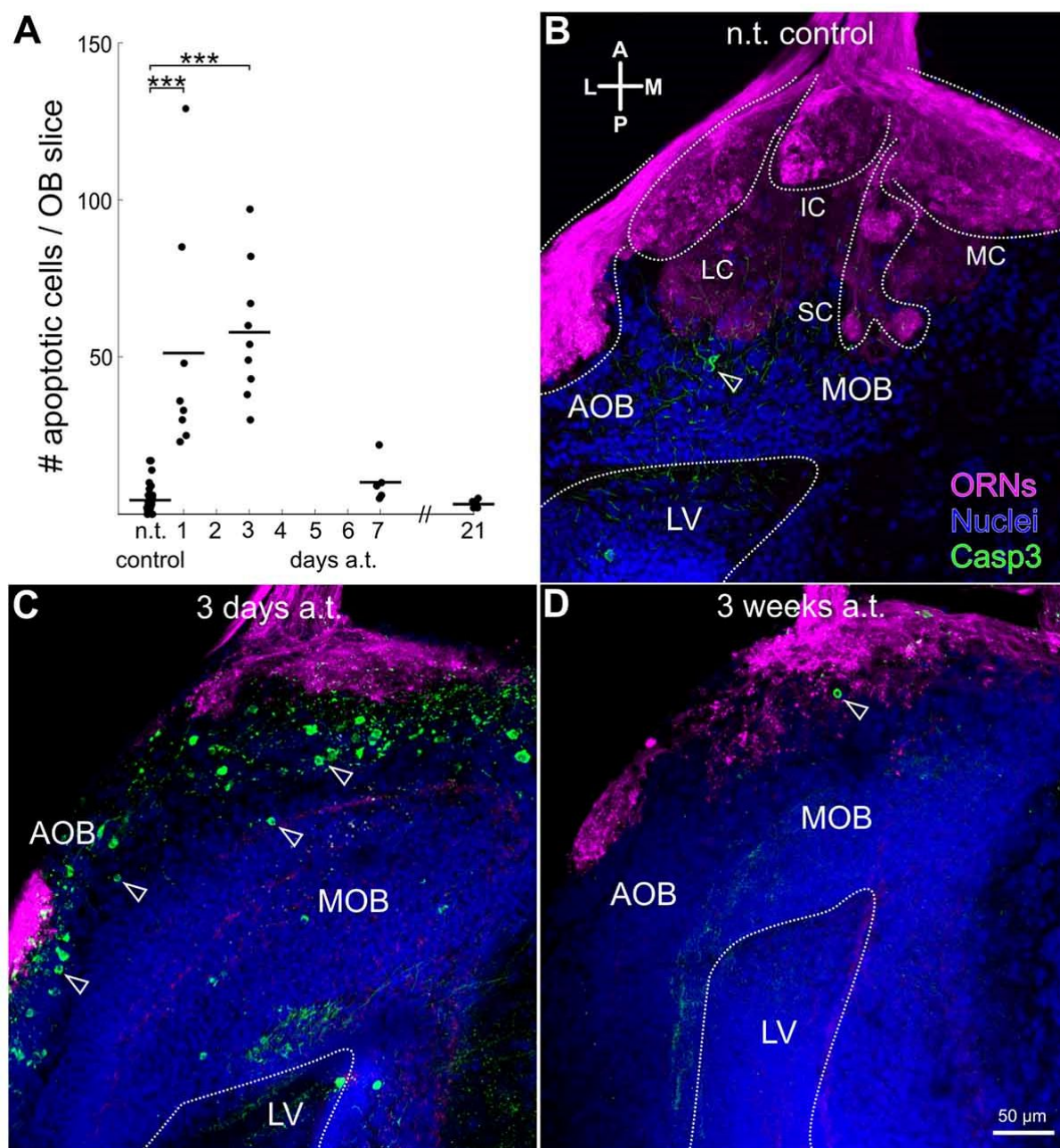


Figure 2.4 Increased levels of apoptotic cells in anterior layers of the olfactory bulb after olfactory nerve transection. (A) Graph depicts changes in the number of apoptotic cells in slices of the OB at different time-points over the course of 3 weeks after ON transection. Maximum projection images of representative slices of the OB of a non-transected control animal (B), an animal killed 3 days post-transection (C) and 3 weeks post-transection (D), with biocytin-streptavidin stained ORNs (magenta), active caspase-3 staining of apoptotic cells (green), and propidium-iodide staining of all cell nuclei (blue). Distinct glomerular clusters and lateral ventricle are outlined with dotted white lines. Open arrow heads highlight cell bodies undergoing apoptosis. A, anterior; AOB, accessory olfactory bulb; a.t., after transection; Casp3, active-Caspase3; IC, intermediate cluster; L, lateral; LC, lateral cluster; LV, lateral ventricle; M, medial; MC, medial cluster; MOB, main olfactory bulb; n.t., non-transected; OB, olfactory bulb; ON, olfactory nerve; ORN, olfactory receptor neuron; P, posterior; SC, small cluster. Statistical

significance was tested using Kruskal-Wallis test followed by Dunn's multiple comparison post hoc test with Holm-Bonferroni correction (**p < 0.001).

Dynamic changes of dendritic tuft complexity in mitral/tufted cells following olfactory nerve transection

As cell death has mostly been observed in the glomerular layer, it imposes the question whether the MTCs located in the deeper OB layers also suffer from consequences related to denervation. In Figure 2.5A different, individual MTCs from ON-transected animals at different time intervals after lesion are presented in comparison to a non-transected control. In *Xenopus*, MTC dendrites have been found to bifurcate and innervate multiple glomeruli (see also (Nezlin and Schild, 2000)). These dendrites end in fine arborizations full of dendritic varicosities, called dendritic tufts (highlighted by squares in Figure 2.5A). Dendritic tufts of MTCs that form the postsynaptic component of a glomerular module were clearly smaller and less complex 1 week post-transection. Complexity of dendritic tufts was quantified using Sholl analysis as depicted in Figure 2.5B. For the representative MTC tufts shown, the number of intersections in general is clearly reduced after 1, and 3 weeks following ON transection (Figure 2.5B). Very complex tufts exhibited a maximum number of intersections well above 20, while minimally complex tufts featured a maximum below 10 intersections (Figures 2.5B–D). In control OBs, a mean maximum number of 12.2 ± 7.0 intersections was measured ($n = 24$ tufts from 12 animals), which was not significantly different from 14.0 ± 7.2 intersections 1 day after transection ($n = 18$ tufts from 13 animals, Figure 2.5D). After the loss of presynaptic input, these structures show a gradual decrease in complexity and tufts were significantly less complex 1 week after transection), with an average maximum of 6.6 ± 3.5 intersections per tuft ($p = 0.039$, $n = 12$ tufts from 9 animals, Figure 2.5C,D). Three weeks after transection and 7 weeks after transection the mean maximum number of intersections was 7.2 ± 1.4 ($n = 9$ tufts from 7 animals) and 12.5 ± 7.7 ($n = 16$ tufts from 8 animals), respectively, no longer significantly different from control. This suggests a tendency for the tufts to become more complex after ORNs have begun to reconnect to the OB (see above). The lowered MTC tuft complexity after 1 week is also visible in the mean linear Sholl plots of the region around the maximum number of intersections (Figure 2.5C). These results indicate that MTC tufts show a highly plastic response to the loss

of their presynaptic partner. Dendritic tuft complexity reached its minimum value right before reconnection of ORN axons to the bulb started and returned to normal morphology after 7 weeks, when glomerular clusters recovered their structure and again resembled the control situation.

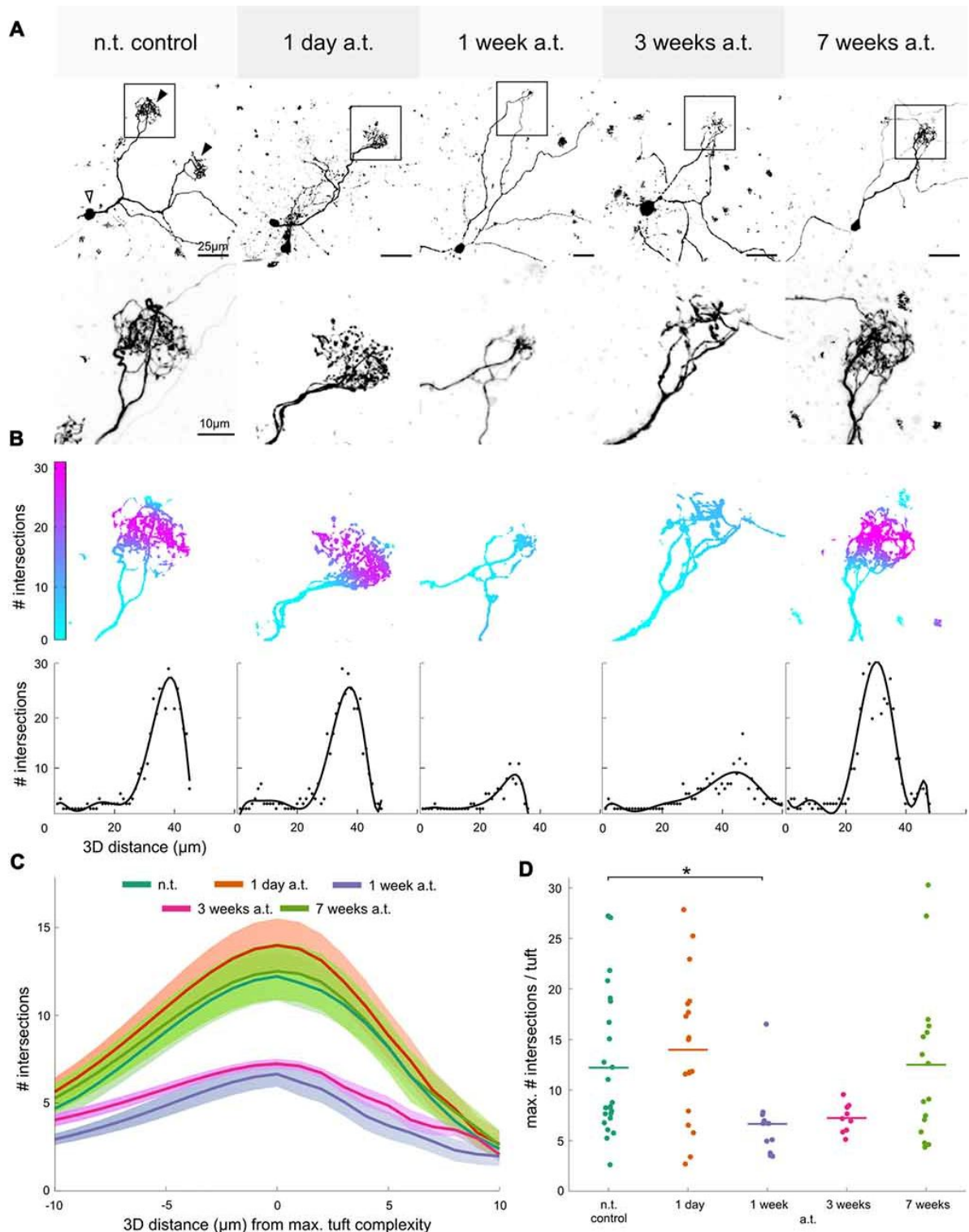


Figure 2.5 *Dynamic changes of mitral/tufted cell dendritic tuft complexity in the olfactory bulb after olfactory nerve transection.* (A) Top row shows individual MTCs stained via sparse cell electroporation. Maximum intensity projections of image stacks of representative MTCs are shown for each time-point after ON transection. Animals were transected unilaterally and MTCs were stained and analyzed on both the non-transected side of the OB, used as control, and on the transected side, 1, 3 and 7 weeks a.t. Bottom row shows a magnification of the tufted regions (boxed outline). (B) Top row illustrates quantification of complexity of the tufts shown in (A) using Sholl analysis. The number of intersections on the three-dimensional tuft is represented as a color gradient on the tuft morphology—blue areas indicate very few intersections and magenta indicates many intersections. Bottom row shows linear Sholl plots for each of the presented tufts with number of intersections indicated as dots and best fit polynomial function as line. (C) The average linear tuft-complexity curves (of all curves as shown in B) for tufts of each respective group are shown. A distance of $\pm 10 \mu\text{m}$ around the maximum is shown. The shaded areas around the curves indicate the SEM within each group. (D) Scatter plot showing the maximum number of intersections for each tuft analyzed in the control group and at each respective time point a.t. Lines show the mean of all analyzed tufts for each time-point. a.t., after transection; MTC, mitral/tufted cell; n.t., non-transected; OB, olfactory bulb; ON, olfactory nerve. Statistical significance was tested using Kruskal-Wallis test followed by Dunn’s multiple comparison post hoc test with Holm-Bonferroni correction (* $p < 0.05$).

Recovery of odorant-induced responses in the glomerular layer and mitral/tufted cells of the olfactory bulb

We performed multi-photon calcium imaging of MTCs to investigate the extent of functional recovery of the olfactory network after ON transection. Calcium responses of the lateral MTC population’s tufts and somata were recorded after application of amino acids to the olfactory epithelium. In animals measured 3 days after transection no odor induced activity could be detected on the postsynaptic level, neither in MTC glomerular tufts nor in MTC somata (Figure 2.6A,D,G; $n = 3$). Only very rarely, somatic calcium signal increases occurred time-correlated with odor stimulus application (Figure 2.6A, arrowheads). Given the high spontaneous activity we observed among the MTCs at this time point as well as the lack of any glomerular responses, it can be assumed that those calcium events were coincidentally time-correlated to the stimulus (Figure 2.6G). In animals measured 3 weeks after transection, glomerular as well as somatic responses to amino acid stimulation were present (Figure 2.6B,E; $n = 3$). Even though the extent of reactive glomerular neuropil and MTC somata varied among the three animals recorded for this time point, odorant induced signals could be detected in each preparation in both the glomerular and MTC layer (Figure 2.6H). In animals

that were measured after 7 weeks post-transection, large portions of the lateral MTC population and the lateral glomerular array were activated by the amino acid stimuli (Figure 2.6C,F; n = 5). Characteristic odorant induced calcium transients were much more distinctly observable in both layers of the OB (Figure 2.6I) and the glomeruli showed individual response profiles to five different, individual amino acids applied (data not shown). In summary, ON transection led to disruption of amino acid induced MTC activity, but the functional OB circuitry was gradually restored over the time course of 7 weeks.

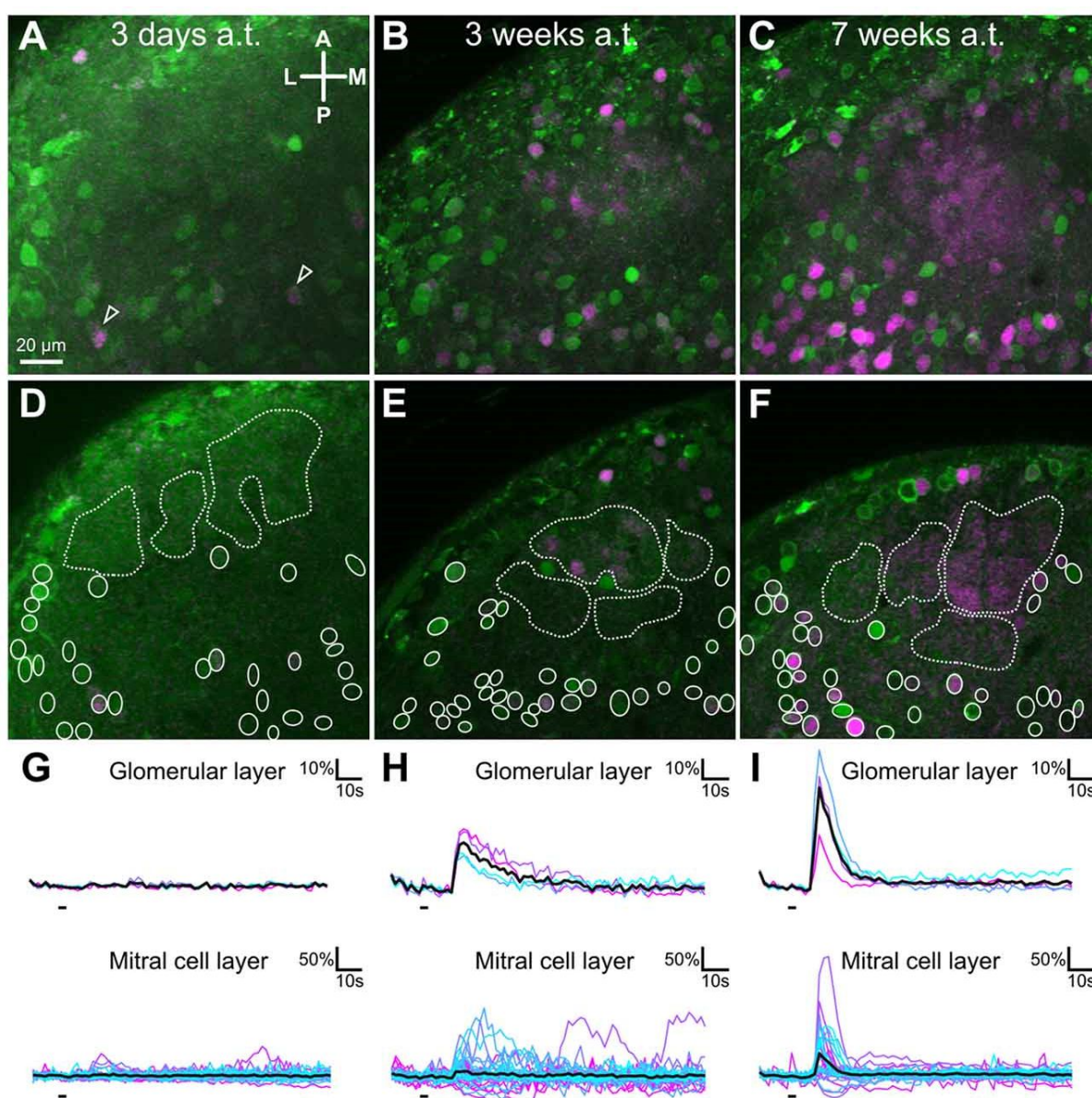


Figure 2.6 Functional changes in mitral/tufted cell and glomerular layer of the lateral glomerular cluster of the olfactory bulb after olfactory nerve transection. Maximum projections of representative examples

of imaged volumes in the ventro-lateral OB of different whole olfactory system explants measured 3 days (A), 3 weeks (B) or 7 weeks (C) post-transection. MTC somata and their tufts were labeled by calcium indicator injection (green) and responses to odorant stimulation of the olfactory organ were recorded. Regions that showed a time-correlated response to stimulation of the MOE with an amino acid mixture are shown in magenta (Difference image of peak response minus pre-stimulus activity). Single planes of the imaged volumes measured 3 days (D), 3 weeks (E) or 7 weeks (F) after ON transection. Dashed white lines surround regions of interest in the glomerular layer, while white ellipses indicate MTC somata. (G–I) Calcium transients of neuropil and individual cells (different shades of blue and magenta, shown as $\Delta F/F$ values) are derived from the regions of interests highlighted in the respective images above. The mean response of all regions of interest in the glomerular neuropil and mitral cell layer are depicted as black traces. Some cells with occasional, spontaneous, time-correlated activity were visible (also highlighted with open arrowheads). A, anterior; a.t., after transection; L, lateral; M, medial; MOE, main olfactory epithelium; MTC, mitral/tufted cell; OB, olfactory bulb; ON, olfactory nerve; P, posterior.

Discussion

Post-developmental neurogenesis is restricted to only a small number of areas in the nervous system. The telencephalic subventricular zone and the peripheral olfactory epithelium are two areas of special interest, as they provide new functional elements to both sides of the fundamental olfactory circuit. On the peripheral side, multipotent stem cells of the BC layer of the olfactory epithelium replenish its different cellular components (Graziadei and Graziadei, 1979; Huard et al., 1998; Leung et al., 2007). ORNs regularly die and have to be replaced with new sensory neurons that reintegrate into a functioning circuit in the brain (Farbman, 1990; Roskams et al., 1996; Schwob, 2002). Beyond that, neurogenesis in the olfactory epithelium can also occur on a larger scale following injury (Schwob, 2002). Severing the ONs of larval *Xenopus laevis* allowed us to successfully eliminate olfactory input to the OB and consequently cause the loss of olfactory function. We show the progression of events that occur after lesion and how the individual components of the olfactory network are transiently recovering, both structurally and functionally.

Timeline for regeneration in the olfactory system of larval *Xenopus laevis* after olfactory nerve transection

Degeneration in the olfactory epithelium is immediately apparent within the first 3 days following ON transection. We observed a pronounced increase in apoptotic cells

throughout the olfactory epithelium, leading to neuronal loss. In particular, a decrease in the overall number of ORNs activated by high K⁺ bath solution and a complete loss of amino acid-responsive ORNs was detected. The overall number of excitable ORNs decreased considerably after transection, but these cells were at no time completely eradicated from the epithelium. This is most likely due to a remaining population of immature ORNs, which have not yet established an axonal connection to the OB and thus are unaffected by ON transection (Schwob, 2002). The morphology of the SC layer was unaltered by ON transection, and the number of cells responsive to purinergic receptor agonists in the SC and BC layers did not decrease at any moment surveyed, indicating that the induced cell death in the olfactory epithelium is restricted mainly to the neuronal population. It has been shown that purinergic signaling pathways influence cell turnover in the healthy MOE (Hassenklöver et al., 2009; Jia et al., 2009), and could potentially play an important role in regulating neuroproliferation during the process of regeneration after lesion (Jia and Hegg, 2010; Jia et al., 2013). After ON transection we found an increase in the number of cells responsive to the application of 2-MeSATP, shown to activate exclusively cells in the BC layer, where the population of stem and progenitor cells of the olfactory epithelium reside (Schwob, 2002; Hassenklöver et al., 2009). This change presumably reflects upregulated proliferative activity in response to lesion and in succession increasing numbers of 2-MeSATP-sensitive progenitor cells. In fact, following injury the stem cell population responds almost immediately to increased neuronal death with a significant increase of BrdU-positive, proliferating cells. Truncated axon terminals of ORNs were subsequently found to be degenerating and no odor-induced activity could be detected on the postsynaptic level in the OB indicating immediate loss of olfactory function following lesion. In the OB, we also saw a significant increase in caspase-mediated cell death in the first 3 days immediately following ON transection. Apoptotic cell somata were restricted mainly to the ON layer and the glomerular layer of the OB, suggesting dying periglomerular cells (Nezlin and Schild, 2000). This is also supported by our recording of spontaneously active neurons in the MTC layer of the OB and our successful labeling of individual MTCs. Thus, we conclude that MTC are not the main cell population of the OB affected by cell death. During the process of regeneration stem cell proliferation in the MOE initiates a compensatory increase in immature neurons expressing NCAM-180 (Cervino et al., 2017). Eventually, this leads to an elevation of functional ORNs over the course of 1 week after ON transection (this

study). This is similar to newborn ORNs in the rodent MOE that are mature after 7–8 days expressing olfactory marker protein (Miragall and Graziadei, 1982). In *Xenopus*, recovery of OMP-expression in newly generated ORNs takes longer than 7 days and remains reduced even 4 weeks post-transection (Cervino et al., 2017). Already after 1 week, other surveyed parameters in the *Xenopus* MOE, e.g., functional odorant responses, return to control levels. This period is comparable to the recovery time of the *Xenopus* MOE after chemical lesion that leads to widespread cell death in multiple cell populations, including SCs and ORNs (Frontera et al., 2016). The network of the OB is still functionally disrupted 1 week post-transection, however, initial signs of a recovering OB are observable as first pioneering ORN axons project into the OB. Axonal reinnervation occurs progressively over the next weeks and already 3 weeks after transection the glomerular cluster organization is coarsely restored. At this point the first odor-evoked responses reappear in the glomerular neuropil of the lateral cluster of the OB. Thus, the functional integration of newborn ORNs into the OB circuitry takes much longer than the structural recovery of the olfactory epithelium. Seven weeks after transection, ORN axons in the OB have reformed glomerular clusters structurally similar to those found in healthy non-transected animals and amino acid-induced responses in the neuropil of the lateral glomerular cluster are comparable to healthy control animals. Nevertheless, it cannot be excluded that some amount of miswiring occurs during recovery after injury. In our study, the structural and functional recovery of the olfactory system of *Xenopus laevis* larvae after ON transection took 7 weeks. A recovery of specific foraging behavior in response to food-odor occurs 3 weeks after ON transection (Cervino et al., 2017). Notably, newly formed ORN synapses in larval *Xenopus* show a high vesicle density in their active zones and can be active before the glomerular units of the OB are fully restored (Terni et al., 2017). In experiments performed on rodents, the average time of recovery is approximately 2.5 months for both ON transection and chemical lesion, notwithstanding differences in the extent of recovery (Kobayashi and Costanzo, 2009; Blanco-Hernández et al., 2012; Cheung et al., 2014; Murai et al., 2016).

Olfactory map recovery and injury-induced dendritic reshaping of second-order neurons

A variety of factors influence the efficacy of olfactory system restoration after injury, and in many cases, the recovery of olfactory network functionality is only partial. When

the ONs and OBs are injured, newly regenerated ORN axons must find their way back to their appropriate OB location and overcome challenging obstacles, like scar tissue formation and gliosis, in order to preserve the spatial mapping of odorants (Kobayashi and Costanzo, 2009). Different from developmental OB network formation, targeting of ORN axons to glomeruli is erroneous in many cases after successful recovery of the olfactory system (Blanco-Hernández et al., 2012; Cheung et al., 2014; Murai et al., 2016). Axonal pathfinding during developmental olfactory map formation is governed by olfactory receptor gene identity, ORN cell type, molecular guidance cues, and activity-dependent mechanisms (for review see (Nishizumi and Sakano, 2015)). At least to some extent these mechanisms are also active in the adult organism (Blanco-Hernández et al., 2012; Cheung et al., 2014). It has been suggested that regenerating ORNs depend more on axon-axon interactions in the adult (Imai and Sakano, 2011), making recovery of the olfactory map after ON transection difficult. Consistent with this idea, chemical lesions to the olfactory epithelium, in which ORNs are not entirely eliminated, do not lead to map distortions that are as severe (Blanco-Hernández et al., 2012). The postsynaptic side of the OB also plays an important role in the formation and recovery of the olfactory map. Dendrites are dynamic structures whose main function consists of integrating synaptic input, a process on which they depend in order to maintain structural integrity (Tavosanis, 2012). This is attributed largely to the delivery of neurotrophins from the pre-synapse that enhance dendritic growth and branching as well as synaptogenesis (Imamura and Greer, 2009). In the OB, the axons of receptor neurons form glutamatergic synapses with dendrites of MTCs and periglomerular cells (Nagayama et al., 2014). In mammals, mitral cell dendrites are reshaping during an early postnatal phase (Meisami and Safari, 1981; Malun and Brunjes, 1996), but remain stable in the adult olfactory system (for review see (Mizrahi and Katz, 2003)). Elimination of ORN axons during early developmental stages, before formation of mature dendritic tufts, leads to atrophy of mitral cell dendrites (Couper Leo and Brunjes, 2003). In the adult mouse, ON transection initiates dendritic retraction of mature mitral cells and re-establishment of connectivity is reduced even after ORN projection recovery (Murai et al., 2016). In non-mammalian vertebrates, like zebrafish, extensive loss of dendritic branches occurs after ablation of the MOE, transection or chemical damage to ORNs (Byrd, 2000). In our study, we found that the dendritic tufts of MTCs in the OB substantially lose complexity and dendritic varicosities within 1 week after ON transection. The lack of input from the ORN axons

appears to have a degenerative effect on the fine branches of the MTCs, which retract and gradually lose their primary synaptic contact site. However, our results show that in the amphibian olfactory system, MTCs retain the capacity to recover their complexity upon reinnervation, and the olfactory system is eventually functionally restored. Structural integrity of MTC dendrite tufts and the OB in general seems to be dependent on afferent innervation. In *Xenopus*, it has previously been shown that, after removal of the telencephalon, reconnection of the ON is essential for recovery of the OB to occur (Yoshino and Tochinai, 2006). The effect of afferent fibers on their target regions seems crucial to prevent continuous degradation of the OB structure. This has also been demonstrated to be true during development, as a quantitative correlation has been found between the number of ORNs reaching the OB and the number of MTCs in the developing OB of *Xenopus laevis* (Byrd and Burd, 1991, 1993). We showed that when ORNs are not allowed to reconnect to the OB, due to continuous weekly transections of the ON, a progressive decrease in OB volume with no apparent recovery was observed. This decrease in volume was significantly larger from experiments with only a single nerve transection. A reduction in OB volume is also caused by sensory deprivation in other animal models and permanent denervation can reduce OB volume by up to -50% when compared to control (rabbit: (Matthews and Powell, 1962); frog: (Graziadei and DeHan, 1973); rat: (Meisami and Safari, 1981); zebrafish: (Byrd, 2000)). This is an indication that extensive damage and cell loss is occurring in the OB in consequence of longer periods without afferent innervation. It seems that MTCs have evolved the ability to survive the loss of their presynaptic partner, at least temporarily and to a certain extent. This is especially relevant in the *Xenopus* olfactory system that undergoes extensive changes during the process of metamorphosis, which occurs shortly after recovery is complete in our experiments. Animals were chosen for this study according to their stage of larval development in order to ensure that the changes that occur in the olfactory system of larval *Xenopus laevis* during metamorphosis would not overlap with our time window of investigation (Dittrich et al., 2016). During metamorphic reorganization of the olfactory organ, whole ORN populations perish, shift locations and a substantial functional rewiring of the system takes place (Dittrich et al., 2016; Syed et al., 2017). Thus during the process of normal development, MTCs of *Xenopus* need to be capable of surviving an extended period with diminished axonal input. This might also be advantageous during recovery after injury. Maintaining the ability to survive without peripheral input is helpful

in a system where continual neurogenesis occurs, but it is still unclear what factors limit the survival of MTCs. It is known that a population of stem cells exists in the subventricular zone that is responsible for the lifelong turnover of interneurons (Kaplan and Hinds, 1977), but post-developmental generation of MTCs and recapitulation of complex wiring to higher brain centers seems impossible. Previous studies have shown that during the process of regeneration after lesion in larval *Xenopus*, there is an increase in BCs expressing BDNF, as well as an increase in the ON and OB (Frontera et al., 2015). In the developing mammalian olfactory system, there is evidence that MTCs express the TrkB neurotrophin receptor, and that BDNF affects dendritic morphology and stimulates branching (Imamura and Greer, 2009). We could speculate that the permissive environment that allows circuit restoration is related in part to the presence of neurotrophic factors. It could be that larval *Xenopus* exhibit elevated neurotrophic support to sustain the viability of MTCs during neuroregeneration and olfactory network reorganization that the adult mammalian system is lacking.

Conclusion

The larval *Xenopus* olfactory system shows a high degree of resilience to injury and a robust capacity for olfactory network recovery. Over the course of approximately 2 months, the structure and function of the OB degenerates (cell death is increased, axons degrade, glomerular clusters disappear and dendritic tuft complexity of second order neurons is reduced), and subsequently recovers (reinnervation with new ORNs occurs, cluster organization is restored, second order neurons regain complexity and glomerular responses return). Our study forms the basis for further investigations on factors that can influence successful olfactory system recovery after injury. It is not yet known what specific changes occur in the MTC population after the loss of their presynaptic partner. Of special interest could also be to assess the precision of the restored olfactory map and to investigate mechanisms beneficial for recovery of olfactory perception.

Chapter 3:

Restoration of distinct odor processing streams in the olfactory bulb underlies the recovery of odor-guided behavior after injury in larval *Xenopus laevis*

Manuscript in preparation

Authors and affiliations:

Sara J. Hawkins¹, Yvonne Gaertner², Thomas Offner¹, Lukas Weiss¹, Guido Maiello³, Thomas Hassenklöver^{1*} and Ivan Manzini^{1*}

¹ Institute of Animal Physiology, Department of Animal Physiology and Molecular Biomedicine, Justus-Liebig-University Giessen, 35392 Giessen, Germany

² Department of Neurology, Focus Program Translational Neuroscience (FTN) and Immunotherapy (FZI), Rhine Main Neuroscience Network (rmn2), University Medical Center of the Johannes Gutenberg University Mainz, 55131 Mainz, Germany

³ Department of Experimental Psychology, Justus-Liebig-University Giessen, 35394 Giessen, Germany

Keywords:

olfactory receptor neurons, neuronal stem cells, olfactory nerve transection, degeneration, regeneration, glomerular clusters, transduction mechanisms

Author contributions:

The experiments were conceived and designed by TH, IM and SJH. The experiments were performed by SJH and YG. SJH, LW, TO and GM analyzed the data. SJH, GM, TH and IM wrote the article. All authors participated in the discussion of the data and in the production of the manuscript.

Abstract

Across species, the olfactory system exhibits the uncommon feature of lifelong neuronal turnover. Stem cells located in the olfactory epithelium in the nose give rise to new olfactory receptor neurons (ORNs). These newly formed neurons can adequately replace dying ORNs during both developmental and adult phases, and in many cases after severe lesion. Olfactory receptor neurons replenished from the stem cell population must form synapses with target neurons in the olfactory bulb (OB) in order to relay chemosensory information about their surroundings. In *Xenopus laevis* larvae, previous work has shown that this rewiring process occurs between three and seven weeks after olfactory nerve transection. It remains unknown whether post-lesion rewiring follows the same structure as that of the previously intact system. It is also unknown what level of rewiring is required to restore odor-guided behavior. Here we investigate the effects of olfactory nerve transection and describe the process of ORN rewiring in the glomerular layer of the OB of larval *Xenopus laevis*. We analyze odorant representations in the OB and the consequential transmission of synaptic information that leads to behavioral changes. We observe that post-lesion rewiring matches the wiring structure of the intact system. After three and seven weeks of recovery from olfactory nerve transection, we show that ORNs reform two functionally and spatially distinct glomerular clusters in the OB, akin to those found in non-transected *Xenopus* larvae. However, only at seven weeks after transection do we find all the same odorant response tuning profiles observed in the OB of non-transected larvae, demonstrating that the OB recovers neural function at this time. Next, we develop a reliable experimental protocol for assessing odor-guided behavior in larval *Xenopus*, and show that odor stimuli influence swimming velocity and environment exploration. Such behavioral responses are absent after olfactory nerve transection but recover in seven to nine weeks. Taken together, our findings demonstrate that the restoration of accurate OB representations leads to the recovery of odor-guided behavior.

Introduction

Across vertebrate species, neurogenesis occurs well beyond embryonic stages, but only in certain areas of the nervous system (Altman and Das, 1965; Altman, 1969; Kaplan and Hinds, 1977; Graziadei and Graziadei, 1979; Kaslin et al., 2008; Kempermann and Gage, 2008). The olfactory system is one such region that shows neurogenesis throughout life (Brann and Firestein, 2014), making it a sensory system of great neurophysiological and evolutionary interest (Hoover, 2010).

Olfaction is a form of chemosensation in which molecules in the environment directly interact with olfactory receptor proteins expressed by olfactory receptor neurons (ORNs; (Buck and Axel, 1991; Breer, 2003; Gaillard et al., 2004; Spehr and Munger, 2009; Manzini et al., 2022). The cell body of ORNs is located in the olfactory epithelium (OE) which resides inside the nasal cavity. Olfactory receptor neurons extend their axons via the olfactory nerve (ON) into the olfactory bulb (OB) in the brain. When ORNs are activated by the binding of odorants to their odorant receptors, synaptic activity ensues (Buck, 1996; Manzini et al., 2022). Their axons synapse with second order neurons, i.e. mitral/tufted cells (MTCs) and interneurons in neuropil clusters called glomeruli within the OB (Ressler et al., 1994; Vassar et al., 1994; Mombaerts et al., 1996). Upon activation by ORN synaptic activity, and after various intrabulbar processing steps, MTCs subsequently relay information to higher olfactory centers (Manzini et al., 2022). This sequence of cell activation and processing of olfactory information ultimately gives meaning to the surrounding environment and influences behavioral outcomes. Such olfactory guided behavior is essential for survival and reproduction, specifically in tasks such as finding mates, shelter, and food sources, as well as in avoiding predators (Ache and Young, 2005; Manzini et al., 2022).

The peripheral location of ORNs permits odorant detection, but leaves these neurons vulnerable to potential noxious substances in the surrounding environment. It is assumed that for this reason, these neurons have a limited lifespan (Cowan and Roskams, 2002; Leung et al., 2007), and eventually undergo caspase-mediated cell death (Cowan and Roskams, 2002). To counteract this loss, a pool of stem cells residing in the basal layer of the OE provide new neurons to replenish those lost (Graziadei and Metcalf, 1971; Graziadei, 1973; Schwob et al., 2017). After stem cell proliferation and differentiation, newly formed ORNs must integrate into the central

nervous system in order to maintain olfactory function. This process of cell death and stem cell proliferation occurs both during the process of natural cell turnover (Graziadei and Metcalf, 1971; Graziadei, 1973; Brann and Firestein, 2014), as well as in some cases after severe lesion (Schwob, 2002; Brann and Firestein, 2014; Schwob et al., 2017). Substantial recovery from lesion to the olfactory circuit has been shown to occur in multiple vertebrate animal models (e.g. mouse, Schwob et al., 1999; Schwob, 2002; St John and Key, 2003; McMillan Carr et al., 2004; Blanco-Hernández et al., 2012; Cheung et al., 2014; zebrafish, Godoy et al., 2020; Calvo-Ochoa et al., 2021). *Xenopus laevis* larvae in particular have been found to withstand a variety of lesions to the olfactory system and recover, at least to a certain degree (Kobayashi and Costanzo, 2009; Frontera et al., 2016; Hawkins et al., 2017). As the organization of the *Xenopus* olfactory system is similar to that of other vertebrates (Manzini et al., 2022), *Xenopus* larvae are thus a promising animal model in which to investigate the general principles of neural recovery after lesion.

As in most other vertebrates, the *Xenopus* olfactory system includes a variety of ORNs that differ in morphology, olfactory receptor protein expression, and transduction mechanisms employed. These varied ORNs all project their axons along the ON and synapse with MTCs and interneurons in glomeruli in the OB (Nezlin and Schild, 2000; Gliem et al., 2013; Manzini et al., 2022). In our previous study, (Hawkins et al., 2017) we found that ON transection in larval *Xenopus laevis* leads to the immediate death of ORNs and an increased proliferation of stem cells in the OE. Within one week after transection, new ORNs repopulate the OE and begin exhibiting functional responses to natural odorants. These newly active ORNs begin to reconnect to the MTCs in the OB, where odorant-induced responses can then be observed in three to seven weeks after transection. While this suggests that by this point the system has recovered, it is yet unknown whether this rewiring is structurally and functionally equivalent to an unlesioned system.

To investigate whether the process of rewiring produces the same structure as that of the previously intact system, we tested whether the same spatially segregated odor processing streams found in unlesioned animals (Gliem et al., 2013) are also present in transected animals after recovery. In *Xenopus laevis*, multiple characteristic glomerular clusters have been described based on the ORNs they are innervated by (Manzini et al., 2007; Gliem et al., 2013). One prominent *laterally* located glomerular

cluster found in the main OB is innervated by ORNs that employ a phospholipase C (PLC) and diacylglycerol (DAG) -dependent transduction cascade to transmit information to MTCs (Gliem et al., 2013; Sansone et al., 2014). These receptor neurons very likely have a microvillous morphology and express vomeronasal receptors that mainly respond to amino acid odorants (Manzini et al., 2002; Gliem et al., 2013). One prominent *medially* located glomerular cluster is instead innervated by ORNs presumably of ciliated morphology that employ a cAMP-dependent transduction cascade and respond to alcohols, aldehydes and ketones (Nakamuta et al., 2011; Gliem et al., 2013). These two clusters, one lateral and one medial, are thus well defined and clearly spatially segregated in unlesioned *Xenopus* larvae. We therefore tested whether this spatially segregated wiring structure recovers after ON transection. To do so, in a series of imaging experiments we first identified lateral and medial glomerular clusters in unlesioned animals. We identified the laterally located glomerular cluster through its activity in response to amino acids, which activate ORNs that employ PLC-DAG-dependent transduction mechanisms. We identified the medially located glomerular cluster through its activity in response to the adenylate cyclase agonist Forskolin, which instead activates ORNs that employ a cAMP-dependent transduction mechanism. Then, we tested whether it is possible to identify the same clusters, in the same spatial locations, in animals at three and seven weeks of recovery from bilateral ON transection. Having assessed that the olfactory system recovers its wiring structure after bilateral ON transection, we next analysed odorant tuning profiles in responsive regions in the OB. The olfactory system must be able to identify not just individual odorants, but also interpret combinations of multiple odorants. To test whether the olfactory system recovers its function after lesion, we thus attempted to identify, in both unlesioned and recovered animals, OB regions tuned to multiple different odorants. In the same set of imaging experiments used to assess the system structure, we stimulated the OE with a series of multiple odorants, and measured the odorant response tuning profiles occurring throughout the OB. If the *Xenopus* olfactory system recovers neural function after bilateral ON transection, we expected to identify the same set of odorant response tuning profiles across OB regions in both unlesioned and recovered *Xenopus* larvae.

Whether the process of rewiring after a traumatic lesion leads to a full recovery of function cannot, however, only be assessed by measuring brain activity. To claim that

rewiring leads to restored function, we must assess whether rewiring restores odor-guided behavior. For this reason, we further performed a set of odor-guided behavioral experiments to determine if and when, during the process of reinnervation after ON transection, larval *Xenopus laevis* would exhibit behavioral responses to odor stimuli, indicative of the recovery of function of the olfactory system. Behavioural responses are challenging to detect as little is known about how larval amphibians interpret specific odorant stimuli and it is possible for similar stimuli to evoke opposing behaviours. Therefore, we first developed a robust experimental protocol for detecting odor-guided behavioural responses in unlesioned *Xenopus* larvae. We then performed the same behavioural procedures and analyses with two groups of *Xenopus* larvae that had undergone ON transection – one group between a period of 3 to 5 weeks of recovery, another group between 7 to 9 weeks of recovery.

The aim of this study was to advance our understanding of the process of recovery of the olfactory system after injury. We found that after severe lesions that bilaterally sever the ON the system is quickly able to rewire itself following its previous architectural structure. We show that this rewiring leads to the restoration of complex neural response patterns in the OB, as well as the recovery of odor-guided behaviour. This suggests that the restoration of the two spatially and functionally distinct glomerular representation of odorants in the OB, during the process of ORN reinnervation, underlies the recovery of odor-guided behavior. These results demonstrate that the rewiring of the *Xenopus* olfactory system after injury is structurally and functionally equivalent to an unlesioned system. These findings thus showcase the remarkable neuroregenerative ability of this animal model and open up further avenues of investigation on the topic of neuroregeneration.

Material and methods

Animal care

All *Xenopus laevis* larvae used in this study were bred and kept in water tanks with constant water circulation at a temperature of approximately 20°C at the animal facility of the University of Giessen. Before any animal experiment, such as bulk electroporation of ORNs, ON transection, or killing, *Xenopus* larvae were first

anesthetized using 0.02% MS-222 (ethyl 3-aminobenzoate methanesulfonate; Sigma-Aldrich) dissolved in tap water. Developmental stages of *Xenopus* larvae were determined according to Nieuwkoop and Faber (Nieuwkoop and Faber, 1994) and all animals used were between stage 46 and 56 (both included). After developmental stage 56 major metamorphic remodeling of the olfactory system begins to occur and therefore animals past this stage of development were not used. All animal procedures were performed following the guidelines of Laboratory animal research of the Institutional Care and Use Committee of the University of Giessen (V 54 – 19 c 20 15 h 01 GI 15/7 Nr. G 2/2019; 649_M; V 54 – 19 c 20 15 h 02 GI 15/7 kTV 7/2018).

Bulk electroporation of olfactory receptor neurons and olfactory nerve transection

For bulk electroporation of ORNs, we placed dried dye crystals of a fluorophore-coupled dextran (Cal 520 dextran conjugate, AAT Bioquest, 10 kDa, 3 mM in frog Ringer's solution) in the nostrils of anesthetized *Xenopus* larvae and applied six electric square pulses using two platinum electrodes (15 V, 25 ms duration at 2 Hz with alternating polarity) to each nostril (for detailed protocol see Weiss et al., 2018). *Xenopus* larvae were then left to recover for at least 24 hours before performing further experiments.

To transect the ON we followed the same procedures previously developed in (Hawkins et al., 2017). Anesthetized *Xenopus* larvae were placed under a microscope and their nerves were carefully severed, using fine scissors to preserve surrounding tissue. Olfactory neurons were transected at the mid-line of each nerve between the nose and the brain. After ON transection *Xenopus* larvae were kept in tanks in the animal facility and used in further experiments carried out at different time points during the process of recovery from ON transection.

Functional calcium imaging and image data processing

Functional calcium imaging experiments were performed on unlesioned *Xenopus* larvae and on larvae at different time points after ON transection (non-transected, n=4; three weeks after ON transection, n=4; seven weeks after ON transection, n=10).

To perform calcium imaging experiments, ORNs were first loaded with a calcium sensitive dextran coupled dye via bulk electroporation (Weiss et al., 2018) as

described above. Animals were then anesthetized and killed by severing the connection between the brainstem and the spinal cord. A tissue block containing the olfactory system (the nose, the ONs, and the rostral portion of the telencephalon, containing the OB; see Results, Figure 3.1A) was carefully excised and kept in frog Ringer’s solution to preserve tissue vitality. The ventral palatal tissue and a small portion of tissue surrounding the OE were removed to facilitate imaging and direct the flow of odorants into the nasal cavity. The tissue block was positioned in a recording chamber, held in place by a platinum grid with nylon strings, and placed on the stage of a multiphoton microscope (Nikon A1R-MP). A constant flow of Ringer’s solution across the tissue block was maintained throughout the experimental procedure – a perfusion manifold (Milli Manifold; ALA Scientific) connected to a multi-channel gravity-fed perfusion system (ALA-VM-8 Series; Scientific) was placed directly in front of one nasal cavity, and solution was removed from the opposing end of the recording chamber. Fast volumetric resonant scanning of the ORN axon terminals in the glomeruli of the OB was performed (780 nm excitation wavelength) as individual stimuli were applied at different time intervals, creating a time series of 3D virtual image stacks (axial dimensions: 180–300 μm , inter-plane distance 4 μm ; lateral dimensions: 509 x 509 μm , 512 x 512 pixel), acquired at 0.5–1 Hz/image stack (for detailed information see Offner et al., 2020). Stimuli used, shown in Table 3.1, were applied with a duration of 5 seconds and an inter-stimulus interval of 60 seconds and repeated twice.

Stimuli	Composition
Amino acid mixture	L-valine, L-leucine, L-isoleucine, L-methionine, glycine, L-serine, L-threonine, L-cysteine, L-arginine, L-lysine, L-histidine, L-tryptophan, L-phenylalanine, L-alanine, L-proline (100 μM in frog Ringer’s solution)
Amine mixture	2-phenylethylamine, tyramine, butylamine, cyclohexylamine, hexylamine, 3-methylbutylamine, N,N-dimethylethylamine, 2-methylbutylamine, 1-formylpiperidine, 2-methylpiperidine, N-ethylcyclohexylamine, 1-ethylpiperidine, piperidine (100 μM in frog Ringer’s solution)
Bile acid mixture	taurocholic acid, cholic acid, glycolic acid, deoxycholic acid (100 μM in frog Ringer’s solution);
Forskolin	direct stimulant of the adenylate-cyclase and the cAMP second messenger pathway (stock 10 mM dissolved in DMSO; 100 μM in frog Ringer’s solution)

Table 3.1 *Stimuli used during calcium imaging experiments in the olfactory bulb of larval Xenopus.* Alongside these stimuli, a positive control made of all stimuli (with the exception of forskolin, L-proline and L-alanine), acohols and aldehydes (50 μ M in frog Ringer's solution; also see Gliem et al., 2013) and a negative control made solely of frog Ringer's solution were used. All chemicals were purchased from Sigma Aldrich. Amino acids, bile acids and amines were selected as odorant stimuli as they are made up of water soluble molecules and are known to be olfactory stimuli for animals that live in aquatic environments (amino acids, Caprio and Byrd, 1984; Kang and Caprio, 1995; Manzini et al., 2002; Manzini and Schild, 2003, 2004; Schild and Manzini, 2004; bile acids, Kang and Caprio, 1995; Sato and Suzuki, 2001; amines, Carr and Derby, 1986; Carr et al., 1990; Rolen et al., 2003).

Image analysis of 3D calcium image stacks and data evaluation were performed using Python. Motion artifacts were removed from images using a motion correction algorithm (Pnevmatikakis and Giovannucci, 2017). Denoised and deconvolved calcium imaging data was generated using the CalmAn toolkit (Friedrich et al., 2017; Giovannucci et al., 2019). Fluorescence intensity difference maps were created by calculating the difference between peak fluorescence intensity of post-stimulus responses (averaged from three timeframes) and baseline fluorescence prior to stimulus onset (averaged from five frames). Note that fluorescence intensity difference maps were used to create maximum intensity projections along the z-axis shown in Figures 3.1 and 3.2 (in Results). Individual timeframes had a duration between 1.5–2 seconds. The following criteria were used to define responding regions:

- I. Area of regions had to be larger than 100 pixels;
- II. Regions had to be responsive to at least one stimulus, i.e. evoking a fluorescence intensity amplitude that exceeded the median value of all amplitudes in the dataset;
- III. The deconvolved timeseries were compared to their corresponding raw traces as quality control;
- IV. Finally, any regions outside the boundaries of the glomerular clusters were discarded.

Fluorescence timetraces of selected responding regions were baseline corrected using asymmetric least squares smoothing (Eilers and Boelens, 2005) and normalized by their response peak amplitude (baseline = 0, maximum = 1). A threshold of 12,5% was defined below which to ignore amplitude peaks within the expected peak response interval. Response tuning profiles of responding regions were therefore defined by the set of stimuli that led to response amplitudes above 12.5% of the

maximum amplitude of the respective time series. To analyse the spatial distribution of response tuning profiles in the OB, responsive regions were first sorted into forskolin-responsive and non-forskolin-responsive regions. Each subset was then further subcategorized based on responses to other stimuli used, and the position within glomerular clusters was determined in relation to manually defined points at the medial-lateral and anterior-posterior edges of each individual OB. Along these two axes, the density of responsive regions was determined using Gaussian kernel density estimates. Scott's rule was implemented in the Python library SciPy (<https://scipy.org/>) and used to calculate the bandwidth of estimation (Scott, 1992; Virtanen et al., 2020).

Odor-guided behavior assay

Odor-guided behavior experiments were performed on unlesioned *Xenopus laevis* larvae and on larvae at different time points after ON transection. We tested 28 non-transected *Xenopus* larvae, 18 larvae that had recovered 3 to 5 weeks after ON transection, and 15 larvae that had recovered 7 to 9 weeks after ON transection.

Before odor-guided behavior experiments were performed, *Xenopus* larvae were kept for 24 hours in individual tanks filled with normal tap water, without food. After 24 hours in this environment of reduced external stimuli, individual *Xenopus* larvae were placed in a partially separated choice tank filled with 1 liter of normal tap water (see Results, Figure 3.3A,B). An infra-red light panel was placed under the tank, and a camera was fixed above the tank, at a distance that would allow recording of the position of the larval *Xenopus* in all regions of the tank. The choice tank was comprised of three regions, all freely accessible to the larvae – two separate 'areas of interest' of the tank, of equal size (area = 58,5 cm²), and a third, larger area (110 cm²), used solely to allow the animal to enter and leave the areas of interest freely. Although the position of the *Xenopus* larvae in this third region was recorded, these data were not used in any statistical analysis. After a habituation period of two hours in which *Xenopus* larvae were left to swim freely in the tank without disturbances, we introduced simultaneously, through a gravity fed perfusion system, 5 ml of an amino acid mixture (100 µM dissolved in water; mixture described above), as an odor stimulus, to one area of interest of the tank, and 5 ml of normal tap water to the other (as a control stimulus). Stimuli entered the tank at a speed of 2 ml/min. In pilot testing, we released food

coloring dye in the areas of interest of the tank, through the gravity fed perfusion system, and observed that the dye diffused beyond the regions of interest after approximately 20 minutes. We therefore set a 20-minute exclusion threshold – data collected from animals that did not visit the areas of interest within the first 20 minutes after application of stimulus were excluded from further analyses. A total of 46 larval *Xenopus* were included in the final analyses (n=18 non-transected; n=13 at 3-5 weeks after ON transection; n=15 at 7-9 weeks after ON transection).

Behavior parameters were extrapolated from position tracking data using video tracking software (EthoVision XT, by Noldus). These parameters were – frequency of visits to each area of interest (visits/minute); time spent in each area of interest per visit (seconds/visit); percentage of time spent in each area of interest for each time period analysed (%); swimming velocity in each area of interest (centimeters/second). Each parameter was measured during the two-hour habituation period and over the course of 5, 10, 20, 40, and 60 minutes, starting from the time of first entry of larvae in each area of interest after stimuli application. The average parameter values measured during the two-hour habituation period, where no stimuli were applied, were used as baseline for comparison to values obtained after stimulus application. For each parameter recorded after the application of stimuli, we computed the absolute value of the parameter's change from baseline. To obtain a single value describing the change in behavior from baseline, we first fit the data with a log parabolic function in the form: $f(x) = \log(ax^2 + bx + c)$. Then, we took the area under the curve (*AUC*) of the fitted function, normalized to the measurement duration, as a metric of change in behavior from baseline. Figure 3.5C exemplifies this sequence of computations for two example non-transected *Xenopus* larvae.

Analyses of behavioral responses to odor stimuli in non-transected *Xenopus* larvae

In non-transected larval *Xenopus*, behavioral variables were compared across areas of interest during the two-hour habituation period to exclude any differences between these areas at baseline. Then, *AUC* values computed for each parameter were compared across areas of interest to identify which parameters showed greater change from baseline in the area of interest where amino acids had been applied compared to the area of interest where normal tap water had been applied. After

having identified which behaviour parameters signalled statistically significant responses to the amino acid odorant stimulus, we computed a robust metric of behavioural response. We defined, for each parameter, an odorant response index (*ORI*) as a ratio of the absolute change in behaviour in the amino-acid compartment (AUC_{aa}) minus the absolute change in behaviour in the water compartment (AUC_w), divided by the absolute change in behaviour in the water compartment:

$$ORI = \sqrt[3]{\frac{AUC_{aa} - AUC_w}{AUC_w}}$$

The cube root transformation was applied to remove the skewness in these proportion data. Positive (>0) values of this *ORI* indicate a behavioural response. We then combined the *ORI* of parameters (time per visit and swimming velocity) that showed a significant behavioural response by taking their average. This combined *ORI* was taken as a robust metric of behavioural response to odorant stimuli.

Analyses of behavioral responses to odor stimuli in transected *Xenopus* larvae

The previous set of analyses determined, in non-transected *Xenopus* larvae, which parameters showed significant behavioural responses to odor stimuli. These parameters were then employed, using the same set of analyses, to test for the recovery of odor-guided behaviour in *Xenopus* larvae after ON transection. Specifically, in larval *Xenopus* between 3-5 and 7-9 weeks after ON transection, we compared the *AUC* values for time per visit and swimming velocity parameters across areas of interest to test whether these parameters showed greater change from baseline in the area of interest where amino acids had been applied. We then computed the *ORI* for both parameters, as well as the combined *ORI*, and tested whether these indexes signalled behavioural responses to the odor stimuli in the two groups of transected *Xenopus* larvae.

Statistical analyses

Differences between groups were assessed using one- or two-tailed Wilcoxon signed-rank or rank-sum test tests, as appropriate. The Pearson correlation coefficient was employed to assess the degree of linear dependency between behavioral parameters. Statistical significance was set at $\alpha < .05$. Calcium imaging analyses were performed in Python; behavioral analyses were performed in Matlab (version R2019b).

Results

Odorant-induced receptor neuron axon terminal activity within glomerular clusters in the olfactory bulb of larval *Xenopus laevis*

We performed fast volumetric calcium imaging of the OB and recorded ORN axon terminal activity in the glomerular layer of *Xenopus laevis* larvae, while applying a sequence of odorant mixtures and forskolin as stimuli to the OE (Figure 3.1A,B). Odorant mixtures included a mixture of amino acids, a mixture of bile acids and a mixture of amines (see Material and Methods for information about the exact composition of stimuli used). Forskolin was applied to stimulate cAMP-dependent cell signaling. A mixture of all odorant mixtures was applied as positive control and frog Ringer's solution as negative control. Figure 3.1C shows a maximum projection image of ORN axon terminal activity (shown in white) in the OB of a non-transected larval *Xenopus* in response to all odorant/stimuli applications used in these experiments. Figure 3.1D shows the OB of the same non-transected larva deconstructed into regions responsive to individual odorants and forskolin, that can be seen in different colors (from left to right), and at different levels across the ventral and dorsal axes of the OB (shown as z-plane bundles, top to bottom). In this example, responses to the mixture of amino acids (third column, blue) can be seen to occur predominantly in ventral-lateral areas of the OB, whereas responses to forskolin (sixth column, yellow) occur in dorsal-medial regions. Responses to bile acids and amines (fourth and fifth column, cyan and magenta) occur slightly more medially. Olfactory receptor neuron axon regions can respond to one single odorant (or solely to forskolin) or to several, therefore each region can be defined by its location in the OB as well as by its stimuli-induced response profile. Examples of stimuli-induced response profiles of specific axon terminal regions (outlined in white) are included as traces at the bottom of each panel (inlays in white).

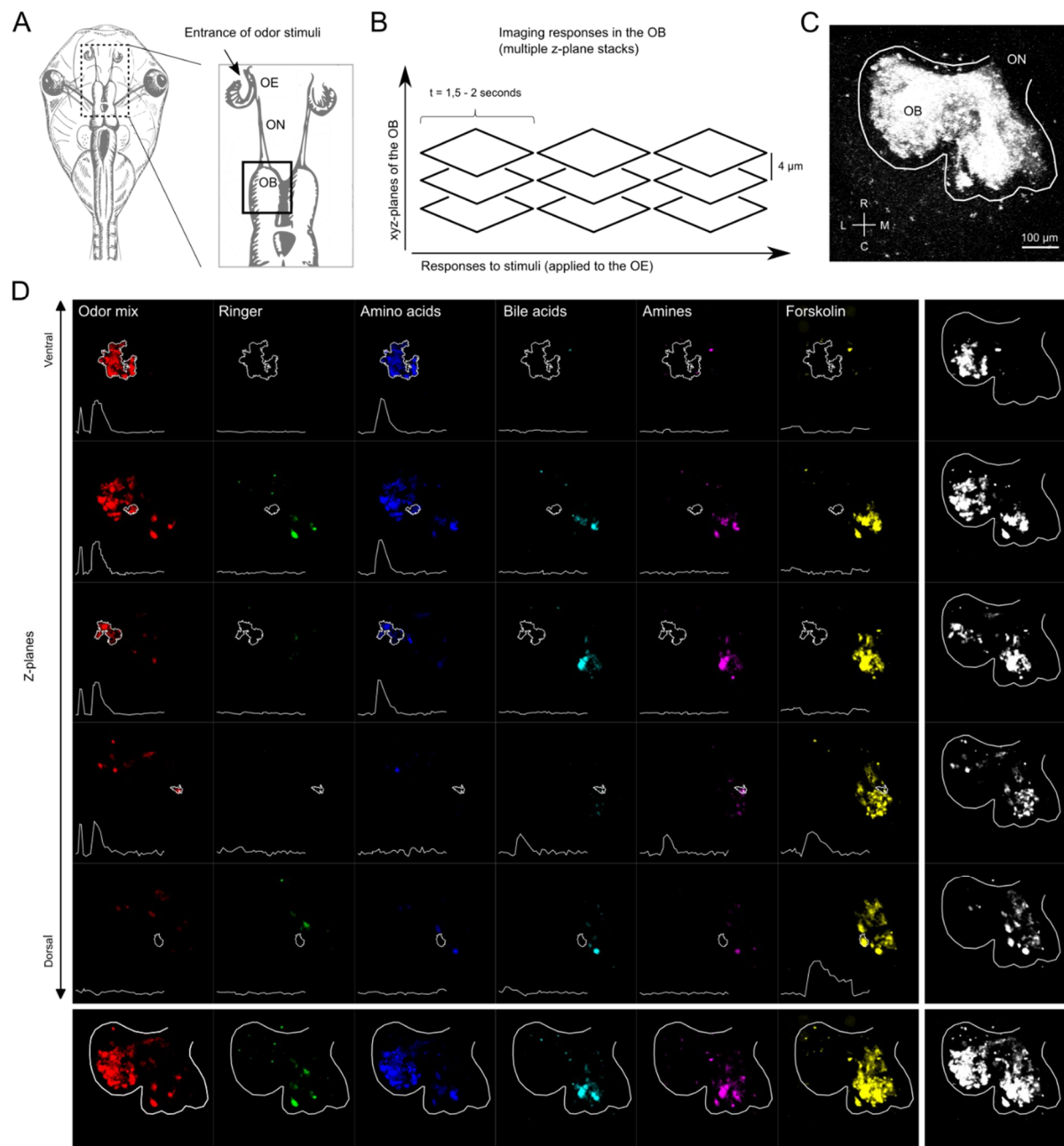


Figure 3.1 Odor-induced receptor neuron axon terminal activity in the olfactory bulb of larval *Xenopus*. (A) Illustration of the dorsal view of a larval *Xenopus laevis* highlighting the olfactory system (rectangular dashed outline). The olfactory system is shown in close up to the right, and includes: the nasal cavities, lined by the olfactory epithelium (OE); the olfactory nerves (ONs), made up of olfactory receptor neuron axons; and the olfactory bulb (OB), located in the anterior telencephalon. The area where odor stimuli enter the nasal cavity is indicated with an arrow. The black square highlights the area of the brain where the OB (one hemisphere) is located, where fast volumetric resonant scanning was performed. (B) Simplified illustration of fast volumetric resonant scanning using a multi-photon microscope. Multiple z-plane stacks of the OB (one hemisphere) were obtained over time in order to identify 3D volumes within the OB that exhibit a peak in fluorescence (indicative of an increase in intracellular calcium levels) upon stimulation with different odorant mixtures and forskolin. (C) A maximum projection image (raw data)

shows all responsive regions (in white) in the olfactory bulb (one hemisphere, outlined in white) of a non-transected larval *Xenopus* (developmental stage 53). (D) Example maximum projection images (difference maps) of z-plane bundles of the olfactory bulb of a non-transected larval *Xenopus* (developmental stage 53, same as shown in C) are shown distributed from most ventral to most dorsal (top to bottom) and over the course of stimuli application (left to right), showing areas responsive to each odor stimulus. The order of stimulus application was: all odorant mixtures (positive control), frog Ringer's solution (negative control), amino acids, bile acids, amines, and forskolin. This visualization shows both the location and temporal activation pattern of responsive regions in the brain. Overlays of all responsive regions over time for each z-plane bundle are shown in white at the far right. Overlays of all ventral to dorsal regions responsive to each individual stimulus are shown at the bottom. In all overlay figures, the outline of the olfactory bulb is shown for reference. Raw traces of odor response profiles are included (white traces as inlays) for specific responsive regions (outlined in white) in each z-plane bundle. OE, olfactory epithelium; ON, olfactory nerve; OB, olfactory bulb; R, rostral; L, lateral; M, medial; C, caudal.

Reintegrating olfactory receptor neurons reestablish distinct odor processing streams in the olfactory bulb after olfactory nerve transection

Fast volumetric calcium imaging of the OB was performed on non-transected *Xenopus* larvae and on larvae that had recovered for different periods of time after ON transection, allowing us to detect odorant- and forskolin-induced activity of ORN axon terminal regions throughout the OB. We were able to identify a considerable amount of odorant/stimulus-induced activity throughout the OB of non-transected and transected and recovered *Xenopus* larvae alike (Figure 3.2A, top row). In line with (Hawkins et al., 2017), this suggests that a substantial amount of reinnervation of the OB by new ORNs has already occurred after 3 weeks of recovery from ON transection. By separating the OB activity (Figure 3.2A, bottom row) in responses to odorant mixtures (blue) and in responses to forskolin (yellow), we observe that some anatomical segregation of ORN axon terminals that respond to these different stimuli is visible in both non-transected and transected *Xenopus* larvae. We next proceeded to quantify this observation at the group level, across all tested larvae.

To do so, from all the calcium imaging data acquired, we identified individual, specialized regions within the OB of the larval *Xenopus* examined. A “region” was defined as a group of adjacent voxels that responded to the same combination of stimuli, i.e. exhibiting the same odorant/stimulus tuning profile. Each region was thus distinguished by its specific tuning profile and its 3D spatial location in the OB. We

were able to identify a total of 435 such regions of ORN axon fibers across all animals. In non-transected *Xenopus* larvae, 86 responsive regions with distinct anatomical locations were found in the OB (n=4, one hemisphere/animal – average of 21,5 regions/hemisphere). In *Xenopus* larvae that had recovered for 3 weeks after ON transection, 82 responsive regions with distinct anatomical location were found (n=4, one hemisphere/animal – 20,5 regions/hemisphere). In *Xenopus* larvae that had recovered for 7 weeks after ON transection, 267 responsive regions with distinct anatomical location were found (n=10, one hemisphere/animal – 26,7 regions/hemisphere). Regions varied widely in size but were not significantly different across time points (before, 3 weeks, and 7 weeks after ON transection). In non-transected *Xenopus* larvae the mean size of responsive regions was $1400,95 \pm 1991,61 \mu\text{m}^2$. After 3 weeks of recovery from ON transection the mean size of responsive regions was $900,21 \pm 1719,08 \mu\text{m}^2$ and 7 weeks after recovery the mean size of responsive regions was $958,36 \pm 1641,40 \mu\text{m}^2$.

Having identified these specialized regions, we employed them to quantify the extent to which the two anatomically and functionally segregated odor processing streams—one lateral PLC-DAG-dependent and one medial cAMP-dependent (see introduction and Gliem et al., 2013) recover during the process of ORN reinnervation of the OB after ON transection. Specifically, we estimated the probability density function of these regions along two spatial axes. In Figure 3.2B we show the spatial distribution of regions responsive to forskolin (orange; fsk+, cAMP-dependent) and of regions responsive to stimuli other than forskolin (blue; fsk-, cAMP-independent), along the medial-lateral and anterior-posterior axis for all time points (before and after ON transection). In non-transected *Xenopus* larvae, regions responding to forskolin (fsk+), and therefore innervated by ORNs that have cAMP-dependent transduction mechanisms, make up 46,6% of responding regions and are generally distributed more medially and rostral. Conversely, regions that respond to other stimuli but not forskolin (fsk-) are distributed more laterally and caudal. In *Xenopus* larvae that recovered for 3 weeks after ON transection, 48,7% of responding regions were fsk+, and after 7 weeks 62,5% were fsk+. At 3 weeks after transection, even though some distinction is already visible, there is substantially more overlap between forskolin-responsive and non-responsive regions. At 7 weeks after transection the spatial and functional distribution is indistinguishable from that of non-transected *Xenopus* larvae.

These results thus demonstrate the progressive reestablishment of spatially-segregated cAMP-dependent and cAMP-independent odor processing streams in the OB over the course of reinnervation by newly formed ORNs after ON transection.

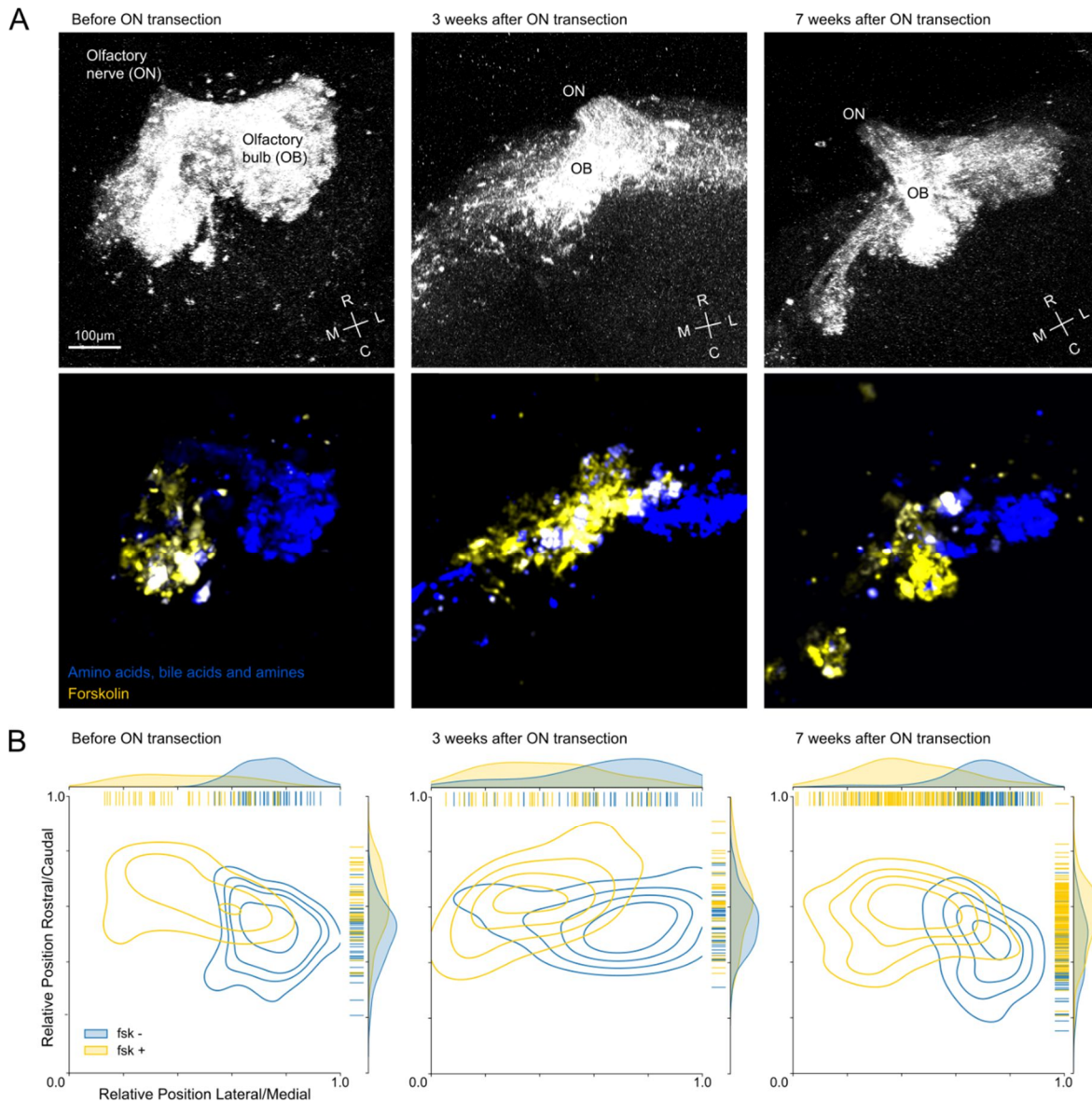


Figure 3.2 Receptor neuron reinnervation of the olfactory bulb shows spatially and functionally distinct glomerular clusters are reformed after nerve transection in larval *Xenopus*. (A) Maximum projection images of the olfactory bulb of three representative animals: left panels show data from one non-transected larval *Xenopus*, middle and right panels show data from animals at 3 and 7 weeks of recovery after transection of the olfactory nerve. Images in top panels (raw data) show all regions in the olfactory bulb which responded to stimuli (in white). Lower panels (difference maps) show responses to all odor mixtures (blue) and to forskolin (yellow). (B) Density plots showing the spatial distribution of forskolin positive (yellow) and forskolin negative (blue) response profiles along medial to lateral and caudal to rostral axes for *Xenopus* larvae before and 3 weeks and 7 weeks after olfactory nerve

transection (shown from right to left). Each individual responsive region, classified as forskolin positive (fsk+, yellow lines) or forskolin negative (fsk-, blue lines) collected from each larval *Xenopus* is shown in the rag plots in the upper and right axes borders. R, rostral; C, caudal; M, medial; L, lateral.

Reintegrating olfactory receptor neurons reestablish multi-stimulus response tuning profiles throughout the olfactory bulb after olfactory nerve transection

To investigate the recovery of neural function, we next analyzed in more detail the specific odorant/stimulus tuning profiles of different responsive glomerular regions. Across all non-transected and transected *Xenopus* larvae, we found 15 distinct tuning profiles, corresponding to all possible combinations of stimuli. The most common response profile across all animals was that of responsive regions that showed activity solely to amino acids (Figure 3.3A). The 2nd most common profile in non-transected *Xenopus* larvae and larvae 7 weeks after ON transection was the one responding to forskolin (this was the 3rd most common profile in *Xenopus* larvae 3 weeks after ON transection). We also found large proportions of regions exhibiting responses to combinations of stimuli. For example, the 3rd most common profile in non-transected *Xenopus* larvae (4th most common in larvae 7 weeks after transection) was that of regions responding to both amines and forskolin.

By looking at the percentage of regions exhibiting each of the 15 distinct tuning profiles (Figure 3.3B), we observed that all 15 response profiles were present in non-transected animals. Conversely, only 12 out of the 15 response profiles found in non-transected *Xenopus* larvae were found in larvae 3 weeks after ON transection. Specifically, in *Xenopus* larvae 3 weeks after ON there were no regions that responded exclusively to amines, or to both bile acids and amines, or to amino-acids and bile acids and amines. All 15 odor response profiles found in non-transected *Xenopus laevis* larvae were however once again found in larvae 7 weeks after ON transection. (Figure 3.3A,B).

These experiments highlight how the transmission of information to the glomeruli is re-established following transection and shows that this rewiring reliably reestablishes the olfactory network as it was before ON transection. Nevertheless, this does not answer the question of whether re-establishing the wiring structure in the glomeruli of the OB is sufficient to recover odor-guided behavior after ON transection. To establish whether and when this is the case, we next developed and executed a set of

experiments investigating odor-guided behavior, using amino acids as olfactory stimuli.

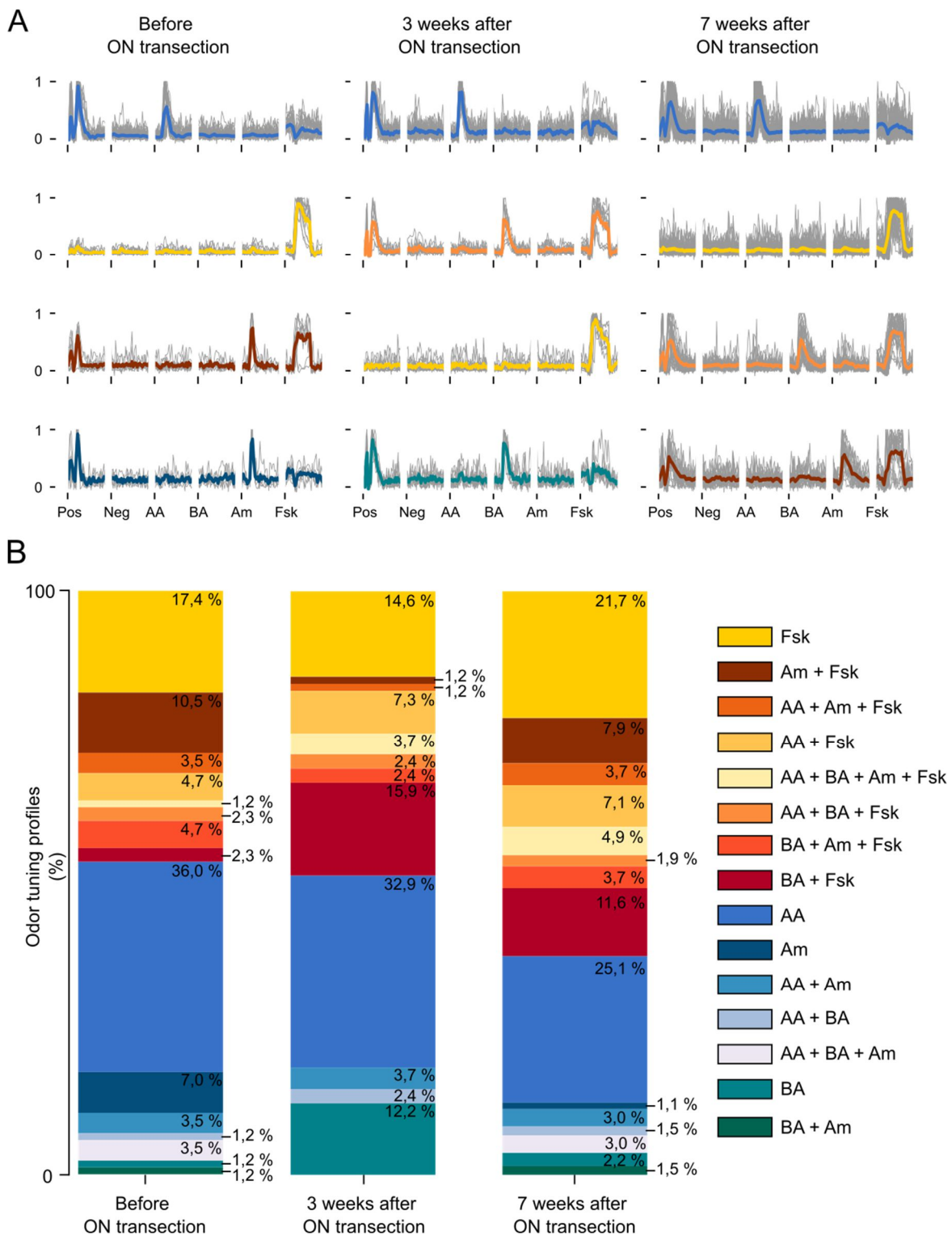


Figure 3.3 *Tuning profiles of olfactory receptor neuron axon terminal regions in the olfactory bulb of larval *Xenopus* – before and during recovery from olfactory nerve transection.* (A) Odorant/stimulus response profiles found in the OB of *Xenopus laevis* larvae. Left, middle, and right columns shows profiles found in non-transected animals, animals 3 weeks after transection, and animals 7 weeks after transection. From top to bottom, we show the four most common profiles found in each group. Normalized response profiles of individual regions are shown as gray traces. Average traces plotted as overlays follow the color code shown in B. (B) Percent of olfactory neuron axon terminal regions exhibiting different odorant/stimuli-induced tuning profiles in the olfactory bulb of non-transected *Xenopus laevis* larvae (left column) and larvae 3 weeks (middle column) and 7 weeks (right column) after olfactory nerve transection. Numbers are shown as percentages of the total number of regions found – non-transected larvae (4 animals, total of 86 responsive regions), 3 weeks post-transection (4 animals, total of 82 responsive regions), 7 weeks post-transection (10 animals, 267 responsive regions). ON, olfactory nerve; Pos, positive control; Neg, negative control; Fsk, forskolin; Am, amines; AA, amino-acids; BA, bile acids; om, odorant mix; rc, ringer control.

Odorant-guided behavioral responses in unlesioned larval *Xenopus laevis*

To investigate odor-guided behaviour, we performed behavioural experiments by tracking the 2D position of individual *Xenopus laevis* larvae placed in a partially separated choice tank (Figure 3.4A). During a two-hour habituation period, in which no odorants were applied to the choice tank, freely swimming *Xenopus* larvae explored the whole volume of the tank. The example tadpole shown in Figure 3.4B exhibits a preference for wall following, a typical behavior previously described in the literature (e.g. Hänzi and Straka, 2018). From these motion tracking data in the two areas of interest of the tank (areas A and B), we extracted four parameters: the time spent per visit in seconds; the frequency of visits per minute; the percent of time spent in each area; the swimming velocity in centimeters per second. As expected, during the two-hour habituation period without odor stimulation we found no significant differences between the two areas of interest for any of these four parameters (Figure 3.4C, all $p > .05$). Across areas of interest and animals ($n=18$), the average time per visit was 25 ± 25 s (mean \pm sd), the average frequency of visits to each compartment was 0.8 ± 0.5 visits/min, the average percentage of time spent per area was 20 ± 8 %, and the average swimming velocity was 1.1 ± 0.6 cm/s. Additionally, these parameters were all significantly correlated across animals and measurement time points (all $p < .05$), with the strongest correlation being between time per visit and velocity parameters ($r = -0.52$, $p < .001$; Figure 3.4D). This suggests that these parameters capture common

sources of variance in the animals' behaviour. For example, the negative correlation between time per visit and velocity parameters sensibly indicates that when *Xenopus* larvae swam at slow speeds, they also tended to remain in the same portion of the tank for longer.

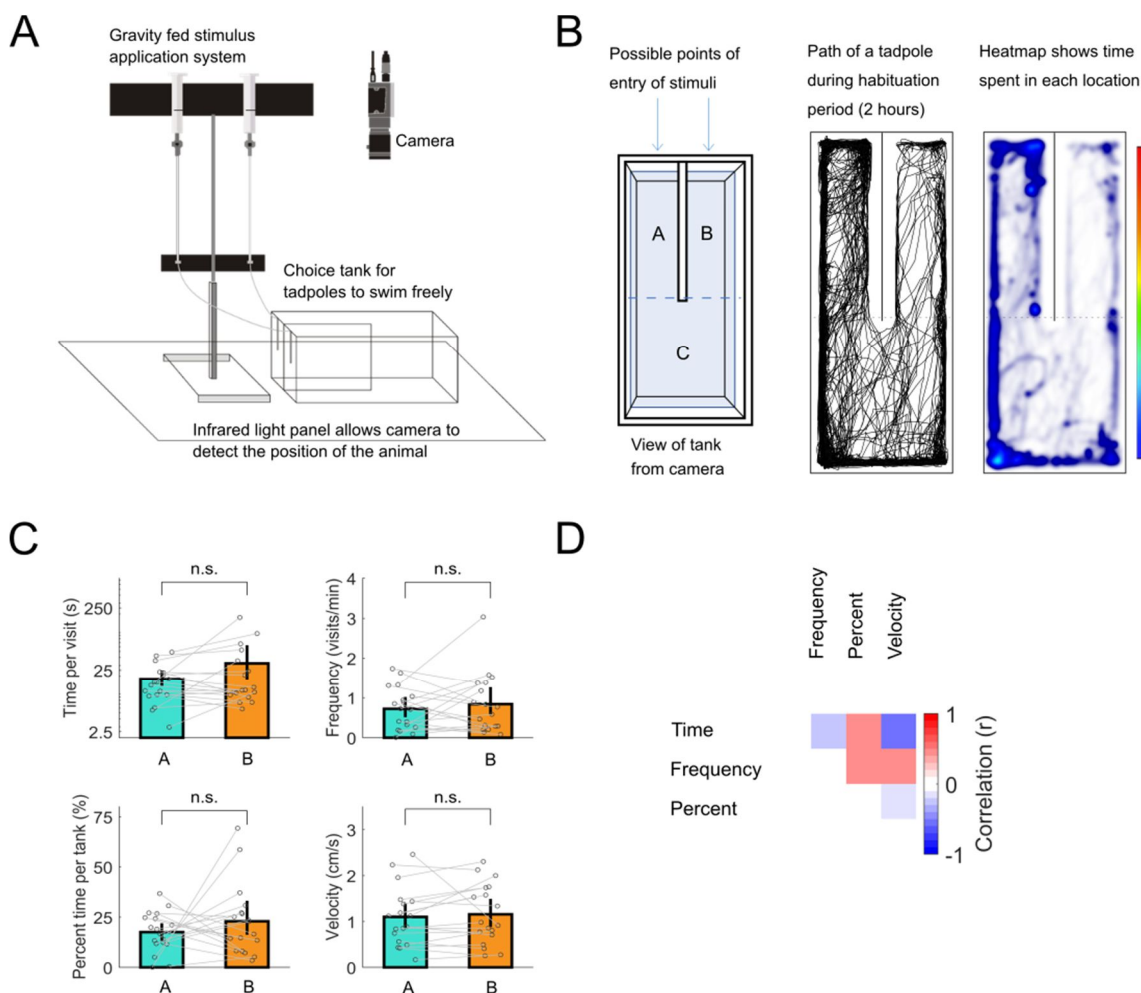


Figure 3.4 Motion tracking experimental setup and larval *Xenopus* behavior without application of odorant stimuli. (A) Illustration of the experimental setup used for odor-guided behavior experiments. *Xenopus* larvae were placed in a partially separated choice tank. A video camera, located above the tank, was used to record an animal's location as it swam freely in the tank. A gravity fed perfusion system was used to apply odorants directly into specific compartments of the tank. The IR light panel, located below the tank, allowed the camera to record the animal's position during the experiments. (B) Schematic of the partially separated choice tank (as seen from camera), followed by raw movement traces, and the spatial distribution of explored tank locations for one representative tadpole during a two-hour habituation period where no odor stimulus was applied. Areas A and B were the areas of interest from which motion tracking data were collected and analysed. Area C was a compartment connecting the two areas of interest so that *Xenopus* larvae could freely move between areas A and B or retreat from both. Motion tracking data from area C was not analysed. (C) Behavioural parameters

extracted from the motion tracking data during the two-hour habituation period in compartments A and B (no odor stimulus applied) for all animals (n=18). Bars are means, and error bars are 95% bootstrapped confidence intervals. Connected dots represent data from individual larvae. All paired comparisons $p > .05$. (D) Strength of the correlations between the four parameters extracted from the motion tracking data from all animals (all $p < .0001$).

Having established that there were no intrinsic differences in the behavior of larval *Xenopus* within the two areas of interest of the tank, we next proceeded to identify odor-guided behavioral responses. At the end of the two-hour habituation period, an amino acid odor solution was applied to one of the areas (AA area) while simultaneously water, as a control, was applied to the other area (W area, Figure 3.5A). The odor stimulus was the same mixture of amino acids used in the calcium imaging experiments. The *Xenopus* larvae continued to swim freely in the tank for 60 minutes while we tracked their movements (Figure 3.5B). In order to detect a behavioural response to the odor stimuli, we monitored how each behavioural parameter extracted from the movement traces varied compared to baseline.

Even though amino acids are known to be olfactory stimuli for animals that live in aquatic environments (Caprio and Byrd, 1984; Kang and Caprio, 1995; Manzini et al., 2002; Manzini and Schild, 2003, 2004; Schild and Manzini, 2004), it is unknown exactly what these stimuli signify to *Xenopus* larvae. For example, these stimuli could signal food sources and/or the presence of predators, and lead to complex and even dichotomous response behaviors (e.g. De Franceschi et al., 2016). For this reason, we expected that changes in value for each parameter, signaling a change in behavior, could take place as an increase or decrease from baseline, i.e. the average parameter value during the two-hour habituation period. For example Figure 3.5C (left panels) shows data on the swimming velocity of two example non-transected larvae. The top tadpole shows a decrease in swimming velocity after the first entrance in the AA area, while the swimming velocity in the area where water was applied shows no apparent change. The second tadpole (bottom) exhibits an increase in swimming velocity in both areas, and this increase is greater in the AA area. Therefore, to obtain a single value describing the change in behavior from baseline, we took the absolute value of the change from baseline, and we fit these data with log parabolic functions (Figure 3.5C, middle panels). Then, we took the area under the curve (AUC) of these fitted functions, normalized to the measurement duration, as our metric of change in

behavior from baseline (rightmost panels in Figure 3.5C). The change in behavior from baseline in the water compartment (blue) represents random changes in each animal's behavior with time. Any additional change in behavior in the AA area (orange) should be attributable to the animals detecting the odorant stimulus in the water.

We applied this method across all animals for each of the four parameters extracted from the movement traces (Figure 3.5D). We did not find statistically significant differences between the AA and W areas in terms of the frequency of visits per area ($Z = -1.7$, $p = 0.96$), or percentage of time spent per area ($Z = 0.13$, $p = 0.45$). Conversely, we found that behaviour in the AA area was significantly different than in the W area with respect to the time per visit ($Z = 2.7$, $p = 0.0035$) and the velocity parameters ($Z = 2.13$, $p = 0.016$). In the AA area, *Xenopus* larvae modified their behaviour by changing how quickly they swam and how much time they spent in the AA area during each visit. These parameters were also moderately correlated with each other (Figure 3.4D). This suggests it should be possible to combine these two parameters into a single, robust index of behavioural response to the amino-acid stimuli. To do so, for each parameter we first defined a unitless odorant response index (*ORI*, see *Methods* for precise mathematical formulations). Values of these indices around zero mean that no odor-induced change in behaviour is detected. Only the indices defined from the time per visit and velocity parameters were significantly greater than zero (Figure 3.5E, $Z = 2.87$, $p = 0.0020$; $Z = 2.96$, $p = 0.0015$), whereas indices defined from the frequency of visits and percentage of time per compartment parameters were not different from zero ($Z = -1.05$, $p = 0.85$; $Z = 0.91$, $p = 0.18$). We thus combined the indices derived from the time per visit and velocity parameters into a single index of behavioural response to the odorant stimuli. Indeed, a simple average of these two indices was robustly greater than zero, signalling a clear behavioural response to the odorant stimuli in the AA area (right-most bar in in Figure 3.5E, $Z = 3.14$, $p < .001$).

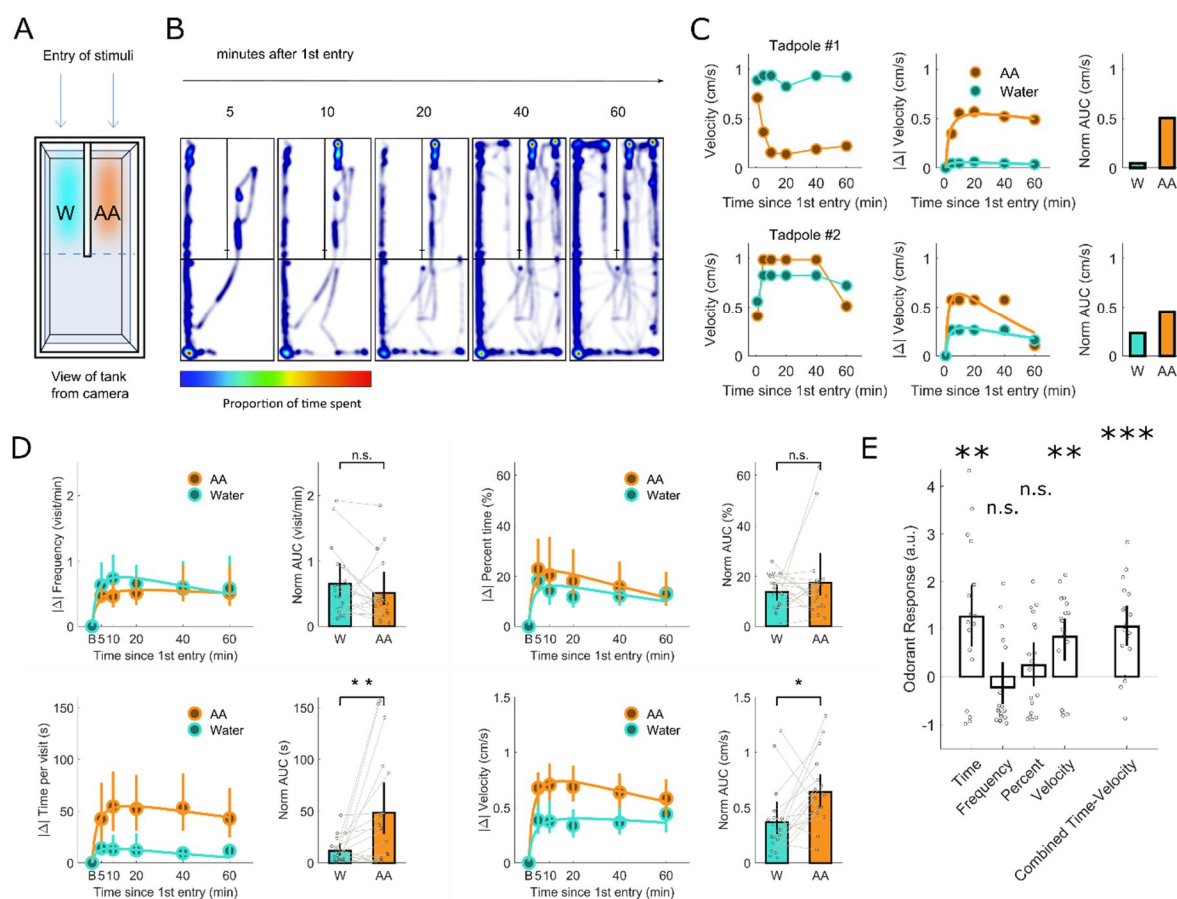


Figure 3.5 Behavioral responses to odor stimuli in non-transected *Xenopus* larvae. (A) Illustration of the partially separated choice tank as seen from the camera. An amino acid mixture and water were simultaneously introduced, via gravity feed, into two separate locations of the choice tank (AA and W areas). Arrows show the location where the stimuli were introduced in the two areas of interest in the tank. The two areas of interest end at the dashed line. Behavioral parameters were extracted from motion tracking data recorded within these two areas of interest. (B) For one representative tadpole, the cumulative distributions of explored tank locations at different time points after the first entry in AA and W areas. (C) For two representative *Xenopus* larvae, leftmost plots show swimming velocity in the areas of the tank where we introduced AA (orange) and W (blue), at baseline ($t=0$) and as a function of time since first entry in each area of interest. Tadpole 1 (top) exhibits a decrease in velocity in the AA area, whereas tadpole 2 (bottom) exhibits an increase in velocity in the AA area. Middle plots show the absolute value of the change in velocity from baseline as a function of time from 1st entry in the AA and W areas. Curves are log parabolic functions fit to the data. In rightmost plots, change in behavior from baseline was computed as the normalized area under the curve (AUC) of the fitted log parabolic functions. AUC data show that both *Xenopus* larvae exhibited greater change in velocity in the AA areas, even though this change was in different directions for the two larvae. (D) For each of the four measured parameters, the left plots show the absolute value of the change from baseline as a function of time from 1st entry in the AA (orange) or W (blue) areas. Dots are means across larvae; error bars are 95% bootstrapped confidence intervals of the mean. Lines are the average best fitting log parabolic functions through the data. Right plots show change in behaviour from baseline computed as the

normalized area under the curve (AUC) of the fitted log parabolic functions (small connected dots represent values for individual larvae). (E) Odorant response index (ORI) for all parameters and combined time-velocity ORI. Positive (>0) values signal a greater change in behaviour from baseline in the AA area compared to the W area. Bars are means, error bars are 95% bootstrapped confidence intervals, dots represent individual larvae. $n=18$; * $p<.05$; ** $p<.01$; *** $p<.001$

Neural rewiring of the olfactory bulb after olfactory nerve transection re-establishes odorant-guided behaviour in larval *Xenopus laevis*

Having determined which parameters reflect odor-guided behavioural responses in non-transected *Xenopus* larvae, we used these parameters to test whether lesioned animals would recover such odor-guided behavioural responses. To do so, the same experiments previously performed on unlesioned animals were performed on animals at different time points during the process of recovery from ON transection.

In *Xenopus* larvae that had recovered 3-5 weeks after ON transection ($n=13$) we found no evidence of behavioral response to odorant stimuli (Figure 3.6A). We did not find statistically significant differences between the AA and W areas in terms of time per visit ($Z = -1.7$, $p = 0.96$) or velocity ($Z = 0.13$, $p = 0.45$), and none of the ORIs were significantly greater than zero (Figure 3.6C, all $p>.05$). In this group, none of our analyses could thus detect odor-guided behavioural responses.

The situation was however different for *Xenopus* larvae that had recovered 7-9 weeks after ON transection ($n=15$; Figure 3.6B). In this group we did find statistically significant differences between the AA and W areas in terms of both time per visit ($Z = -1.7$, $p = 0.96$) and velocity ($Z = 0.13$, $p = 0.45$). Further, both ORIs were significantly greater than zero (Figure 3.6D, all $p<.05$), indicating that *Xenopus* larvae in this group modified their behaviour from baseline in the AA area more than in the W area.

Figure 3.6E concisely summarises our behavioural results across non-transected and transected animals using the combined Time-Velocity odorant response index. The combined ORI was significantly greater than zero—and thus detected odor-guided behavioural responses—in non-transected *Xenopus* larvae ($p < .001$) and in larvae that had recovered 7-9 weeks after ON transection ($p=.0085$), but not in larvae that had recovered 3-5 weeks after ON transection ($p=.31$).

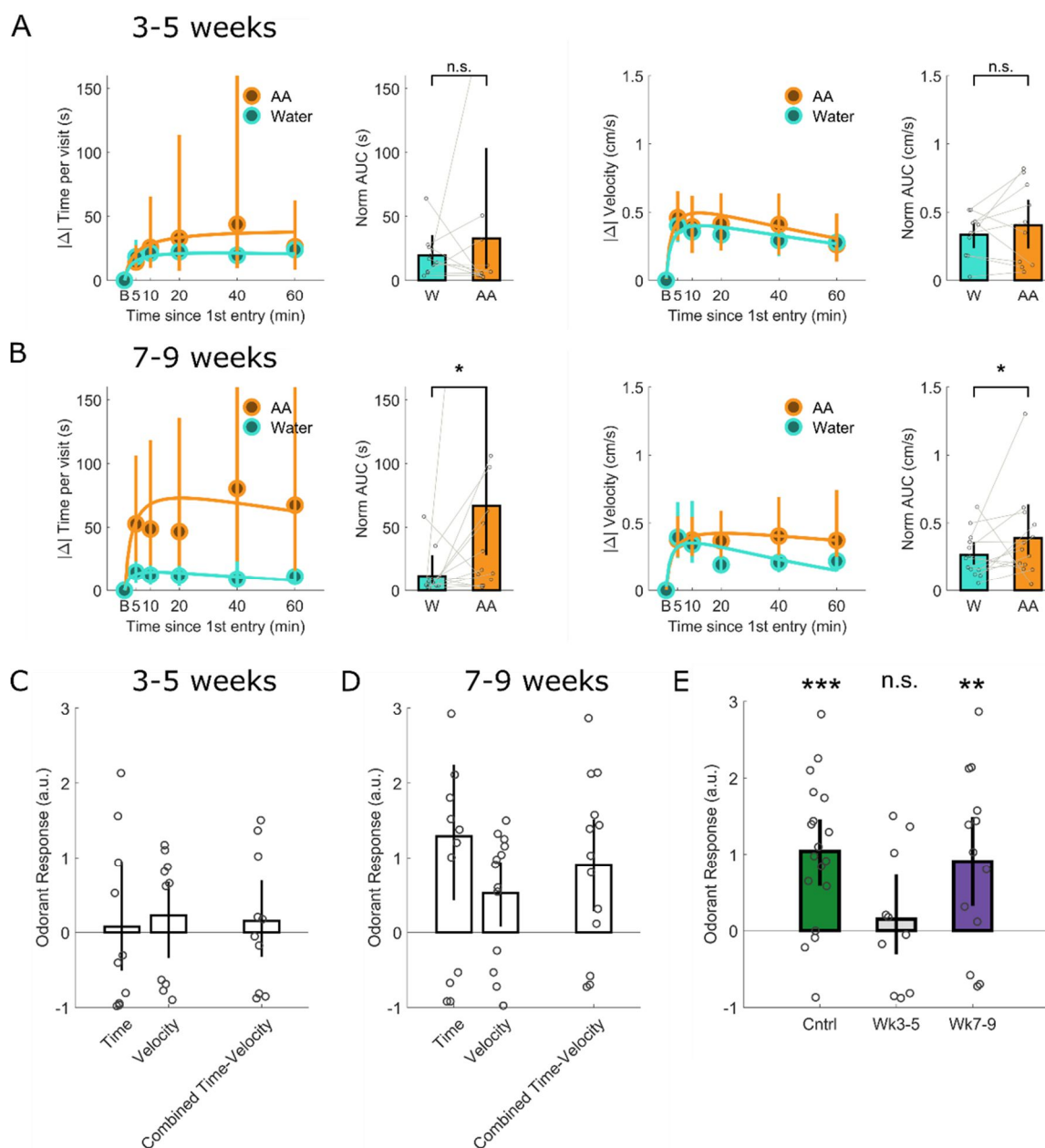


Figure 3.6 Behavioral responses to odor stimuli in transected *Xenopus* larvae at different time-points during recovery from olfactory nerve transection. (A) Time per visit and velocity parameters in *Xenopus* larvae that had recovered 3-5 weeks after ON transection ($n=13$). Left plots show the absolute value of the change from baseline as a function of time from 1st entry in the AA (orange) or W (blue) areas. Dots are means across larvae; error bars are 95% bootstrapped confidence intervals of the mean. Lines are the average best fitting log parabolic functions through the data. Right plots show change in behaviour from baseline computed as the normalized area under the curve (AUC) of the fitted log parabolic functions (small connected dots represent values for individual larvae). (B) Same as in A, for animals that had recovered 7-9 weeks after ON transection ($n=15$). (C) Odor response indexes computed from time per visit and velocity parameters at 3-5 weeks after ON transection. Positive (>0) values signal a greater change in behaviour from baseline in the AA area compared to the W area. Bars are means, error bars are 95% bootstrapped confidence intervals, dots represent individual larvae. (D) Same as in

C, for animals that had recovered 7-9 weeks after ON transection. (E) Combined Time-Velocity index as a single parameter that shows behavioral response to odor stimuli. A significant behavioural response to odor stimuli can be seen in non-transected *Xenopus* larvae and in larvae 7-9 weeks after ON transection. No significant response was found in larvae 3-5 weeks after ON transection. * $p < .05$; ** $p < .01$; *** $p < .001$

Discussion

Distinct subsets of olfactory receptor neurons show odorant and forskolin-induced activity in the olfactory bulb 3 weeks after olfactory nerve transection

In all vertebrates investigated to date, peripheral disruptions of the olfactory system, e.g. lesions of the OE and/or the ON, can generally be compensated its well known regenerative capacity. After damage, new ORNs are generated from a pool of neuronal stem cells in the OE and functionally reconnect in the OB (Costanzo, 2005; Brann and Firestein, 2014; Cheung et al., 2014).

As in other vertebrates (Manzini et al., 2022), ORNs in the OE of larval *Xenopus* interact with odor molecules from the environment and transmit olfactory information to the OB and higher brain centers for further processing (Manzini and Schild, 2010). After bilateral ON transection responses to odorant stimuli are disrupted (Hawkins et al., 2017). Over the course of recovery, with the formation of new ORNs in the OE and their axonal reconnection in the OB, odorant responses are restored (Hawkins et al., 2017). However, before newly formed ORN axons of premetamorphic *Xenopus* can reinnervate the OB, regenerative processes must occur in the OE in order to reconstitute the cells lost after injury. Previous work has shown that during the first days after mechanical lesion to the ON apoptosis in the ORN cell layer and stem cell proliferation in the basal cell layer of the OE occur at significantly higher rates than in control animals (Cervino et al., 2017; Hawkins et al., 2017). Due to massive ORN death, mature ORNs decrease significantly in the first days following lesion and are completely absent in the OE after 1 week (Cervino et al., 2017). At this point of complete loss of mature ORNs, immature ORNs start to appear in the OE (Cervino et al., 2017). This is also the point in which responses to amino acid-odorants begin to reappear in ORNs in the OE and new ORN axons reach the OB (Hawkins et al., 2017). This suggests that 1 week after ON transection the OE is repopulated with a large number of immature ORNs that show responses to amino acids in the OE, but have

not yet fully developed into mature neurons. The maturation of these newly formed ORNs seems to be completed about 3 weeks after transection, as responses in glomeruli are reestablished at this time (Hawkins et al., 2017). Loss of ORN axon innervation in larval *Xenopus* is presumed to be the cause of a significant decrease in OB volume over the course of two weeks after ON transection (Hawkins et al., 2017). The volume of the OB begins to increase again 3 weeks after ON transection, presumably due, at least in part, to further ORN axon reinnervation (Hawkins et al., 2017). During the first week after ON transection in the larval *Xenopus* OB, MTCs lose their glomerular tufts. These tufts reappear about 3 weeks after transection and are completely reestablished after 7 weeks (Hawkins et al., 2017). This is also the period when amino acid-induced MTC responses reappear (Hawkins et al., 2017). A reduction of the OB volume and alterations in MTC dendritic morphology after introducing chemical or physical lesions in the OE has also been observed in zebrafish (Calvo-Ochoa et al., 2021). Similar results have also been obtained in mice (Murai et al., 2016). After partial transection of the ON in mouse, coarse axonal targeting of ORNs is disrupted, and MTCs lose dendritic connectivity to glomeruli that, in contrast to *Xenopus* larvae, does not fully recover over time.

In the present study we investigated the functional recovery of the *Xenopus* olfactory system in more detail. We found that 3 weeks after recovery from ON transection, in addition to the amino acid-sensitive ORN subset (Hawkins et al., 2017), all other known ORN subsets (see Gliem et al., 2013) with distinct transduction mechanisms (cAMP-dependent and PLC-DAG-dependent) and distinct odorant response profiles (amino acids, bile acids, and amines) are mostly reconnected to the OB glomerular layer. These results were obtained by locating, in 3D space, regions of ORN axon innervation responsive to multiple odorants and forskolin.

Accurate neural rewiring in the olfactory bulb after olfactory nerve transection leads to the reformation of two segregated odor processing streams

Although a precise anatomical and functional glomerular map for odor recognition has yet to be described, *Xenopus laevis* larvae have been shown to employ two functionally and anatomically segregated odor processing streams in the OB – a lateral glomerular cluster, innervated by ORNs that employ cAMP-independent transduction mechanisms, and a medial glomerular cluster, innervated by ORNs that employ

cAMP-dependent transduction mechanisms (Gliem et al., 2013). A similar glomerular clustering is also present in the OB of fishes (Sato et al., 2005; Olivares and Schmachtenberg, 2019). We examined the connectivity pattern of different subsets of ORNs in non-transected *Xenopus laevis* larvae and in larvae that had recovered from bilateral ON transection for 3 and 7 weeks to determine the accuracy of ORN axonal rewiring in the OB.

In rodents it has been shown that the recovery from chemical lesions of the OE results in a more accurate rewiring of ORN axons to the OB (Schwob, 2002) than after damage or transection of the ON (Christensen, 2001). An accurate recovery of bulbar responses after chemical lesion of the OE has also been described in the mouse olfactory system (Cheung et al., 2014). The rewiring after ON damage or transection results in a rather distorted odor map in the OB (Costanzo, 2005; Murai et al., 2016). Olfactory nerve damage leads to a fast depletion of ORN axons. As ORN axons are thought to act as an essential scaffold for the maintenance of the olfactory circuit, the decline of this scaffolds might result in olfactory circuit. The reason for this inaccurate rewiring in rodents might prevent an accurate reformation of the olfactory circuitry (Murai et al., 2016).

In concordance with the results obtained by Gliem and coworkers (Gliem et al., 2013), in the present work we found that in non-transected *Xenopus* larvae the location of cAMP-dependent responses were located with highest density in the medial region of the OB, and cAMP-independent responses were located more laterally. After 3 weeks of recovery from ON transection the two main odor processing streams that occur in non-transected *Xenopus laevis*, begin to reform as the OB is re-innervated by new ORNs. Already at 3 weeks post transection there is an initial anatomical and functional distinction between responsive regions which becomes increasingly more segregated during the following weeks. At 7 weeks post-transection the segregation of cAMP-dependent and -independent ORN axons in a medial and lateral glomerular clusters reaches control levels. Our results suggest that axonal guidance mechanisms in *Xenopus laevis* larvae lead to the accurate rewiring of the OB, relative to the two anatomically and functionally segregated odor processing streams. Although, several axonal guidance mechanisms in the olfactory system have been investigated in vertebrates, mainly in rodents (Mori and Sakano, 2011; Lodovichi, 2021), the axonal

guidance mechanisms at play in *Xenopus* are yet to be defined. Obviously, there is a substantial difference between rodents and larval *Xenopus*, as differently as in rodents, in *Xenopus* ORN axons appear to rewire more accurately after ON damage.

Also, we found that only 12 out of the 15 odor tuning response profiles, i.e, bulbar regions that differently respond to a variety of odorants and forskolin, found in the OB of non-transected control *Xenopus* larvae were found in larvae 3 weeks after ON transection. After further odor processing segregation after 7 weeks of recovery all 15 response profiles found in non-transected larvae were once again reestablished in the OB. Notably, the full recovery of odorant tuning response profiles after ON transection coincides with the time it takes for MTCs to recover from the loss of dendritic tuft complexity (Hawkins et al., 2017). This is also the point in which MTCs regain the ability to respond to odorants (amino acids; Hawkins et al., 2017).

Accurate reinnervation of the OB by ORNs, accompanied by the recovery of odor tuning response profiles in the OB, suggests substantial recovery of the odor detection and processing capability.

Odorant-guided behavior is reestablished 7-9 weeks after recovery from olfactory nerve transection

In an attempt to determine if and when, during the process of recovery from ON transection, *Xenopus laevis* larvae regain a fully functional olfactory system and odor-guided behaviour, we investigated odor-induced changes in behavior in control larvae and in larvae at different timepoints after ON transection.

In our behavioral experiments we employed amino acids as odorants. In aquatic species, amino acids are well-established odorants, and in various fish species these stimuli have been shown to signal the presence of food and thus to attract animals (Valentinčič and Caprio, 1997; Hara, 2006; Olivares and Schmachtenberg, 2019). Amino acids are suitable odorants also in larval *Xenopus*. This has been shown in numerous publications (e.g. Manzini et al., 2002; Manzini and Schild, 2010; Gliem et al., 2013; Syed et al., 2017) and amino acid odorants have been used also in the functional calcium imaging experiments performed in the present study. In the present study we have shown that indeed the most common odorant responses found in the OB were responses to amino acids.

We first found that when control *Xenopus* larvae were in contact with amino acids this affected their swimming velocity and the amount of time they remained in the amino acid enriched environment of the behaviour choice tank. We then proceeded to determine if odor-induced behavior returns during olfactory system recovery after ON transection and at which time point after transection the larvae showed the same odor-induced behavioral change as under control conditions. Although at 3 weeks after ON transection high levels of recovery seem to be present relative to ORN reinnervation and amino acid induced activity of glomerular clusters in the OB (see above, Figure 3.2), we found that the recovery of olfactory guided behavior only begins to occur within the 7 to 9 week range after transection. This confirmed our strong suspicion that the recovery of amino acids-induced responses in the ORN axonal projections in the OB is not sufficient for the recovery of odor-induced behavior. Our behavioral results are in line with our morphological results and our functional calcium imaging results that showed that only about 7 weeks after ON transection MTCs regained their glomerular tufts and started responding to epithelial odorant application. In order to generate a behavioural response, MTCs, the projection neurons of the OB, need to relay the odorant information to higher brain centers that process these information and in turn generate behavioral outputs (Kermen et al., 2013; Mori and Sakano, 2021; Manzini et al., 2022).

A fast return of olfactory-guided behavior after ON transection has also been observed in goldfish (Hoyk et al., 1993; Zippel, 2000). These researchers showed that after bilateral ON axotomy, regenerated ON fibres and terminals became again visible in the OB about 10 days and two weeks post transection. This rewiring timeframe is in line with our results in *Xenopus* larvae (Hawkins et al., 2017). The same authors report that within the same timeframe after ON axotomy also odor-guided behaviour returns (von rekowski and Zippel, 1993; Zippel, 2000). This suggests that in goldfish the regeneration of the whole olfactory system and the sense of smell may be faster than in *Xenopus* larvae.

Interestingly, using a similar lesion technique in which the ON was transected in both pre-metamorphic *Xenopus laevis* and *Xenopus tropicalis* larvae, Terni and co-workers (Terni et al., 2017) found that odor-guided behavior no longer occurs in the days following lesion but recovers after 4 days. They show that the ON disappears after lesion but quickly forms a new connection with the OB after 3-4 days of recovery, after

which it progressively thickens. Comparing anatomically defined glomeruli in non-transected *Xenopus* larvae to larvae post-transection, these authors found that new glomeruli could be found after 8 days and after 15 days glomeruli were similar to those found in control animals. Given their results they conclude that the formation of glomeruli in the OB requires up to some weeks, however, they suggest that this is not required to convey olfactory information to higher brain centers. Our results contradict the results of Terni and co-workers (Terni et al., 2017) and indicate that the time frame in which odor-guided behavior returns coincides with the accurate rewiring and fully segregated odor processing streams in the OB, the recovery of specific odor tuning response profiles as well as the recovery of MTCs dendritic complexity and their ability to respond to odorants (our present work and (Hawkins et al., 2017)). We propose that the rapid recovery and rewiring of the ORN population in the OB may be necessary, as suggested by Murai and co-workers (Murai et al., 2016), to maintain MTCs capability to make dendritic connections to ORN axons. However, although necessary, we have evidence that this does not immediately provide the OB with the ability to successfully relay odor information to higher brain centers, as the MTCs only recover full dendritic tuft complexity and the ability to respond to odorants (amino acids) after 7 weeks (Hawkins et al., 2017). The necessity for second order neurons to regain tuft complexity in response to new synaptic connections and their ability to relay information to higher brain centers could very likely account for this delay between ORN rewiring and activity in the OB and recovery of the sense of smell. There may also be a necessity for refinement of ORN wiring and formation of synaptic connections during the process of building the two archetypical odor processing projection fields found in *Xenopus laevis* larvae. Our data suggests this, as a more prominent segregation of odor processing streams and recovery of all specific odor tuning response profiles only occurs after 7 weeks, and odor guided changes in behavior occur between 7 and 9 weeks. The recovery of odor-guided behavior strongly suggests recovery of complete olfactory function in higher brain centers after disruption of the olfactory network by ON transection.

Chapter 4: General discussion

The olfactory system is a complex neuronal network, that detects and interprets environmental cues, ultimately providing species-specific environmental adaptability. Surprisingly, over the course of evolution, the basic structure and function of the olfactory system has remained similar across phyla – suggesting that there are basic but optimal biological mechanisms for detection and discrimination of molecular features (Eisthen, 2002; Manzini et al., 2022). One of the main sources of phylogenetic variation in the olfactory system, that allows different species to detect highly varied chemical cues, is the large number of receptor gene families retained in the genome of each species (Eisthen, 2002).

The olfactory system is not only an interesting model system to study evolutionary processes, but it is also a fascinating model to study functional neurogenesis (Schwob, 2002; Sokpor et al., 2018). Both peripheral and central nervous system components of the olfactory system maintain the ability to generate new neurons and interneurons during development, as well as throughout adult life. After olfactory system development is complete, newly generated neurons and interneurons continuously integrate in a functional neuronal network, from both input and output circuit regions, – ORNs in the OE (Graziadei and Graziadei, 1979; Hinds et al., 1984), and interneurons in the OB (Altman, 1969; Lim and Alvarez-Buylla, 2016). In addition to this lifelong piecemeal turnover, the olfactory system is also capable of recovering from direct injury or damage (Schwob, 2002). This unique ability distinguishes the olfactory system of vertebrates from other sensory systems and network regions in the central nervous system (Takahashi et al., 2018). The reintegrative input of new ORNs generated post-lesion will be the main focus of my discussion.

Regulation of stem cell proliferation in the olfactory epithelium

In the BC layer of the mammalian OE two populations of cells can be distinguished, both of which exhibit stem cell-like characteristics (Graziadei, 1971, 1973; Graziadei and Metcalf, 1971; Murdoch and Roskams, 2007). It is in this layer that cells proliferate, differentiate and lead to the formation of new ORNs in the OE during natural cell turnover and after lesion (Andres, 1965; Graziadei and Graziadei, 1979; Schwob, 2002; Schnittke et al., 2015; Suzuki et al., 2015; Weng et al., 2016; Schwob et al.,

2017). Unsurprisingly, the complete loss of this stem/progenitor cell population has been shown to lead to the complete degeneration of the OE (Schwob et al., 1995). The two cell populations found in the basal mammalian OE include the so called globose BCs and the horizontal BCs (Calof et al., 2002). Globose BCs are round in shape, lie above horizontal BCs and have high proliferative activity (Schwartz Levey et al., 1991; Huard and Schwob, 1995) leading to the formation and regeneration of both ORNs and non-neuronal cell types of the OE (Schwartz Levey et al., 1991; Caggiano et al., 1994; DeHamer et al., 1994; Goldstein et al., 1998; Schwob, 2002, 2005; Chen et al., 2004; Beites et al., 2005). Horizontal BCs have a flattened morphology and lie adjacent to the basal lamina (Holbrook et al., 1995; Carter, 2004). These cells express cytokeratin and the stem cell markers Pax6 and Sox2 (Calof and Chikaraishi, 1989; Mackay-Sim and Kittel, 1991; Holbrook et al., 1995; Sansom et al., 2009; Guo et al., 2010; Suzuki et al., 2015). They are mostly quiescent, but have been found to proliferate after lesion (Holbrook et al., 1995; Carter, 2004; Leung et al., 2007; Iwai et al., 2008; Suzuki et al., 2013, 2015; Schwob et al., 2017).

For stem cells to become ORNs or non-neuronal cell types they need physiological instructions to proliferate and differentiate as needed to maintain olfactory function (Murdoch and Roskams, 2007; Kam et al., 2014; Schwob et al., 2017). The process of neurogenesis in the OE generally begins with the death of ORNs (Schwartz Levey et al., 1991; Carr and Farbman, 1992, 1993; Schwob et al., 1992), stimulating proliferation of stem/progenitor cells. How cell death in OE stimulates this proliferation is still not fully understood. After proliferation, progenitor cells differentiate and become committed to a certain cell fate (Schwob, 2002). In mouse, immature ORNs arise from the proliferation and differentiation of OE stem cells, and are located immediately above the BC layer (Graziadei and Graziadei, 1979; Calof and Chikaraishi, 1989; Bachmann et al., 2016). These immature ORNs have been found to express specific marker proteins, such as Lhx2, Cux2, HuC/D, β -tubulin, NCAM, GAP43 and SCGIO (Calof and Chikaraishi, 1989; Roskams et al., 1994; Pellier-Monnin et al., 2001). As they mature ORNs begin to form apical dendritic appendages and their axons project into the OB where they form functional synaptic connections with neurons of the OB (de Lorenzo, 1957; Frisch, 1967; Menco, 1980; Ronnett and Moon, 2002). Although complete ORN maturity is difficult to define it has been found to take approximately 1 week for new ORN axons to reach target synaptic areas in the OB (Miragall and

Graziadei, 1982; Schwob et al., 1992). The level of ORN maturity is generally associated with the expression of olfactory marker protein (OMP), a protein whose function is still not fully understood several decades after its discovery (Dibattista et al., 2021). The population of OMP-positive cells make up about 75 to 80% of the cell population in the adult mouse OE (Farbman and Margolis, 1980; Bachmann et al., 2016).

The complex process of generating new populations of functional cells in the OE involves highly regulated spatiotemporal expression of genes by transcription and epigenetic factors (Sokpor et al., 2018), including transcription factors Pax6, Mash1, Ngn1 and NeuroD (Nicolay et al., 2006), as well as and chromatin remodeling factors and non-coding RNA activity (Sokpor et al., 2017). Interestingly, transcription factor expression in the mouse OE has been found to be similar during embryonic and postnatal development as well as during lesion induced regeneration (Cau et al., 1997, 2002; Manglapus et al., 2004). This suggests that the regulation of cell renewal in the OE has highly overlapping characteristics during development, maintenance and repair. Both positive and negative regulatory factors have been found to be involved in the process of proliferation and differentiation of BCs in the rodent OE (**Table 1**).

Proliferation promoting	Proliferation inhibiting	Involved in differentiation
LIF <i>Bauer et al., 2003</i>	GDF-11 <i>Wu et al., 2003</i>	Neurotrophins <i>Simpson et al., 2003</i>
FGF <i>DeHamer et al., 1994</i>		PACAP <i>Hegg et al., 2003</i>
EGF <i>Carter et al., 2004</i> <i>Farbman and Buchholz, 1994</i>	TGF- β <i>Wu et al., 2003</i>	Dopamine <i>Feron et al., 1999</i>
TGF- α <i>Carter et al., 2004</i> <i>Farbman and Buchholz, 1994</i>		Nitric Oxide <i>Sulz and Bacigalupo, 2006</i>
BMPs at low concentrations <i>Shou et al., 1999; Shou et al., 2000</i>	BMPs at high concentrations <i>Shou et al., 1999; Shou et al., 2000</i>	IGF-1 <i>McCurdy et al., 2005</i>
		BDNF <i>Buckland and Cunningham, 1998</i>
		GDNF <i>Buckland and Cunningham, 1998</i>
		CNTF <i>Buckland and Cunningham, 1998</i>

Table 4.1. Factors that influence proliferation and differentiation of stem/progenitor cells in the basal cell layer of the mammalian olfactory epithelium. LIF, leukemia inhibitory factor; FGF, basic fibroblast growth factor; EGF, epidermal growth factor; TGF- α , transforming growth factor α ; BMPs, bone morphogenic proteins; GDF-11, growth and differentiation factor 11; TGF- β , transforming growth factor-

β; PACAP, pituitary adenylate cyclase-activating polypeptide; IGF-1, insulin-like growth factor 1; BDNF, brain-derived neurotrophic factor; GDNF, glial cell line-derived neurotrophic factor; CNTF, ciliary neurotrophic factor.

Nucleotides have also been found to play an important role in stem cell proliferation in the OE of larval *Xenopus laevis* (Hassenklöver et al., 2009). In larval *Xenopus* two distinct populations of basal cells have been described based on their morphology and location in the BC layer of the OE (Hassenklöver et al., 2009). The BC layer makes up about 1/3 of the *Xenopus* OE and contains stem/progenitor cells and some immature ORNs, as well as the end foot terminal regions of SCs that contact the basal lamina (Hassenklöver et al., 2009). Basal cells immediately adjacent to the basal lamina are elongated and are in close contact with each other as well as SC terminal regions (Hassenklöver et al., 2009). Between this layer of elongated basal cells and the ORN layer of the OE, polyhedral basal cells are found that do not contact the basal lamina (Hassenklöver et al., 2009). Both populations of BCs show proliferative activity under normal physiological conditions (Hassenklöver et al., 2009). In larval *Xenopus laevis*, these basal cells have been found to express metabotropic P2Y receptors, and show purinergic agonist-induced calcium transients (Hassenklöver et al., 2009). When these receptors are inhibited a substantial reduction of proliferative activity can be seen in the BC layer, indicating that purinergic signaling plays an important role in regulating stem cell proliferation in the OE of larval *Xenopus laevis* (Hassenklöver et al., 2009).

A distinction between BC populations can also be found in the fish OE, much like in the *Xenopus* and mammalian OE. In Zebrafish, two BC populations have been distinguished – based on their location in the OE; their differential expression of stem cell markers; and their differing proliferative activity. One population is continuously active, while the other activates after injury (Iqbal and Byrd-Jacobs, 2010; Bayramli et al., 2017; Demirler et al., 2020; Calvo-Ochoa et al., 2021). In the zebrafish OE, globose-like BCs express neuronal differentiation markers and are mitotically active under normal physiological conditions (Bayramli et al., 2017); whereas horizontal-like BCs are located in direct contact with the basal lamina, express different markers and proliferate after lesion (Demirler et al., 2020). In zebrafish, purinergic signaling also plays a part in stem cell turnover, but has been found to mainly be involved in

maintenance processes and not during lesion induced recovery of the OE (Demirler et al., 2020).

Injury-induced regeneration of the olfactory system of larval *Xenopus laevis*

The olfactory system, as well as its regenerative abilities, have most frequently been studied in rodents. To investigate neuroregenerative processes, several different lesion techniques have been used to damage the olfactory system of rodents, including ON transection, aspiration or ablation of the OB, or direct chemical lesions to the OE. All of these lesions cause harm to different cell populations and damage the olfactory system to different extents, subsequently varying in potential for recovery (Brann and Firestein, 2014; Steuer et al., 2014; Brann et al., 2015). In larval *Xenopus laevis* similar lesion techniques have been used to damage the olfactory system in order to study regenerative processes. In my work I transected the ON of larval *Xenopus* in order to determine key factors that lead to functional recovery (Hawkins et al., 2017, in prep). Other studies on larval *Xenopus*, using similar techniques (Manzini, 2015; Cervino et al., 2017; Terni et al., 2017) corroborate many of my findings as well as add additional information on the processes of degeneration and recovery of the olfactory system post-lesion.

I found that transection of the ON in larval *Xenopus laevis* leads to a massive increase in caspase mediate ORN cell death, which quickly returns to control levels 3 days post-lesion (Hawkins et al., 2017), similar to results found by (Cervino et al., 2017). The direct lesion to ORN axons in the ON does not noticeably affect the structure and activity of SCs, mostly targeting ORNs (Hawkins et al., 2017). The structural integrity of SCs after nerve transection was shown using immunohistochemical staining for *Xenopus* SC markers, as well as functional integrity by nucleotide stimulation (Hawkins et al., 2017). This suggests that with this lesion model, as opposed to other forms of lesion, such as chemical lesions that affect all OE cell types, SCs maintain their main biological functions in the OE during the process of regeneration. This could potentially lead to an increase in the neurogenic ability of the OE as SCs have been shown to be involved in purinergic signaling mechanisms in the OE that promote stem cell proliferation (Hassenklöver et al., 2009). In addition to an increase in ORN apoptosis, I found that odor-induced activity, – to amino acids, a natural

odorant that is known to induce responses in the ORN layer of the OE, – were no longer found in the days immediately following transection (Hawkins et al., 2017), indicating that ON transection potentially leads to the loss of all odorant responsive ORNs. However, I also used a high K^+ bath solution to stimulate all ORNs, independently of their olfactory receptor identity, and found that some responsive cells still remain in the OE in the days following transection (Hawkins et al., 2017). High K^+ bath solution responsive cells were located adjacent to the BC layer of the OE, indicating that the remaining responsive ORNs after nerve lesion are most likely progenitor cells or immature ORNs in the process of neuronal differentiation, whose axons were preserved as they had not yet extended past the site of axon transection (Hawkins et al., 2017). The complete loss of mature ORNs after ON transection is shown by the loss of all OMP-positive cells in the OE after ON transection (Cervino et al., 2017).

This massive loss of ORNs stimulates proliferative activity in stem/progenitor cells, however, the mechanisms involved in this compensatory process of neuron replacement are not fully understood. I found an increase in BrdU-positive cells in the basal cell layer of the OE, and show that a peak in proliferative activity occurs at 3 days post-transection (Hawkins et al., 2017), also shown in (Cervino et al., 2017)) coinciding with the loss of amino acid responses in the OE (Hawkins et al., 2017). I stimulated the OE with a purinergic agonist, shown to provoke responses in BCs of larval *Xenopus*, and found a massive increase in responsive cells in the basal cell layer, 3 days post-transection (Hawkins et al., 2017). This is an indication of increased proliferation of stem cells due to ORN cell death, as purinergic intraepithelial cell signaling has been found to occur in the OE and regulate neurogenesis (Hassenklöver et al., 2009). The potential interplay of SCs and BCs in the *Xenopus* OE due to purinergic signaling mechanisms (Hassenklöver et al., 2009), might potentially promote post-injury recovery of the OE.

One week after transection, BrdU-positive cells were found to return to control levels in the basal cell layer of the OE, accompanied by an increase in immature ORNs, shown by the increase in NCAM-180-positive cells (Cervino et al., 2017). After 1 week of recovery from ON transection I found a recovery of functional responses to odorant stimuli, i.e. amino acids and an increase in cells responsive to high K^+ bath solution (Hawkins et al., 2017). Using biocytin ON backfills accompanied by

immunohistochemical staining and analysis of the OE, I found a significant repopulation of ORNs in the OE after one week post-transection (Hawkins et al., 2017). This indicates that 1 week after transection, new ORNs are incorporated in the OE, due to compensatory stem cell proliferation and differentiation.

I found that the massive loss of ORNs, caused by ON transection, is accompanied by the degeneration of ORN axons in the ON and in the OB over the course of 1 week (Hawkins et al., 2017). To confirm that denervation of the OB post transection leads to the loss of olfactory function I performed calcium imaging experiments in which odor stimuli were applied to the OE and activity in the OB was recorded (Hawkins et al., 2017). I found a complete loss of odor induced activity in response to amino acids in the lateral glomerular cluster after ON transection (Hawkins et al., 2017). The lateral glomerular cluster has been functionally and anatomically described in the OB of larval *Xenopus* and has been shown to respond to amino acid stimulation under normal physiological conditions (Manzini et al., 2007; Gliem et al., 2013). I found that the loss of pre-synaptic innervation is accompanied by an increase in apoptotic somata and axons in the nerve and glomerular layer of the OB during the first 3 days post-transection (Hawkins et al., 2017). I found that cell death in these OB layers return to control levels after 1 week, however a major decrease in OB volume is found (Hawkins et al., 2017). The nerve layer of the OB, under normal physiological conditions, is primarily made up of ORN axons and juxtglomerular cells, and is surrounded by OECs that reside in the nerve layer periphery. The cell death I found in and around the nerve layer would indicate that potentially affected cell populations include juxtglomerular cells and OECs. Although surprising, I did not find any cell death in the MTC layer, where under normal physiological conditions MTCs somata are found. However, although these cells do not die as a consequence of denervation they are affected by the loss of their pre-synaptic partner. I found that 1 week post transection MTCs show a massive decrease in dendritic tuft complexity (Hawkins et al., 2017). This suggests that the functional synaptic connections with ORN axons lost after transection, lead to degradation of tuft complexity, presumably due to the loss of trophic support from the periphery.

I found that, after 1 week of recovery from ON transection, the first axons of newly formed ORNs reach the OB, and progressively rewire over the course of 2, 3 and 7 weeks post-transection (Hawkins et al., 2017). After 7 weeks of recovery, reinnervated

olfactory clusters can be anatomically distinguished in the OB (Hawkins et al., 2017), including all 4 clusters found under normal physiological condition in the OB of larval *Xenopus laevis* (Gliem et al., 2013). During this period of reinnervation, MTC dendrites begin to recover tuft complexity, starting at 3 weeks post-transection, leading to full recovery at 7 weeks post-transection (Hawkins et al., 2017). I also found that the OB recovers volume after 7 weeks, but does not fully reach control values (Hawkins et al., 2017). Our results suggest that newly innervated ORNs presumably provide trophic support to MTCs and interneurons as they reinnervate the OB, leading to the recovery of MTC dendritic tuft complexity and control levels of apoptosis in the nerve layer of the OB (Hawkins et al., 2017). However OB cell loss and full ORN reinnervation may not be complete, as the OB does not fully recover volume (Hawkins et al., 2017).

After 3 weeks of recovery, ORN axons in the glomerular layer of the OB show responses to odorant stimuli (amino acids, bile acids and amines; Hawkins et al., 2017, in prep). As ORNs reinnervate, they begin to reform the two distinct olfactory pathways in the OB (Hawkins et al., in prep) – one lateral glomerular cluster, presumably innervated by microvillar ORNs expressing V1R- or V2R-type receptors, that transmit olfactory information via cAMP-independent mechanisms (upon stimulation with amino acids); and one medial glomerular cluster, presumably innervated by ciliated ORNs expressing OR- and TAAR-type receptors, that transmit olfactory information via cAMP-dependent mechanisms (that can be stimulated by forskolin; see (Gliem et al., 2013)). I found that after ON transection these two prominent glomerular clusters are lost due to complete ORN axon degradation in the OB (Hawkins et al., 2017), but begin to be partially distinguishable after 3 weeks of recovery (Hawkins et al., 2017, in prep).

I found that under normal physiological conditions, responses of ORN axons in the OB to different stimuli could be grouped into odorant tuning profiles (Hawkins et al., in prep), presumably based on ORN odorant receptor identity and consequently odorant sensitivity. In non-transected control *Xenopus* larvae, 15 different ORN innervated regions with distinct odorant tuning profiles were found, in response to amino acid, bile acids, amines and the cAMP activator forskolin (Hawkins et al., in prep).

Although the olfactory processing pathways (lateral and medial) can already be partially distinguished in the OB after 3 weeks of recovery, a loss of specific odorant

tuning profiles in ORNs can be seen (Hawkins et al., in prep). After 3 weeks of recovery from ON transection only 12 out of the 15 distinct tuning profiles were found in the OB of larval *Xenopus* (Hawkins et al., in prep). After 7 weeks of recovery from ON transection the two olfactory processing pathways are again completely distinguishable in the OB, accompanied by the recovery of all odor tuning profiles in ORN axon innervation areas in the OB (Hawkins et al., in prep).

These findings suggests that there is a potential for recovery of odor perception in the olfactory system of larval *Xenopus laevis* post injury, as a vast amount of cell replacement and rewiring occurs over the course of 7 weeks after ON transection (Cervino et al., 2017; Hawkins et al., 2017, in prep). In previous studies, buccal pumping frequency has been shown to be related to feeding behavior, which is presumed to increase in the presence of food related odors, such as those emitted by spirulina (Cervino et al., 2017). During experiments performed on larval *Xenopus* before ON transection, 50% of larvae showed an increase in buccal pumping frequency upon stimulation with spirulina, whereas after 3 and 4 weeks of recovery, 20% of larvae showed an increase in buccal pumping frequency (Cervino et al., 2017), indicating partial recovery of olfactory function during the 4 week time period analyzed (Cervino et al., 2017).

I found that changes in behavior in larval *Xenopus laevis* can also be found upon stimulation with amino acids (Hawkins et al., in prep). I found that these changes are lost during a 3-5 week period of recovery from ON transection (Hawkins et al., in prep), most likely due to the fact that MTCs have still not fully regained dendritic tuft complexity or the capability to transmit olfactory information to higher olfactory brain centers (Hawkins et al., 2017). After 7-9 weeks of recovery from ON transection, *Xenopus laevis* larvae show recognition of odorant stimuli by change swimming velocity and environmental exploration, as seen in non-transected control larvae (Hawkins et al., in prep), indicating some recovery of olfactory function. The recovery of odorant-guided behavioral changes suggests that sufficient functional rewiring has formed that allows for appropriate detection, transmission, modulation and processing of olfactory information, which involves both peripheral and central nervous system areas.

Together, these results provide an interesting foundation for further research on the olfactory system's capability to sustain massive lesion and recover adequate odor representations that allow for odor discrimination and behavioral output. It is also interesting to note, that as the larval *Xenopus* matures, it goes through various stages of metamorphosis (Dittrich et al., 2016). During these stages a complete rewiring of the olfactory system takes place, which includes, much like after ON transection, ORN cell death and renewal, as well as ORN axon rewiring in the OB. However, during metamorphosis these events occur in a more progressive fashion.

Cell death, neurogenesis and network rewiring in the olfactory system of *Xenopus laevis* during metamorphosis

During larval stages *Xenopus* has a fully aquatic lifestyle and develops a functional olfactory system around developmental stage 40 (Nieuwkoop and Faber, 1994). Its sensory olfactory epithelia are located in two separate olfactory organs in the nose (Hansen et al., 1998), that house ORNs specialized in detecting waterborne odorants (Reiss and Burd, 1997; Nezlin and Schild, 2000; Manzini et al., 2002, 2007; Manzini and Schild, 2003). Olfactory receptor neurons from the principal cavity and the vomeronasal organ project their axons to the OB where they innervate the main OB and the accessory OB, respectively. During pro-metamorphic and metamorphic stages (54/55-58 and 58-66, respectively) the olfactory system is presumed to maintain some level of function (Hawkins et al., 2017; Syed et al., 2017), while a complete rearrangement of the olfactory circuit takes place (Nieuwkoop and Faber, 1994; Reiss and Burd, 1997; Hansen et al., 1998; Dittrich et al., 2016). During these stages, massive cell death occurs in the OE, which leads to the renewal of a majority of the ORN population (Dittrich et al., 2016). During this period an additional cavity (middle cavity) lined with olfactory sensory epithelia is formed (Reiss and Burd, 1997; Hansen et al., 1998; Gascuel and Amano, 2013). After metamorphosis is complete, the adult frog possesses a principal cavity that functions as a “air nose” and a middle cavity that functions as a newly formed “water nose”, along side the adult vomeronasal organ (Reiss and Burd, 1997; Hansen et al., 1998; Gascuel and Amano, 2013). The major repopulation the OE with new ORNs that occurs during metamorphosis, and subsequent necessity for rewiring glomeruli in the OB, leads to the formation of the

fully functional adult olfactory system, that can detect both water and airborne odorants (Weiss et al., 2021).

These metamorphic phases of massive ORN death and renewal, followed by rewiring in the OB, are similar in many ways to what occurs during recovery from ON transection. This would suggest that the olfactory system of larval *Xenopus* is more readily adapted to sustain high levels of ORN loss, at least during these metamorphic stages. Our results show that after ON transection, performed on *Xenopus* larvae around stages 48-52, before metamorphic changes would take place, some mechanisms that support the functional regenerative capacity during metamorphosis might also play a part in the capacity for recovery from lesion. It is also likely that the olfactory system of larval *Xenopus* might retain some developmental-like characteristics that are more permissive for extensive recovery from injury.

Injury induced regeneration of the mammalian olfactory system

The recovery of olfactory function in mammalian olfactory systems has been found to be highly variable and dependent on the location and severity of the lesion. In mammalian olfactory systems, the transection of the ON has been found to mostly preserve the OB, in the sense that synaptic targets are maintained intact for newly generated ORNs to reinnervate (Yee and Costanzo, 1995, 1998; Koster and Costanzo, 1996; Costanzo, 2000; Christensen, 2001). However, the structure and blood supply to the ON has been found to be disrupted (Schwob, 2002), as well as a notable invasion of macrophages at the lesion site (Berger, 1971; Taskinen and Røyttä, 1997). Similarly, my results show that the second order neurons in the OB of larval *Xenopus* remain intact as potential synaptic targets, as they do not undergo apoptosis after nerve transection (Hawkins et al., 2017), and possibly provide trophic support to newly innervating ORNs.

Transection of the ON in the mammalian olfactory system has been found to lead to apoptosis of ORNs whose axons transverse the site of lesion, leading to the subsequent degeneration of axonal projections in the ON and OB (Graziadei and Graziadei, 1979; Holcomb et al., 1995). This ORN cell death was found to lead to an increase in proliferation of globose BCs (Schwartz Levey et al., 1991), while other cells in the OE were not noticeably affected (SCs and immature ORNs). After recovery, however, a higher level of proliferation was found to remain in the BC layer,

comparatively to non-transected animals, as well as a higher proportion of immature ORNs (Costanzo, 1984; Christensen, 2001). My results also show that massive ORN cell death leads to BC proliferation, while SCs remain mostly unaffected, and that some possibly immature ORNs may remain in the OE after lesion (Hawkins et al., 2017). Whether a higher proportion of immature ORNs remain after recovery is unknown, however (Cervino et al., 2017) show that the intermediate layer of the OE remains reduced over the course of 4 weeks of recovery from ON transection.

Aspiration or ablation of the OB in the mammalian olfactory system was found to lead to ORN apoptosis and degeneration of all ORN axons that had previously innervated the OB (Graziadei and Graziadei, 1979; Holcomb et al., 1995). This loss of ORNs, in turn was found to lead to the increase of proliferation of stem cells in the basal cell layer of the OE (Graziadei and Graziadei, 1979; Holcomb et al., 1995). Here again SCs and immature ORNs were not found to be directly affected by the lesion. With aspiration or ablation of the OB, full recovery of the OE was not found, presumably due to the lack of trophic support that comes from the OB (Carr and Farbman, 1992, 1993; Schwob et al., 1992). Additionally, the ORN population after injury was found to remain mostly immature (Graziadei and Monti Graziadei, 1983; Verhaagen et al., 1990; Schwob et al., 1992), likely due to the lack of synaptic targets which in turn lead to ORN degeneration (Schwob et al., 1992). In (Hawkins et al., 2017), I show that weekly ON transection leads to continual degeneration of the OB, shown by a reduction in volume. This would suggest that trophic support is between the OE and the OB is mutual. The OB cannot recover from lesion without pre-synaptic input and trophic support from the periphery, and vice-versa.

Chemical lesions, directly applied in solution to the OE, such as ZnSO₄ and Triton X-100, have been found to cause cell death in all olfactory epithelial cell population (Schultz, 1941, 1960; Smith, 1951; Mulvaney and Heist, 1971; Matulionis, 1975, 1976; Harding et al., 1978; Burd, 1993), and severe lesions were found to lead to the complete loss of OE regions (Schwob et al., 1995). The inhalation of methyl bromide, another toxic agent, can also be used to directly lesion the OE, and has been found to lead to a more successful recovery, as some cells in the BC layer are spared. After 8 weeks of recovery after methyl bromide inhalation the OE was found to be similar to control non-lesioned animals (Hurtt et al., 1988; Schwob et al., 1995).

With each lesion model discussed, regenerated ORNs have been found to express olfactory receptor protein types in the correct anatomical locations in the OE (Costanzo, 2000; Iwema and Schwob, 2003). However, a higher percentage of immature ORNs are found in the OE post-lesion (Verhaagen et al., 1989, 1990; Schwob et al., 1992, 1995; Loo et al., 1996), presumably due to the unsuccessful retargeting of ORN axons in the OB. In both ON transection and direct OE damage by toxic chemical substances, reinnervation of the OB has been found to take around 2-3 weeks (Graziadei et al., 1980; Schwob et al., 1999; Christensen, 2001), at which point a substantial amount of innervation of the olfactory neuron layer and the glomerular layer can be seen (Yee and Costanzo, 1995; Costanzo, 2000).

Although substantial recovery can be seen also in the mammalian olfactory system after injury, errors in axon targeting in the glomerular layer of the OB can be found after newly formed ORN establish synaptic connections (Ring et al., 1997; Schwob et al., 1999; Gogos et al., 2000; Christensen, 2001; Cheung et al., 2014). These errors in ORN axon targeting could alter odor representations in the brain which could potentially lead to olfactory dysfunction (Murai et al., 2016). Altered connectivity affects spatial mapping at the glomerular level, which is important for accurate odor perception and can affect behavior. After recovery from ON transection, rodents have been found to be able to perform simple odorant discrimination tasks successfully (Yee and Costanzo, 1995, 1998). After 2 months of recovery from direct lesion to the rodent OE by inhalation of methyl bromide, animals were found to be capable of correctly performing odorant identification tasks, learned before lesion (Youngentob et al., 1997). However, subtle alterations of olfactory encoding in the OB were found to affect the performance in some animals (Youngentob et al., 2001).

Olfactory dysfunction and odor representations in the olfactory bulb

Olfactory dysfunction in humans can occur after head trauma or infections that damage the olfactory system (Doty et al., 1997; Meisami et al., 1998). As mentioned previously, the disruption of odor perception after damage may be caused by the mistargeting of ORN axons during reinnervation of the OB (Yee and Costanzo, 1998; Vedin et al., 2004). Recovery from lesions in the mammalian OE, if not too severe, generally leads to the complete ORN repopulation of the OE with substantial accuracy, in terms of OE topography of olfactory receptor identity (Schwob et al., 1999; Iwema,

2004). However, these newly formed ORNs must project their axons into the OB and form functional connections in the appropriate in order to adequately transmit olfactory information. During normal development and maintenance of the olfactory system of mammals, ORNs with the same olfactory receptor identity, project their axons to specific subsets of glomeruli in the OB (Mombaerts et al., 1996), creating a representative topographical map of receptor identity in the central nervous system (Strotmann et al., 2000; Schaefer et al., 2001; Costanzo and Kobayashi, 2010). Subsets of ORNs with their corresponding olfactory receptor identities are distributed in different domains of the OE and target different glomerular regions in the OB, creating a representation of these OE domains in the central nervous system (Bozza et al., 2009; Pacifico et al., 2012). Studies on the rodent olfactory systems ability to recover from lesion have shown that errors occurs during the process of ORN reinnervation of the OB (Schwob et al., 1999; Costanzo, 2000; St John and Key, 2003; McMillan Carr et al., 2004; Blanco-Hernández et al., 2012). Targeting errors seem to disrupt ORNs ability to converge their axons onto the appropriate glomerular structure, leading to the formation of small dispersed glomerular-like structures (Costanzo, 2000; St John and Key, 2003; Blanco-Hernández et al., 2012; Cheung et al., 2014). However, functional experiments have shown the glomeruli can recover to a large extent in the correct OB domains after the loss of ORN input, and show equivalent response magnitudes to odor stimuli (Cheung et al., 2014). This coarse recovery of odor processing streams indicates that some axon targeting mechanisms are still active in the adult olfactory system (Cheung et al., 2014). Axon targeting mechanisms include olfactory receptor protein expression (Singer et al., 1995; Mombaerts et al., 1996; Wang et al., 1998; Feinstein et al., 2004), glial cell responses to damage (Kafitz and Greer, 1998, 1999; Bartolomei and Greer, 2000), and axon interactions. Lesions that cause the complete loss of all ORNs have been found to lead to higher mistargeting of ORNs in the OB, which may be caused by reduced axon-axon interactions along the ON that usually provide guidance to newly formed ORN axons as they make their way to the appropriate location in the OB. An important relationship that promotes accurate axon targeting exists between ORNs and OECs. These cells enwrap hundreds of ORN axons as they exit the OE, along the ON and along the periphery of the ON layer in the OB (Doucette, 1991; Schwob, 2002; Barraud et al., 2010). This enwrapment maintains axon-axon interactions between ORNs and help segregate ORN bundles targeted for different regions of the OB (Schwob, 2002).

These OECs can migrate from the OE along the ON to the OB (Windus et al., 2007, 2011; Chehrehasa et al., 2012), and provide axon growth promoting properties (Ramón-Cueto and Valverde, 1995; Imaizumi et al., 1998).

In larval *Xenopus laevis* a comprehensive description of ORN receptor identity in the OE and the exact target locations in the OB have yet to be discovered. However, it is clear that some axon guidance mechanisms are still in place as two distinct olfactory processing pathways are reformed in the OB after ON transection (Hawkins et al., in prep). This process of ORN reinnervation leads to the recovery of second order neurons in the OB and the reformation of odor representations in the brain, to an extent sufficient for the recovery of odor-guided behavior (Hawkins et al., in prep).

Summary

The olfactory system is a window to the chemical world, that permits each species to adapt to novel spaces and situations. Despite the various phylogenetic adaptations, this sensory system maintains similar functional and structural features (Eisthen, 2002). One of these shared features is the regenerative capability of the olfactory system, due to the maintenance of stem cell niches that replace neurons throughout life and after lesion. The disruption and damage of olfactory systems in different species allows us to compare these neurogenic processes and potentially find features that are more or less permissive for the recovery of function, potentially providing clinical relevance (Lledo and Valley, 2016; Shohayeb et al., 2018).

I lesioned the olfactory system of larval *Xenopus laevis*, by severing the olfactory nerve, causing loss of olfactory function. Over the course of approximately 2 months, distinct populations of ORNs are regenerated, capable of accurately rewiring in the OB, leading to the morphological and functional recovery of second order neurons and consequently to the recovery of odor representations in the brain that allow for odor recognition (Hawkins et al., 2017; Hawkins et al., in prep). I show that odor-guided behavioral changes are lost after ON transection, and recover after a 7 to 9 week period after lesion (Hawkins et al., in prep). My findings show a clear interplay between peripheral and central nervous system trophic support during the process of recovery from damage. Further comparative analyses of recovery from olfactory system lesion between vertebrate phyla would contribute to the understanding of what factors or mechanisms promote or inhibit the recovery of odor perception.

Acknowledgements

It is difficult to find the words to thank everyone in the way that I would like to. I am so grateful for my family and childhood friends, for all our adventures and misfortunes, and for the never ending support on my quest to understand life. I would like to thank Guido Maiello for always being there to lift me up when life gets tough, putting up with my grumpy potato vibes, for being my personal MasterChef, and for showing me how to enjoy the beautiful moments. Here's to many more beautiful moments with you. I would like to thank my scientific supervisors, Ivan Manzini and Thomas Hassenklöver, for all the time and effort they have put into improving my work over the past 7 years. All Manzini Lab Group members, past and present, thank you for accompanying me on this PhD adventure, for all the late lab nights, the inside jokes and for always being my substitute lablings. And finally I would like to express my gratitude to all CMPB program leaders, staff and members, as well as my TAC members for providing me with this opportunity, for their guidance and scientific advice.

List of abbreviations

Abbreviations used in the introduction and general discussion:

- AA:** amino acid
ACIII: adenylyl cyclase III
ANO: anoctamin
ATP: adenosine triphosphate
AUC: area under the curve
BC: basal cell
BrdU: bromodeoxyuridine
cAMP: cyclic adenosine monophosphate
Cux2: cut like homeobox 2
DAG: diacylglycerol
DMSO: dimethyl sulfoxide
FPR: formyl-peptide receptors
Fsk: forskolin
GAP43: growth associated protein 43
GDP: guanosine diphosphate
GPCR: G protein coupled receptor
GTP: guanosine triphosphate
IP3: inositol triphosphate
Lhx2: LIM homeobox 2
MS: ethyl 3-aminobenzoate methanesulfonate
MS4A: membrane-spanning 4A receptors
MTC: mitral/tufted cell
NCAM: neural cell adhesion molecule
NeuroD: neurogenic differentiation
Ngn1: neurogenin 1
OB: olfactory bulb
OE: olfactory epithelium
OEC: olfactory ensheathing cell
OlfC: OR class C-related
OMP: olfactory marker protein

ON: olfactory nerve

OR: odorant receptor

ORA: OR class A-related

ORI: odorant response index

ORN: olfactory receptor neuron

PLC: phospholipase C

PN: projection neuron

SC: supporting cell

TAAR: trace amine associated receptor

TRPC2: transient receptor potential cation channel 2

V1R: vomeronasal type-1 receptor

V2R: vomeronasal type-2 receptor

VR: vomeronasal receptor

W: water

List of figures and tables

Figure 1.1: General wiring structure of the vertebrate olfactory system and proliferative activity in the olfactory bulb (adapted from Manzini et al., 2022).

Figure 1.2: General structure of the vertebrate olfactory epithelium and proliferative activity (adapted from Manzini et al., 2022).

Figure 1.3: Features and wiring characteristics in the olfactory system of larval *Xenopus laevis* (adapted from Weiss et al., 2021).

Figure 2.1: Olfactory nerve transection as a model injury to induce neuronal damage in the olfactory system of larval *Xenopus laevis*.

Figure 2.2: Timeline of structural and functional changes in the main olfactory epithelium after olfactory nerve transection.

Figure 2.3: Olfactory nerve transection induces transitional olfactory bulb volume reduction due to axonal degradation of olfactory receptor neurons and subsequent reinnervation by new neurons.

Figure 2.4: Increased levels of apoptotic cells in anterior layers of the olfactory bulb after olfactory nerve transection.

Figure 2.5: Dynamic changes of mitral/tufted cell dendritic tuft complexity in the olfactory bulb after olfactory nerve transection.

Figure 2.6: Functional changes in mitral/tufted cell and glomerular layer of the lateral glomerular cluster of the olfactory bulb after olfactory nerve transection.

Table 3.1: Stimuli used during calcium imaging experiments in the olfactory bulb of larval *Xenopus*.

Figure 3.1: Odor-induced receptor neuron axon terminal activity in the olfactory bulb of larval *Xenopus*.

Figure 3.2: Receptor neuron reinnervation of the olfactory bulb shows spatially and functionally distinct glomerular clusters are reformed after nerve transection in larval *Xenopus*.

Figure 3.3: Tuning profiles of olfactory receptor neuron axon terminal regions in the olfactory bulb of larval *Xenopus* – before and during recovery from olfactory nerve transection.

Figure 3.4: Motion tracking experimental setup and larval *Xenopus* behavior without application of odorant stimuli.

Figure 3.5: Behavioral responses to odor stimuli in non-transected *Xenopus* larvae.

Figure 3.6: Behavioral responses to odor stimuli in transected *Xenopus* larvae at different time-points during recovery from olfactory nerve transection.

Table 4.1: Factors that influence proliferation and differentiation of stem/progenitor cells in the basal cell layer of the mammalian olfactory epithelium.

References

- Ache BW, Young JM (2005) Olfaction: Diverse Species, Conserved Principles. *Neuron* 48:417–430.
- Alioto TS, Ngai J (2006) The repertoire of olfactory C family G protein-coupled receptors in zebrafish: candidate chemosensory receptors for amino acids. *BMC Genomics* 7:309.
- Altman J (1969) Autoradiographic and histological studies of postnatal neurogenesis. IV. Cell proliferation and migration in the anterior forebrain, with special reference to persisting neurogenesis in the olfactory bulb. *The Journal of Comparative Neurology* 137:433–457.
- Altman J, Das GD (1965) Autoradiographic and histological evidence of postnatal hippocampal neurogenesis in rats. *The Journal of Comparative Neurology* 124:319–335.
- Altner H (1962) Untersuchungen über Leistungen und Bau der Nase des sudafrikanischen Krallenfrosches *Xenopus laevis* (Daudin, 1803). *Zeitschrift für Vergleichende Physiologie* 45:272–306.
- Amano T, Gascuel J (2012) Expression of Odorant Receptor Family, Type 2 OR in the Aquatic Olfactory Cavity of Amphibian Frog *Xenopus tropicalis* Matsunami H, ed. *PLoS ONE* 7:e33922.
- Amjad A, Hernandez-Clavijo A, Pifferi S, Maurya DK, Boccaccio A, Franzot J, Rock J, Menini A (2015) Conditional knockout of TMEM16A/anoctamin1 abolishes the calcium-activated chloride current in mouse vomeronasal sensory neurons. *Journal of General Physiology* 145:285–301.
- Andres KH (1965) Differenzierung und Regeneration von Sinneszellen in der Regio olfactoria. *Die Naturwissenschaften* 52:500–500.
- Bachmann C, Nguyen H, Rosenbusch J, Pham L, Rabe T, Patwa M, Sokpor G, Seong RH, Ashery-Padan R, Mansouri A, Stoykova A, Staiger JF, Tuoc T (2016) mSWI/SNF (BAF) Complexes Are Indispensable for the Neurogenesis and Development of Embryonic Olfactory Epithelium Hamilton BA, ed. *PLOS Genetics* 12:e1006274.
- Bakalyar HA, Reed RR (1990) Identification of a Specialized Adenylyl Cyclase That May Mediate Odorant Detection. *Science* 250:1403–1406.
- Barraud P, Seferiadis AA, Tyson LD, Zwart MF, Szabo-Rogers HL, Ruhrberg C, Liu KJ, Baker CVH (2010) Neural crest origin of olfactory ensheathing glia. *Proceedings of the National Academy of Sciences* 107:21040–21045.
- Bartolomei JC, Greer CA (2000) Olfactory Ensheathing Cells: Bridging the Gap in Spinal Cord Injury. *Neurosurgery* 47:1057–1069.

- Bartoshuk LM (1989) The Functions of Taste and Olfaction. *Annals of the New York Academy of Sciences* 575:353–362.
- Bayramli X, Kocagöz Y, Sakizli U, Fuss SH (2017) Patterned Arrangements of Olfactory Receptor Gene Expression in Zebrafish are Established by Radial Movement of Specified Olfactory Sensory Neurons. *Scientific Reports* 7:5572.
- Bear DM, Lassance J-M, Hoekstra HE, Datta SR (2016) The Evolving Neural and Genetic Architecture of Vertebrate Olfaction. *Current Biology* 26:R1039–R1049.
- Beites CL, Kawauchi S, Crocker CE, Calof AL (2005) Identification and molecular regulation of neural stem cells in the olfactory epithelium. *Experimental Cell Research* 306:309–316.
- Benzekri NA, Reiss JO (2012) Olfactory metamorphosis in the coastal tailed frog *Ascaphus truei* (Amphibia, Anura, Leiopelmatidae). *Journal of Morphology* 273:68–87.
- Berger B (1971) Etude Ultrastructurale de la Dégénérescence Wallérienne Expérimentale d'un Nerf Entièrement Amyélinique: le Nerf Olfactif. *Journal of Ultrastructure Research* 37:105–118.
- Blanco-Hernández E, Valle-Leija P, Zomosa-Signoret V, Drucker-Colín R, Vidaltamayo R (2012) Odor Memory Stability after Reinnervation of the Olfactory Bulb Ravel N, ed. *PLoS ONE* 7:e46338.
- Blaustein AR, O'hara RK (1982) Kin recognition in *Rana cascadae* tadpoles: maternal and paternal effects. *Animal Behaviour* 30:1151–1157.
- Boesveldt S, Parma V (2021) The importance of the olfactory system in human well-being, through nutrition and social behavior. *Cell and Tissue Research* 383:559–567.
- Bozza T, Vassalli A, Fuss S, Zhang J-J, Weiland B, Pacifico R, Feinstein P, Mombaerts P (2009) Mapping of Class I and Class II Odorant Receptors to Glomerular Domains by Two Distinct Types of Olfactory Sensory Neurons in the Mouse. *Neuron* 61:220–233.
- Brann JH, Ellis DP, Ku BS, Spinazzi EF, Firestein S (2015) Injury in aged animals robustly activates quiescent olfactory neural stem cells. *Frontiers in Neuroscience* 9.
- Brann JH, Firestein SJ (2014) A lifetime of neurogenesis in the olfactory system. *Frontiers in Neuroscience* 8.
- Breer H (2003) Olfactory receptors: molecular basis for recognition and discrimination of odors. *Analytical and Bioanalytical Chemistry* 377:427–433.
- Buck L, Axel R (1991) A novel multigene family may encode odorant receptors: A molecular basis for odor recognition. *Cell* 65:175–187.

- Buck LB (1996) Information Coding in the Vertebrate Olfactory System. *Annual Review of Neuroscience* 19:517–544.
- Burd GD (1993) Morphological study of the effects of intranasal zinc sulfate irrigation on the mouse olfactory epithelium and olfactory bulb. *Microscopy Research and Technique* 24:195–213.
- Bushdid C, Magnasco MO, Vosshall LB, Keller A (2014) Humans Can Discriminate More than 1 Trillion Olfactory Stimuli. *Science* 343:1370–1372.
- Byrd CA (2000) Deafferentation-induced changes in the olfactory bulb of adult zebrafish. *Brain Research* 866:92–100.
- Byrd CA, Burd GD (1991) Development of the olfactory bulb in the clawed frog, *Xenopus laevis*: A morphological and quantitative analysis. *The Journal of Comparative Neurology* 314:79–90.
- Byrd CA, Burd GD (1993) The quantitative relationship between olfactory axons and mitral/tufted cells in developing *Xenopus* with partially deafferented olfactory bulbs. *Journal of Neurobiology* 24:1229–1242.
- Caggiano M, Kauer JS, Hunter DD (1994) Globose basal cells are neuronal progenitors in the olfactory epithelium: A lineage analysis using a replication-incompetent retrovirus. *Neuron* 13:339–352.
- Calof AL, Bonnin A, Crocker C, Kawauchi S, Murray RC, Shou J, Wu H-H (2002) Progenitor cells of the olfactory receptor neuron lineage. *Microscopy Research and Technique* 58:176.
- Calof AL, Chikaraishi DM (1989) Analysis of neurogenesis in a mammalian neuroepithelium: Proliferation and differentiation of an olfactory neuron precursor in vitro. *Neuron* 3:115–127.
- Calvo-Ochoa E, Byrd-Jacobs CA, Fuss SH (2021) Diving into the streams and waves of constitutive and regenerative olfactory neurogenesis: insights from zebrafish. *Cell and Tissue Research* 383:227–253.
- Caprio J, Byrd RP (1984) Electrophysiological evidence for acidic, basic, and neutral amino acid olfactory receptor sites in the catfish. *Journal of General Physiology* 84:403–422.
- Carr VM, Farbman AI (1993) The Dynamics of Cell Death in the Olfactory Epithelium. *Experimental Neurology* 124:308–314.
- Carr VMcM, Farbman AI (1992) Ablation of the olfactory bulb up-regulates the rate of neurogenesis and induces precocious cell death in olfactory epithelium. *Experimental Neurology* 115:55–59.
- Carr WES, Derby CD (1986) Chemically stimulated feeding behavior in marine animals: Importance of chemical mixtures and involvement of mixture interactions. *Journal of Chemical Ecology* 12:989–1011.

- Carr WES, Gleeson RA, Trapido-Rosenthal HG (1990) The role of perireceptor events in chemosensory processes. *Trends in Neurosciences* 13:212–215.
- Carter LA (2004) Olfactory Horizontal Basal Cells Demonstrate a Conserved Multipotent Progenitor Phenotype. *Journal of Neuroscience* 24:5670–5683.
- Cau E, Casarosa S, Guillemot F (2002) *Mash1* and *Ngn1* control distinct steps of determination and differentiation in the olfactory sensory neuron lineage. *Development* 129:1871–1880.
- Cau E, Gradwohl G, Fode C, Guillemot F (1997) Mash1 activates a cascade of bHLH regulators in olfactory neuron progenitors. *Development* 124:1611–1621.
- Caviness VS, Takahashi T, Nowakowski RS (1995) Numbers, time and neocortical neurogenesis: a general developmental and evolutionary model. *Trends in Neurosciences* 18:379–383.
- Cervino AS, Paz DA, Frontera JL (2017) Neuronal degeneration and regeneration induced by axotomy in the olfactory epithelium of *Xenopus laevis*: Olfactory Neurogenesis After Axotomy. *Developmental Neurobiology* 77:1308–1320.
- Chamero P, Leinders-Zufall T, Zufall F (2012) From genes to social communication: molecular sensing by the vomeronasal organ. *Trends in Neurosciences* 35:597–606.
- Chehrehasa F, Ekberg JAK, Lineburg K, Amaya D, Mackay-Sim A, St. John JA (2012) Two phases of replacement replenish the olfactory ensheathing cell population after injury in postnatal mice. *Glia* 60:322–332.
- Chen X, Fang H, Schwob JE (2004) Multipotency of purified, transplanted globose basal cells in olfactory epithelium. *The Journal of Comparative Neurology* 469:457–474.
- Chen Y, Getchell ML, Ding X, Getchell TV (1992) Immunolocalization of two cytochrome P450 isozymes in rat nasal chemosensory tissue: *NeuroReport* 3:749–752.
- Cheung MC, Jang W, Schwob JE, Wachowiak M (2014) Functional recovery of odor representations in regenerated sensory inputs to the olfactory bulb. *Frontiers in Neural Circuits* 7.
- Christensen MD (2001) Rhinotomy is Disrupted During the Re-innervation of the Olfactory Bulb that Follows Transection of the Olfactory Nerve. *Chemical Senses* 26:359–369.
- Christie KJ, Turnley AM (2013) Regulation of endogenous neural stem/progenitor cells for neural repair—factors that promote neurogenesis and gliogenesis in the normal and damaged brain. *Frontiers in Cellular Neuroscience* 6.
- Coelho DH, Costanzo RM (2016) Posttraumatic olfactory dysfunction. *Auris Nasus Larynx* 43:137–143.

- Costanzo RM (1984) Comparison of neurogenesis and cell replacement in the hamster olfactory system with and without a target (olfactory bulb). *Brain Research* 307:295–301.
- Costanzo RM (2000) Rewiring the Olfactory Bulb: Changes in Odor Maps following Recovery from Nerve Transection. *Chemical Senses* 25:199–205.
- Costanzo RM (2005) Regeneration and Rewiring the Olfactory Bulb. *Chemical Senses* 30:i133–i134.
- Costanzo RM, Kobayashi M (2010) Age-Related Changes in P2 Odorant Receptor Mapping in the Olfactory Bulb. *Chemical Senses* 35:417–426.
- Couper Leo JM, Brunjes PC (2003) Neonatal focal denervation of the rat olfactory bulb alters cell structure and survival: a Golgi, Nissl and confocal study. *Developmental Brain Research* 140:277–286.
- Cowan CM, Roskams AJ (2002) Apoptosis in the mature and developing olfactory neuroepithelium. *Microscopy Research and Technique* 58:204.
- Cummings DM, Snyder JS, Brewer M, Cameron HA, Belluscio L (2014) Adult Neurogenesis Is Necessary to Refine and Maintain Circuit Specificity. *The Journal of Neuroscience* 34:13801–13810.
- Czesnik D, Kuduz J, Schild D, Manzini I (2006) ATP activates both receptor and sustentacular supporting cells in the olfactory epithelium of *Xenopus laevis* tadpoles. *European Journal of Neuroscience* 23:119–128.
- Date-Ito A, Ohara H, Ichikawa M, Mori Y, Hagino-Yamagishi K (2008) *Xenopus* V1R Vomeronasal Receptor Family Is Expressed in the Main Olfactory System. *Chemical Senses* 33:339–346.
- de Lorenzo AJ (1957) ELECTRON MICROSCOPIC OBSERVATIONS OF THE OLFACTORY MUCOSA AND OLFACTORY NERVE. *The Journal of Biophysical and Biochemical Cytology* 3:839–850.
- De Franceschi G, Vivattanasarn T, Saleem AB, Solomon SG (2016) Vision Guides Selection of Freeze or Flight Defense Strategies in Mice. *Current Biology* 26:2150–2154.
- DeHamer MK, Guevara JL, Hannon K, Olwin BB, Calof AL (1994) Genesis of olfactory receptor neurons in vitro: Regulation of progenitor cell divisions by fibroblast growth factors. *Neuron* 13:1083–1097.
- Del Punta K, Puche A, Adams NC, Rodriguez I, Mombaerts P (2002) A Divergent Pattern of Sensory Axonal Projections Is Rendered Convergent by Second-Order Neurons in the Accessory Olfactory Bulb. *Neuron* 35:1057–1066.
- DeMaria S, Berke AP, Van Name E, Heravian A, Ferreira T, Ngai J (2013) Role of a Ubiquitously Expressed Receptor in the Vertebrate Olfactory System. *Journal of Neuroscience* 33:15235–15247.

- Demirler MC, Sakizli U, Bali B, Kocagöz Y, Eski SE, Ergöner A, Alkiraz AS, Bayramli X, Hassenklöver T, Manzini I, Fuss SH (2020) Purinergic signalling selectively modulates maintenance but not repair neurogenesis in the zebrafish olfactory epithelium. *The FEBS Journal* 287:2699–2722.
- Dibattista M, Al Koborssy D, Genovese F, Reisert J (2021) The functional relevance of olfactory marker protein in the vertebrate olfactory system: a never-ending story. *Cell Tissue Res* 383:409–427.
- Dibattista M, Amjad A, Maurya DK, Sagheddu C, Montani G, Tirindelli R, Menini A (2012) Calcium-activated chloride channels in the apical region of mouse vomeronasal sensory neurons. *Journal of General Physiology* 140:3–15.
- Ding X, Coon MJ (1988) Purification and characterization of two unique forms of cytochrome P-450 from rabbit nasal microsomes. *Biochemistry* 27:8330–8337.
- Dittrich K, Kuttler J, Hassenklöver T, Manzini I (2016) Metamorphic remodeling of the olfactory organ of the African clawed frog, *Xenopus laevis*: Metamorphic Remodeling of the Olfactory Organ. *Journal of Comparative Neurology* 524:986–998.
- Doty R (2009) The Olfactory System and Its Disorders. *Seminars in Neurology* 29:074–081.
- Doty RL, Yousem DM, Pham LT, Kreshak AA, Geckle R, Lee WW (1997) Olfactory Dysfunction in Patients With Head Trauma. *Archives of Neurology* 54:1131–1140.
- Doucette R (1991) PNS-CNS transitional zone of the first cranial nerve. *The Journal of Comparative Neurology* 312:451–466.
- Dulac C, Axel R (1995) A novel family of genes encoding putative pheromone receptors in mammals. *Cell* 83:195–206.
- Eilers PH, Boelens HF (2005) Baseline correction with asymmetric least squares smoothing. *Leiden University Medical Centre Report*:5.
- Eisthen HL (1992) Phylogeny of the vomeronasal system and of receptor cell types in the olfactory and vomeronasal epithelia of vertebrates. *Microscopy Research and Technique* 23:1–21.
- Eisthen HL (1997) Evolution of Vertebrate Olfactory Systems. *Brain, Behavior and Evolution* 50:222–233.
- Eisthen HL (2002) Why Are Olfactory Systems of Different Animals So Similar? *Brain, Behavior and Evolution* 59:273–293.
- Falk N, Lösl M, Schröder N, Gießl A (2015) Specialized Cilia in Mammalian Sensory Systems. *Cells* 4:500–519.
- Farbman AI (1990) Olfactory neurogenesis: genetic or environmental controls? *Trends in Neurosciences* 13:362–365.

- Farbman AI (1992) Cell biology of olfaction. Cambridge ; New York, N.Y., USA: Cambridge University Press.
- Farbman AI, Margolis FL (1980) Olfactory marker protein during ontogeny: Immunohistochemical localization. *Developmental Biology* 74:205–215.
- Feinstein P, Bozza T, Rodriguez I, Vassalli A, Mombaerts P (2004) Axon Guidance of Mouse Olfactory Sensory Neurons by Odorant Receptors and the β 2 Adrenergic Receptor. *Cell* 117:833–846.
- Feinstein P, Mombaerts P (2004) A Contextual Model for Axonal Sorting into Glomeruli in the Mouse Olfactory System. *Cell* 117:817–831.
- Ferreira TA, Blackman AV, Oyrer J, Jayabal S, Chung AJ, Watt AJ, Sjöström PJ, van Meyel DJ (2014) Neuronal morphometry directly from bitmap images. *Nature Methods* 11:982–984.
- Ferretti P (2011) Is there a relationship between adult neurogenesis and neuron generation following injury across evolution?: Adult neurogenesis, regeneration and evolution. *European Journal of Neuroscience* 34:951–962.
- Figueres-Oñate M, Sánchez-Villalón M, Sánchez-González R, López-Mascaraque L (2019) Lineage Tracing and Cell Potential of Postnatal Single Progenitor Cells In Vivo. *Stem Cell Reports* 13:700–712.
- Firestein S, Darrow B, Shepherd GM (1991) Activation of the sensory current in salamander olfactory receptor neurons depends on a G protein-mediated cAMP second messenger system. *Neuron* 6:825–835.
- Fredriksson R, Lagerström MC, Lundin L-G, Schiöth HB (2003) The G-Protein-Coupled Receptors in the Human Genome Form Five Main Families. Phylogenetic Analysis, Paralogon Groups, and Fingerprints. *Molecular Pharmacology* 63:1256–1272.
- Freitag J, Beck A, Ludwig G, von Buchholtz L, Breer H (1999) On the origin of the olfactory receptor family: receptor genes of the jawless fish (*Lampetra fluviatilis*). *Gene* 226:165–174.
- Freitag J, Krieger J, Strotmann J, Breer H (1995) Two classes of olfactory receptors in *xenopus laevis*. *Neuron* 15:1383–1392.
- Fried HU, Fuss SH, Korsching SI (2002) Selective imaging of presynaptic activity in the mouse olfactory bulb shows concentration and structure dependence of odor responses in identified glomeruli. *Proceedings of the National Academy of Sciences* 99:3222–3227.
- Friedrich J, Zhou P, Paninski L (2017) Fast online deconvolution of calcium imaging data Vogelstein J, ed. *PLOS Computational Biology* 13:e1005423.
- Frisch D (1967) Ultrastructure of mouse olfactory mucosa. *American Journal of Anatomy* 121:87–119.

- Frontera JL, Cervino AS, Jungblut LD, Paz DA (2015) Brain-derived neurotrophic factor (BDNF) expression in normal and regenerating olfactory epithelium of *Xenopus laevis*. *Annals of Anatomy - Anatomischer Anzeiger* 198:41–48.
- Frontera JL, Raices M, Cervino AS, Pozzi AG, Paz DA (2016) Neural regeneration dynamics of *Xenopus laevis* olfactory epithelium after zinc sulfate-induced damage. *Journal of Chemical Neuroanatomy* 77:1–9.
- Gage FH (2002) Neurogenesis in the Adult Brain. *The Journal of Neuroscience* 22:612–613.
- Gaillard I, Rouquier S, Giorgi D (2004) Olfactory receptors. *Cellular and Molecular Life Sciences (CMLS)* 61:456–469.
- Gascuel J, Amano T (2013) Exotic Models May Offer Unique Opportunities to Decipher Specific Scientific Question: The Case of *Xenopus* Olfactory System: The Case of *Xenopus* Olfactory System. *The Anatomical Record* 296:1453–1461.
- Gelperin A (1999) Oscillatory dynamics and information processing in olfactory systems. *Journal of Experimental Biology* 202:1855–1864.
- Giovannucci A, Friedrich J, Gunn P, Kalfon J, Brown BL, Koay SA, Taxidis J, Najafi F, Gauthier JL, Zhou P, Khakh BS, Tank DW, Chklovskii DB, Pnevmatikakis EA (2019) CalmAn an open source tool for scalable calcium imaging data analysis. *eLife* 8:e38173.
- Glezer I, Malnic B (2019) Olfactory receptor function. In: *Handbook of Clinical Neurology*, pp 67–78. Elsevier.
- Gliem S, Syed AS, Sansone A, Kludt E, Tantalaki E, Hassenklöver T, Korsching SI, Manzini I (2013) Bimodal processing of olfactory information in an amphibian nose: odor responses segregate into a medial and a lateral stream. *Cellular and Molecular Life Sciences* 70:1965–1984.
- Godoy R, Hua K, Kalyn M, Cusson V-M, Anisman H, Ekker M (2020) Dopaminergic neurons regenerate following chemogenetic ablation in the olfactory bulb of adult Zebrafish (*Danio rerio*). *Scientific Reports* 10:12825.
- Gogos JA, Osborne J, Nemes A, Mendelsohn M, Axel R (2000) Genetic Ablation and Restoration of the Olfactory Topographic Map. *Cell* 103:609–620.
- Goldstein BJ, Fang H, Youngentob SL, Schwob JE (1998) Transplantation of multipotent progenitors from the adult olfactory epithelium: *NeuroReport* 9:1611–1617.
- Gradwell N (1971) *Ascaphus* tadpole: experiments on the suction and gill irrigation mechanisms. *Canadian Journal of Zoology* 49:307–332.
- Graziadei PPC (1971) The Olfactory Mucosa of Vertebrates. In: *Olfaction* (Beidler LM, ed), pp 27–58 *Handbook of Sensory Physiology*. Berlin, Heidelberg: Springer Berlin Heidelberg.

- Graziadei PPC (1973) Cell dynamics in the olfactory mucosa. *Tissue and Cell* 5:113–131.
- Graziadei PPC, DeHan RS (1973) NEURONAL REGENERATION IN FROG OLFACTORY SYSTEM. *Journal of Cell Biology* 59:525–530.
- Graziadei PPC, Graziadei GAM (1979) Neurogenesis and neuron regeneration in the olfactory system of mammals. I. Morphological aspects of differentiation and structural organization of the olfactory sensory neurons. *Journal of Neurocytology* 8:1–18.
- Graziadei PPC, Karlan MS, Monti GA, Bernstein JJ (1980) Neurogenesis of sensory neurons in the primate olfactory system after section of the fila olfactoria. *Brain Research* 186:289–300.
- Graziadei PPC, Metcalf JF (1971) Autoradiographic and ultrastructural observations on the frog's olfactory mucosa. *Z Zellforsch* 116:305–318.
- Graziadei PPC, Monti Graziadei AG (1983) Regeneration in the olfactory system of vertebrates. *American Journal of Otolaryngology* 4:228–233.
- Graziadei PPC, Monti Graziadei GA (1978) Continuous Nerve Cell Renewal in the Olfactory System. In: *Development of Sensory Systems* (Jacobson M, ed), pp 55–83 *Handbook of Sensory Physiology*. Berlin, Heidelberg: Springer Berlin Heidelberg.
- Greer PL, Bear DM, Lassance J-M, Bloom ML, Tsukahara T, Pashkovski SL, Masuda FK, Nowlan AC, Kirchner R, Hoekstra HE, Datta SR (2016) A Family of non-GPCR Chemosensors Defines an Alternative Logic for Mammalian Olfaction. *Cell* 165:1734–1748.
- Gudziol V, Hoenck I, Landis B, Podlesek D, Bayn M, Hummel T (2014) The impact and prospect of traumatic brain injury on olfactory function: a cross-sectional and prospective study. *European Archives of Oto-Rhino-Laryngology* 271:1533–1540.
- Guo Z, Packard A, Krolewski RC, Harris MT, Manglapus GL, Schwob JE (2010) Expression of Pax6 and Sox2 in adult olfactory epithelium. *The Journal of Comparative Neurology* 518:4395–4418.
- Haas K, Jensen K, Sin WC, Foa L, Cline HT (2002) Targeted electroporation in *Xenopus* tadpoles in vivo – from single cells to the entire brain. *Differentiation* 70:148–154.
- Hagino-Yamagishi K, Moriya K, Kubo H, Wakabayashi Y, Isobe N, Saito S, Ichikawa M, Yazaki K (2004) Expression of vomeronasal receptor genes in *Xenopus laevis*. *The Journal of Comparative Neurology* 472:246–256.
- Hansen A, Reiss JO, Gentry CL, Burd GD (1998) Ultrastructure of the olfactory organ in the clawed frog, *Xenopus laevis*, during larval development and metamorphosis. *The Journal of Comparative Neurology* 398:273–288.

- Hansson BS, Stensmyr MC (2011) Evolution of Insect Olfaction. *Neuron* 72:698–711.
- Hänzi S, Straka H (2018) Wall following in *Xenopus laevis* is barrier-driven. *Journal of Comparative Physiology A* 204:183–195.
- Hara TJ (2006) Feeding behaviour in some teleosts is triggered by single amino acids primarily through olfaction. *Journal of Fish Biology* 68:810–825.
- Harding JW, Getchell TV, Margolis FL (1978) Denervation of the primary olfactory pathway in mice. V. Long-term effect of intranasal ZnSO₄ irrigation on behavior, biochemistry and morphology. *Brain Research* 140:271–285.
- Hart AC, Chao MY (2010) From Odors to Behaviors in *Caenorhabditis elegans*. In: *The Neurobiology of Olfaction* (Menini A, ed) *Frontiers in Neuroscience*. Boca Raton (FL): CRC Press/Taylor & Francis.
- Hashiguchi Y, Nishida M (2007) Evolution of Trace Amine–Associated Receptor (TAAR) Gene Family in Vertebrates: Lineage-Specific Expansions and Degradations of a Second Class of Vertebrate Chemosensory Receptors Expressed in the Olfactory Epithelium. *Molecular Biology and Evolution* 24:2099–2107.
- Hassenklöver T, Kurtanska S, Bartoszek I, Junek S, Schild D, Manzini I (2008) Nucleotide-induced Ca²⁺ signaling in sustentacular supporting cells of the olfactory epithelium. *Glia* 56:1614–1624.
- Hassenklöver T, Manzini I (2013) Olfactory Wiring Logic in Amphibians Challenges the Basic Assumptions of the Unbranched Axon Concept. *Journal of Neuroscience* 33:17247–17252.
- Hassenklöver T, Manzini I (2014) The Olfactory System as a Model to Study Axonal Growth Patterns and Morphology In Vivo. *JoVE*:52143.
- Hassenklöver T, Schwartz P, Schild D, Manzini I (2009) Purinergic Signaling Regulates Cell Proliferation of Olfactory Epithelium Progenitors. *STEM CELLS* 27:2022–2031.
- Hawkins SJ, Weiss L, Offner T, Dittrich K, Hassenklöver T, Manzini I (2017) Functional Reintegration of Sensory Neurons and Transitional Dendritic Reduction of Mitral/Tufted Cells during Injury-Induced Recovery of the Larval *Xenopus* Olfactory Circuit. *Frontiers in Cellular Neuroscience* 11:380.
- Hawkins SJ, Yvonne G, Offner T, Weiss L, Maiello G, Hassenklöver T, Manzini I (in prep) Restoration of distinct odor processing streams in the olfactory bulb underlies the recovery of odor-guided behavior after injury in larval *Xenopus laevis*.
- Heerema JL, Bogart SJ, Helbing CC, Pyle GG (2020) Olfactory epithelium ontogenesis and function in postembryonic North American Bullfrog (*Rana* (*Lithobates*) *atesbeiana*) tadpoles. *Canadian Journal of Zoology* 98:367–375.

- Herrada G, Dulac C (1997) A Novel Family of Putative Pheromone Receptors in Mammals with a Topographically Organized and Sexually Dimorphic Distribution. *Cell* 90:763–773.
- Hildebrand JG, Shepherd GM (1997) Mechanisms of Olfactory Discrimination: Converging Evidence for Common Principles Across Phyla. *Annual Review of Neuroscience* 20:595–631.
- Hinds JW, Hinds PL, McNelly NA (1984) An autoradiographic study of the mouse olfactory epithelium: Evidence for long-lived receptors. *The Anatomical Record* 210:375–383.
- Holbrook EH, Szumowski KEM, Schwob JE (1995) An immunochemical, ultrastructural, and developmental characterization of the horizontal basal cells of rat olfactory epithelium. *The Journal of Comparative Neurology* 363:129–146.
- Holcomb JD, Mumm JS, Calof AL (1995) Apoptosis in the Neuronal Lineage of the Mouse Olfactory Epithelium: Regulation in Vivo and in Vitro. *Developmental Biology* 172:307–323.
- Holl A-M (2018) Survival of mature mouse olfactory sensory neurons labeled genetically perinatally. *Molecular and Cellular Neuroscience* 88:258–269.
- Hoover KC (2010) Smell with inspiration: The evolutionary significance of olfaction. *American Journal of Physical Anthropology* 143:63–74.
- Hoyk Z, Lago-Schaaf T, Zippel HP, Füzesi G, Halász N (1993) Fast regeneration of the olfactory nerve in goldfish: fine structure and behaviour. *Journal Fur Hirnforschung* 34:461–465.
- Huard JMT, Schwob JE (1995) Cell cycle of globose basal cells in rat olfactory epithelium. *Developmental Dynamics* 203:17–26.
- Huard JMT, Youngentob SL, Goldstein BJ, Luskin MB, Schwob JE (1998) Adult olfactory epithelium contains multipotent progenitors that give rise to neurons and non-neural cells. *The Journal of Comparative Neurology* 400:469–486.
- Hurt ME, Thomas DA, Working PK, Monticello TM, Morgan KT (1988) Degeneration and regeneration of the olfactory epithelium following inhalation exposure to methyl bromide: Pathology, cell kinetics, and olfactory function. *Toxicology and Applied Pharmacology* 94:311–328.
- Hussain A, Saraiva LR, Korsching SI (2009) Positive Darwinian selection and the birth of an olfactory receptor clade in teleosts. *Proceedings of the National Academy of Sciences* 106:4313–4318.
- Imai T, Sakano H (2011) Axon-axon interactions in neuronal circuit assembly: lessons from olfactory map formation: Axon-axon interactions in olfactory map formation. *European Journal of Neuroscience* 34:1647–1654.

- Imaizumi T, Lankford KL, Waxman SG, Greer CA, Kocsis JD (1998) Transplanted Olfactory Ensheathing Cells Remyelinate and Enhance Axonal Conduction in the Demyelinated Dorsal Columns of the Rat Spinal Cord. *The Journal of Neuroscience* 18:6176–6185.
- Imamura F, Greer CA (2009) Dendritic Branching of Olfactory Bulb Mitral and Tufted Cells: Regulation by TrkB Matsunami H, ed. *PLoS ONE* 4:e6729.
- Iqbal T, Byrd-Jacobs C (2010) Rapid Degeneration and Regeneration of the Zebrafish Olfactory Epithelium after Triton X-100 Application. *Chemical Senses* 35:351–361.
- Iwai N, Zhou Z, Roop DR, Behringer RR (2008) Horizontal Basal Cells Are Multipotent Progenitors in Normal and Injured Adult Olfactory Epithelium. *STEM CELLS* 26:1298–1306.
- Iwema CL (2004) Odorant Receptor Expression Patterns Are Restored in Lesion-Recovered Rat Olfactory Epithelium. *Journal of Neuroscience* 24:356–369.
- Iwema CL, Schwob JE (2003) Odorant receptor expression as a function of neuronal maturity in the adult rodent olfactory system. *The Journal of Comparative Neurology* 459:209–222.
- Jia C, Doherty JP, Crudgington S, Hegg CC (2009) Activation of purinergic receptors induces proliferation and neuronal differentiation in Swiss Webster mouse olfactory epithelium. *Neuroscience* 163:120–128.
- Jia C, Hayoz S, Hutch CR, Iqbal TR, Pooley AE, Hegg CC (2013) An IP3R3- and NPY-Expressing Microvillous Cell Mediates Tissue Homeostasis and Regeneration in the Mouse Olfactory Epithelium Mezey E, ed. *PLoS ONE* 8:e58668.
- Jia C, Hegg CC (2010) NPY mediates ATP-induced neuroproliferation in adult mouse olfactory epithelium. *Neurobiology of Disease* 38:405–413.
- Joiner AM, Green WW, McIntyre JC, Allen BL, Schwob JE, Martens JR (2015) Primary Cilia on Horizontal Basal Cells Regulate Regeneration of the Olfactory Epithelium. *The Journal of Neuroscience* 35:13761–13772.
- Junek S, Chen T-W, Alevra M, Schild D (2009) Activity Correlation Imaging: Visualizing Function and Structure of Neuronal Populations. *Biophysical Journal* 96:3801–3809.
- Jungblut LD, Pozzi AG, Paz DA (2012) A putative functional vomeronasal system in anuran tadpoles. *Journal of Anatomy* 221:364–372.
- Kafitz KW, Greer CA (1998) Differential expression of extracellular matrix and cell adhesion molecules in the olfactory nerve and glomerular layers of adult rats. *Journal of Neurobiology* 34:271–282.
- Kafitz KW, Greer CA (1999) Olfactory ensheathing cells promote neurite extension from embryonic olfactory receptor cells in vitro. *Glia* 25:99–110.

- Kam JWK, Raja R, Cloutier J (2014) Cellular and molecular mechanisms regulating embryonic neurogenesis in the rodent olfactory epithelium. *International Journal of Developmental Neuroscience* 37:76–86.
- Kang J, Caprio J (1995) In vivo responses of single olfactory receptor neurons in the channel catfish, *Ictalurus punctatus*. *Journal of Neurophysiology* 73:172–177.
- Kaplan MS, Hinds JW (1977) Neurogenesis in the Adult Rat: Electron Microscopic Analysis of Light Radioautographs. *Science* 197:1092–1094.
- Kaslin J, Ganz J, Brand M (2008) Proliferation, neurogenesis and regeneration in the non-mammalian vertebrate brain. *Philosophical Transactions of the Royal Society B: Biological Sciences* 363:101–122.
- Katada S (2005) Structural Basis for a Broad But Selective Ligand Spectrum of a Mouse Olfactory Receptor: Mapping the Odorant-Binding Site. *Journal of Neuroscience* 25:1806–1815.
- Kauffman SL (1968) Lengthening of the generation cycle during embryonic differentiation of the mouse neural tube. *Experimental Cell Research* 49:420–424.
- Kempermann G, Gage FH (2008) Neurogenesis in the Adult Hippocampus. In: *Novartis Foundation Symposia* (Chadwick DJ, Goode JA, eds), pp 220–241. Chichester, UK: John Wiley & Sons, Ltd.
- Kermen F, Franco LM, Wyatt C, Yaksi E (2013) Neural circuits mediating olfactory-driven behavior in fish. *Frontiers in Neural Circuits* 7.
- Kim S, Ma L, Yu CR (2011) Requirement of calcium-activated chloride channels in the activation of mouse vomeronasal neurons. *Nature Communications* 2:365.
- Kleene S, Gesteland R (1991) Calcium-activated chloride conductance in frog olfactory cilia. *The Journal of Neuroscience* 11:3624–3629.
- Klenoff JR, Greer CA (1998) Postnatal development of olfactory receptor cell axonal arbors. *The Journal of Comparative Neurology* 390:256–267.
- Kobayashi M, Costanzo RM (2009) Olfactory Nerve Recovery Following Mild and Severe Injury and the Efficacy of Dexamethasone Treatment. *Chemical Senses* 34:573–580.
- Kosaka T, Kosaka K (2016) Neuronal organization of the main olfactory bulb revisited. *Anatomical Science International* 91:115–127.
- Koster NL, Costanzo RM (1996) Electrophysiological characterization of the olfactory bulb during recovery from sensory deafferentation. *Brain Research* 724:117–120.
- Kurahashi T, Yau K-W (1993) Co-existence of cationic and chloride components in odorant-induced current of vertebrate olfactory receptor cells. *Nature* 363:71–74.

- Kurian SM, Naressi RG, Manoel D, Barwich A-S, Malnic B, Saraiva LR (2021) Odor coding in the mammalian olfactory epithelium. *Cell and Tissue Research* 383:445–456.
- Larriva-Sahd J (2008) The accessory olfactory bulb in the adult rat: A cytological study of its cell types, neuropil, neuronal modules, and interactions with the main olfactory system. *The Journal of Comparative Neurology* 510:309–350.
- Leinders-Zufall T, Brennan P, Widmayer P, S. PC, Maul-Pavicic A, Jäger M, Li X-H, Breer H, Zufall F, Boehm T (2004) MHC Class I Peptides as Chemosensory Signals in the Vomeronasal Organ. *Science* 306:1033–1037.
- Lepousez G, Valley MT, Lledo P-M (2013) The Impact of Adult Neurogenesis on Olfactory Bulb Circuits and Computations. *Annual Review of Physiology* 75:339–363.
- Leung CT, Coulombe PA, Reed RR (2007) Contribution of olfactory neural stem cells to tissue maintenance and regeneration. *Nature Neuroscience* 10:720–726.
- Li Q, Liberles SD (2015) Aversion and Attraction through Olfaction. *Current Biology* 25:R120–R129.
- Liberles SD, Buck LB (2006) A second class of chemosensory receptors in the olfactory epithelium. *Nature* 442:645–650.
- Liberles SD, Horowitz LF, Kuang D, Contos JJ, Wilson KL, Siltberg-Liberles J, Liberles DA, Buck LB (2009) Formyl peptide receptors are candidate chemosensory receptors in the vomeronasal organ. *Proceedings of the National Academy of Sciences* 106:9842–9847.
- Lim DA, Alvarez-Buylla A (2016) The Adult Ventricular–Subventricular Zone (V-SVZ) and Olfactory Bulb (OB) Neurogenesis. *Cold Spring Harbor Perspectives in Biology* 8:a018820.
- Liman ER, Corey DP, Dulac C (1999) TRP2: A candidate transduction channel for mammalian pheromone sensory signaling. *Proceedings of the National Academy of Sciences* 96:5791–5796.
- Lledo P-M, Gheusi G, Vincent J-D (2005) Information Processing in the Mammalian Olfactory System. *Physiological Reviews* 85:281–317.
- Lledo P-M, Valley M (2016) Adult Olfactory Bulb Neurogenesis. *Cold Spring Harbor Perspectives in Biology* 8:a018945.
- Lodovichi C (2021) Topographic organization in the olfactory bulb. *Cell and Tissue Research* 383:457–472.
- Lois C, Alvarez-Buylla A (1994) Long-Distance Neuronal Migration in the Adult Mammalian Brain. *Science* 264:1145–1148.

- Loo AT, Youngentob SL, Kent PF, Schwob JE (1996) The aging olfactory epithelium: Neurogenesis, response to damage, and odorant-induced activity. *International Journal of Developmental Neuroscience* 14:881–900.
- Lowe G, Gold GH (1993a) Contribution of the ciliary cyclic nucleotide-gated conductance to olfactory transduction in the salamander. *The Journal of Physiology* 462:175–196.
- Lowe G, Gold GH (1993b) Nonlinear amplification by calcium-dependent chloride channels in olfactory receptor cells. *Nature* 366:283–286.
- Lucas P, Ukhanov K, Leinders-Zufall T, Zufall F (2003) A Diacylglycerol-Gated Cation Channel in Vomeronasal Neuron Dendrites Is Impaired in TRPC2 Mutant Mice. *Neuron* 40:551–561.
- Mackay-Sim A, Kittel PW (1991) On the Life Span of Olfactory Receptor Neurons. *European Journal of Neuroscience* 3:209–215.
- Malun D, Brunjes PC (1996) Development of olfactory glomeruli: Temporal and spatial interactions between olfactory receptor axons and mitral cells in opossums and rats. *The Journal of Comparative Neurology* 368:1–16.
- Manglapus GL, Youngentob SL, Schwob JE (2004) Expression patterns of basic helix-loop-helix transcription factors define subsets of olfactory progenitor cells. *The Journal of Comparative Neurology* 479:216–233.
- Manoel D, Makhlof M, Scialdone A, Saraiva LR (2019) Interspecific variation of olfactory preferences in flies, mice, and humans. *Chemical Senses* 44:7–9.
- Manzini I (2015) From neurogenesis to neuronal regeneration: the amphibian olfactory system as a model to visualize neuronal development in vivo. *Neural Regeneration Research* 10:872.
- Manzini I, Frasnelli J, Croy I (2014) How we smell and what it means to us: basic principles of the sense of smell. *HNO* 62:846–852.
- Manzini I, Heermann S, Czesnik D, Brase C, Schild D, Rössler W (2007) Presynaptic protein distribution and odour mapping in glomeruli of the olfactory bulb of *Xenopus laevis* tadpoles: Odour mapping in glomerular clusters. *European Journal of Neuroscience* 26:925–934.
- Manzini I, Rössler W, Schild D (2002) cAMP-independent responses of olfactory neurons in *Xenopus laevis* tadpoles and their projection onto olfactory bulb neurons. *The Journal of Physiology* 545:475–484.
- Manzini I, Schild D (2003) cAMP-independent olfactory transduction of amino acids in *Xenopus laevis* tadpoles. *The Journal of Physiology* 551:115–123.
- Manzini I, Schild D (2004) Classes and Narrowing Selectivity of Olfactory Receptor Neurons of *Xenopus laevis* Tadpoles. *Journal of General Physiology* 123:99–107.

- Manzini I, Schild D (2010) Olfactory Coding in Larvae of the African Clawed Frog *Xenopus laevis*. In: The Neurobiology of Olfaction (Menini A, ed) *Frontiers in Neuroscience*. Boca Raton (FL): CRC Press/Taylor & Francis.
- Manzini I, Schild D, Di Natale C (2022) Principles of odor coding in vertebrates and artificial chemosensory systems. *Physiological Reviews* 102:61–154.
- Matsumoto H, Kobayakawa K, Kobayakawa R, Tashiro T, Mori K, Sakano H, Mori K (2010) Spatial Arrangement of Glomerular Molecular-Feature Clusters in the Odorant-Receptor Class Domains of the Mouse Olfactory Bulb. *Journal of Neurophysiology* 103:3490–3500.
- Matsunami H, Buck LB (1997) A Multigene Family Encoding a Diverse Array of Putative Pheromone Receptors in Mammals. *Cell* 90:775–784.
- Matthews MR, Powell TP (1962) Some observations on transneuronal cell degeneration in the olfactory bulb of the rabbit. *Journal of Anatomy* 96:89–102.
- Matulionis DH (1975) Ultrastructural study of mouse olfactory epithelium following destruction by ZnSO₄ and its subsequent regeneration. *American Journal of Anatomy* 142:67–89.
- Matulionis DH (1976) Light and electron microscopic study of the degeneration and early regeneration of olfactory epithelium in the mouse. *American Journal of Anatomy* 145:79–99.
- McMillan Carr V, Ring G, Youngentob SL, Schwob JE, Farbman AI (2004) Altered epithelial density and expansion of bulbar projections of a discrete HSP70 immunoreactive subpopulation of rat olfactory receptor neurons in reconstituting olfactory epithelium following exposure to methyl bromide. *The Journal of Comparative Neurology* 469:475–493.
- Meisami E, Mikhail L, Baim D, Bhatnagar KP (1998) Human Olfactory Bulb: Aging of Glomeruli and Mitral Cells and a Search for the Accessory Olfactory Bulba. *Annals of the New York Academy of Sciences* 855:708–715.
- Meisami E, Safari L (1981) A quantitative study of the effects of early unilateral olfactory deprivation on the number and distribution of mitral and tufted cells and of glomeruli in the rat olfactory bulb. *Brain Research* 221:81–107.
- Meister M, Bonhoeffer T (2001) Tuning and Topography in an Odor Map on the Rat Olfactory Bulb. *The Journal of Neuroscience* 21:1351–1360.
- Menco BertPhM (1984) Ciliated and microvillous structures of rat olfactory and nasal respiratory epithelia: A study using ultra-rapid cryo-fixation followed by freeze-substitution or freeze-etching. *Cell and Tissue Research* 235.
- Menco M (1980) Qualitative and quantitative freeze-fracture studies on olfactory and nasal respiratory epithelial surfaces of frog, ox, rat, and dog: II. Cell apices, cilia, and microvilli. *Cell and Tissue Research* 211.

- Mezler M, Konzelmann S, Freitag J, Rössler P, Breer H (1999) Expression of olfactory receptors during development in *Xenopus laevis*. *Journal of Experimental Biology* 202:365–376.
- Miragall F, Graziadei GAM (1982) Experimental studies on the olfactory marker protein. II. Appearance of the olfactory marker protein during differentiation of the olfactory sensory neurons of mouse: an immunohistochemical and autoradiographic study. *Brain Research* 239:245–250.
- Miragall F, Kremer M, Dermietzel R (1994) Intercellular Communications Via Gap Junctions in the Olfactory System. In: *Olfaction and Taste XI* (Kurihara K, Suzuki N, Ogawa H, eds), pp 32–35. Tokyo: Springer Japan.
- Mirza RS, Ferrari MCO, Kiesecker JM, Chivers DP (2006) Responses of American toad tadpoles to predation cues: behavioural response thresholds, threat-sensitivity and acquired predation recognition. *Behaviour* 143:877–889.
- Mizrahi A, Katz LC (2003) Dendritic stability in the adult olfactory bulb. *Nature Neuroscience* 6:1201–1207.
- Mombaerts P (2006) Axonal Wiring in the Mouse Olfactory System. *Annual Review of Cell and Developmental Biology* 22:713–737.
- Mombaerts P, Wang F, Dulac C, Chao SK, Nemes A, Mendelsohn M, Edmondson J, Axel R (1996) Visualizing an Olfactory Sensory Map. *Cell* 87:675–686.
- Monti Graziadei GA, Graziadei PPC (1979) Neurogenesis and neuron regeneration in the olfactory system of mammals. II. Degeneration and reconstitution of the olfactory sensory neurons after axotomy. *Journal of Neurocytology* 8:197–213.
- Mori K, Sakano H (2011) How Is the Olfactory Map Formed and Interpreted in the Mammalian Brain? *Annual Review of Neuroscience* 34:467–499.
- Mori K, Sakano H (2021) Olfactory Circuitry and Behavioral Decisions. *Annual Review of Physiology* 83:231–256.
- Moulton DG (1974) DYNAMICS OF CELL POPULATIONS IN THE OLFACTORY EPITHELIUM. *Annals of the New York Academy of Sciences* 237:52–61.
- Moulton DG, Çelebi G, Fink RP (2008) Olfaction in Mammals—Two Aspects: Proliferation of Cells in the Olfactory Epithelium and Sensitivity to Odours. In: *Novartis Foundation Symposia* (Wolstenholme GEW, Knight J, eds), pp 227–250. Chichester, UK: John Wiley & Sons, Ltd.
- Mouret A, Lepousez G, Gras J, Gabellec M-M, Lledo P-M (2009) Turnover of Newborn Olfactory Bulb Neurons Optimizes Olfaction. *Journal of Neuroscience* 29:12302–12314.
- Mulvaney BD, Heist HE (1971) Regeneration of rabbit olfactory epithelium. *American Journal of Anatomy* 131:241–251.

- Münch J, Billig G, Hübner CA, Leinders-Zufall T, Zufall F, Jentsch TJ (2018) Ca²⁺-activated Cl⁻ currents in the murine vomeronasal organ enhance neuronal spiking but are dispensable for male–male aggression. *Journal of Biological Chemistry* 293:10392–10403.
- Murai A, Iwata R, Fujimoto S, Aihara S, Tsuboi A, Muroyama Y, Saito T, Nishizaki K, Imai T (2016) Distorted Coarse Axon Targeting and Reduced Dendrite Connectivity Underlie Dysosmia after Olfactory Axon Injury. *eneuro* 3:ENEURO.0242-16.2016.
- Murdoch B, Roskams AJ (2007) Olfactory epithelium progenitors: insights from transgenic mice and in vitro biology. *Journal of Molecular Histology* 38:581–599.
- Nagayama S, Homma R, Imamura F (2014) Neuronal organization of olfactory bulb circuits. *Frontiers in Neural Circuits* 8.
- Nakamura T, Gold GH (1987) A cyclic nucleotide-gated conductance in olfactory receptor cilia. *Nature* 325:442–444.
- Nakamuta S, Nakamuta N, Taniguchi K (2011) Distinct axonal projections from two types of olfactory receptor neurons in the middle chamber epithelium of *Xenopus laevis*. *Cell and Tissue Research* 346:27–33.
- Nezlin LP, Heermann S, Schild D, Rössler W (2003) Organization of glomeruli in the main olfactory bulb of *Xenopus laevis* tadpoles: Olfactory Glomeruli in *Xenopus laevis*. *Journal of Comparative Neurology* 464:257–268.
- Nezlin LP, Schild D (2000) Structure of the olfactory bulb in tadpoles of *Xenopus laevis*. *Cell and Tissue Research* 302:21–29.
- Nezlin LP, Schild D (2005) Individual olfactory sensory neurons project into more than one glomerulus in *Xenopus laevis* tadpole olfactory bulb. *The Journal of Comparative Neurology* 481:233–239.
- Nicolay DJ, Doucette JR, Nazarali AJ (2006) Transcriptional Regulation of Neurogenesis in the Olfactory Epithelium. *Cellular and Molecular Neurobiology* 26:801–819.
- Nieuwkoop PD, Faber J eds. (1994) Normal table of *Xenopus laevis* (Daudin): a systematical and chronological survey of the development from the fertilized egg till the end of metamorphosis. New York: Garland Pub.
- Niimura Y, Nei M (2005) Comparative evolutionary analysis of olfactory receptor gene clusters between humans and mice. *Gene* 346:13–21.
- Nishizumi H, Sakano H (2015) Developmental regulation of neural map formation in the mouse olfactory system: Neural Map Formation in the Mouse Olfactory System. *Developmental Neurobiology* 75:594–607.

- Nomura T, Takahashi S, Ushiki T (2004) Cytoarchitecture of the normal rat olfactory epithelium: Light and scanning electron microscopic studies. *Archives of Histology and Cytology* 67:159–170.
- Offner T, Daume D, Weiss L, Hassenklöver T, Manzini I (2020) Whole-Brain Calcium Imaging in Larval *Xenopus*. *Cold Spring Harbor Protocols* 2020:pdb.prot106815.
- Olivares J, Schmachtenberg O (2019) An update on anatomy and function of the teleost olfactory system. *PeerJ* 7:e7808.
- Otsu N (1979) A Threshold Selection Method from Gray-Level Histograms. *IEEE Trans Syst, Man, Cybern* 9:62–66.
- Pace U, Hanski E, Salomon Y, Lancet D (1985) Odorant-sensitive adenylate cyclase may mediate olfactory reception. *Nature* 316:255–258.
- Pacifico R, Dewan A, Cawley D, Guo C, Bozza T (2012) An Olfactory Subsystem that Mediates High-Sensitivity Detection of Volatile Amines. *Cell Reports* 2:76–88.
- Pellier-Monnin V, Astic L, Bichet S, Riederer BM, Grenningloh G (2001) Expression of SCG10 and stathmin proteins in the rat olfactory system during development and axonal regeneration. *The Journal of Comparative Neurology* 433:239–254.
- Pfister P, Rodriguez I (2005) Olfactory expression of a single and highly variable V1r pheromone receptor-like gene in fish species. *Proceedings of the National Academy of Sciences* 102:5489–5494.
- Pinching AJ, Powell TPS (1971a) The Neuropil of the Glomeruli of the Olfactory Bulb. *Journal of Cell Science* 9:347–377.
- Pinching AJ, Powell TPS (1971b) The Neuron Types of the Glomerular Layer of the Olfactory Bulb. *Journal of Cell Science* 9:305–345.
- Pnevmatikakis EA, Giovannucci A (2017) NoRMCorre: An online algorithm for piecewise rigid motion correction of calcium imaging data. *Journal of Neuroscience Methods* 291:83–94.
- Pozzi A (2015) Cytotoxic Effect of 5-Bromo-2-Deoxyuridine on Olfactory Epithelium. *MOJAP* 1.
- Preibisch S, Saalfeld S, Tomancak P (2009) Globally optimal stitching of tiled 3D microscopic image acquisitions. *Bioinformatics* 25:1463–1465.
- Raices M (2020) Evidence of the peptide identity of the epidermal alarm cue in tadpoles of the toad *Rhinella arenarum*. *Herpetological Journal*:230–233.
- Rall W, Shepherd GM, Reese TS, Brightman MW (1966) Dendrodendritic synaptic pathway for inhibition in the olfactory bulb. *Experimental Neurology* 14:44–56.

- Ramón-Cueto A, Valverde F (1995) Olfactory bulb ensheathing glia: A unique cell type with axonal growth-promoting properties: OLFACTORY BULB ENSHEATHING GLIA. *Glia* 14:163–173.
- Reiss JO, Burd GD (1997) Metamorphic remodeling of the primary olfactory projection in *Xenopus*: Developmental independence of projections from olfactory neuron subclasses. *Journal of Neurobiology* 32:213–222.
- Ressler KJ, Sullivan SL, Buck LB (1993) A zonal organization of odorant receptor gene expression in the olfactory epithelium. *Cell* 73:597–609.
- Ressler KJ, Sullivan SL, Buck LB (1994) Information coding in the olfactory system: Evidence for a stereotyped and highly organized epitope map in the olfactory bulb. *Cell* 79:1245–1255.
- Ring G, Mezza RC, Schwob JE (1997) Immunohistochemical identification of discrete subsets of rat olfactory neurons and the glomeruli that they innervate. *The Journal of Comparative Neurology* 388:415–434.
- Rivière S, Challet L, Fluegge D, Spehr M, Rodriguez I (2009) Formyl peptide receptor-like proteins are a novel family of vomeronasal chemosensors. *Nature* 459:574–577.
- Rodriguez-Gil DJ, Bartel DL, Jaspers AW, Mobley AS, Imamura F, Greer CA (2015) Odorant receptors regulate the final glomerular coalescence of olfactory sensory neuron axons. *Proceedings of the National Academy of Sciences* 112:5821–5826.
- Rolen SH, Sorensen PW, Mattson D, Caprio J (2003) Polyamines as olfactory stimuli in the goldfish *Carassius auratus*. *Journal of Experimental Biology* 206:1683–1696.
- Ronnett GV, Moon C (2002) G Proteins and Olfactory Signal Transduction. *Annual Review of Physiology* 64:189–222.
- Roskams A, Bethel M, Hurt K, Ronnett G (1996) Sequential expression of Trks A, B, and C in the regenerating olfactory neuroepithelium. *The Journal of Neuroscience* 16:1294–1307.
- Roskams AJ, Bredt DS, Dawson TM, Ronnett GV (1994) Nitric oxide mediates the formation of synaptic connections in developing and regenerating olfactory receptor neurons. *Neuron* 13:289–299.
- Rosler W (2002) Aggregation of F-Actin in Olfactory Glomeruli: a Common Feature of Glomeruli Across Phyla. *Chemical Senses* 27:803–810.
- Rünnenburger K, Breer H, Boekhoff I (2002) Selective G protein $\beta\gamma$ -subunit compositions mediate phospholipase C activation in the vomeronasal organ. *European Journal of Cell Biology* 81:539–547.
- Ryba NJP, Tirindelli R (1997) A New Multigene Family of Putative Pheromone Receptors. *Neuron* 19:371–379.

- Sansom SN, Griffiths DS, Faedo A, Kleinjan D-J, Ruan Y, Smith J, van Heyningen V, Rubenstein JL, Livesey FJ (2009) The Level of the Transcription Factor Pax6 Is Essential for Controlling the Balance between Neural Stem Cell Self-Renewal and Neurogenesis Hébert JM, ed. *PLoS Genetics* 5:e1000511.
- Sansone A, Hassenklöver T, Syed AS, Korsching SI, Manzini I (2014) Phospholipase C and Diacylglycerol Mediate Olfactory Responses to Amino Acids in the Main Olfactory Epithelium of an Amphibian Reisert J, ed. *PLoS ONE* 9:e87721.
- Saraiva LR, Korsching SI (2007) A novel olfactory receptor gene family in teleost fish. *Genome Research* 17:1448–1457.
- Sato K, Suzuki N (2001) Whole-cell Response Characteristics of Ciliated and Microvillous Olfactory Receptor Neurons to Amino Acids, Pheromone Candidates and Urine in Rainbow Trout. *Chemical Senses* 26:1145–1156.
- Sato Y, Miyasaka N, Yoshihara Y (2005) Mutually Exclusive Glomerular Innervation by Two Distinct Types of Olfactory Sensory Neurons Revealed in Transgenic Zebrafish. *Journal of Neuroscience* 25:4889–4897.
- Schaefer ML, Young DA, Restrepo D (2001) Olfactory Fingerprints for Major Histocompatibility Complex-Determined Body Odors. *The Journal of Neuroscience* 21:2481–2487.
- Schild D, Manzini I (2004) Cascades of response vectors of olfactory receptor neurons in *Xenopus laevis* tadpoles. *European Journal of Neuroscience* 20:2111–2123.
- Schild D, Restrepo D (1998) Transduction Mechanisms in Vertebrate Olfactory Receptor Cells. *Physiological Reviews* 78:429–466.
- Schindelin J, Arganda-Carreras I, Frise E, Kaynig V, Longair M, Pietzsch T, Preibisch S, Rueden C, Saalfeld S, Schmid B, Tinevez J-Y, White DJ, Hartenstein V, Eliceiri K, Tomancak P, Cardona A (2012) Fiji: an open-source platform for biological-image analysis. *Nature Methods* 9:676–682.
- Schnittke N, Herrick DB, Lin B, Peterson J, Coleman JH, Packard AI, Jang W, Schwob JE (2015) Transcription factor p63 controls the reserve status but not the stemness of horizontal basal cells in the olfactory epithelium. *Proceedings of the National Academy of Sciences* 112:E5068–E5077.
- Schultz EW (1941) Regeneration of Olfactory Cells. *Experimental Biology and Medicine* 46:41–43.
- Schultz EW (1960) Repair of the olfactory mucosa with special reference to regeneration of olfactory cells (sensory neurons). *The American Journal of Pathology* 37:1–19.
- Schwartz Levey M, Chikaraishi D, Kauer J (1991) Characterization of potential precursor populations in the mouse olfactory epithelium using immunocytochemistry and autoradiography. *The Journal of Neuroscience* 11:3556–3564.

- Schwob J, Szumowski K, Stasky A (1992) Olfactory sensory neurons are trophically dependent on the olfactory bulb for their prolonged survival. *The Journal of Neuroscience* 12:3896–3919.
- Schwob JE (2002) Neural regeneration and the peripheral olfactory system. *The Anatomical Record* 269:33–49.
- Schwob JE (2005) Restoring Olfaction: A View from the Olfactory Epithelium. *Chemical Senses* 30:i131–i132.
- Schwob JE, Jang W, Holbrook EH, Lin B, Herrick DB, Peterson JN, Hewitt Coleman J (2017) Stem and progenitor cells of the mammalian olfactory epithelium: Taking poietic license: Stem and progenitor cells of the Mammalian OE. *Journal of Comparative Neurology* 525:1034–1054.
- Schwob JE, Youngentob SL, Mezza RC (1995) Reconstitution of the rat olfactory epithelium after methyl bromide-induced lesion. *The Journal of Comparative Neurology* 359:15–37.
- Schwob JE, Youngentob SL, Ring G, Iwema CL, Mezza RC (1999) Reinnervation of the rat olfactory bulb after methyl bromide-induced lesion: Timing and extent of reinnervation. *The Journal of Comparative Neurology* 412:439–457.
- Scott DW (1992) *Multivariate Density Estimation: Theory, Practice, and Visualization*, 1st ed. Wiley.
- Shi L, Javitch JA (2002) The Binding Site of Aminergic G Protein–Coupled Receptors: The Transmembrane Segments and Second Extracellular Loop. *Annual Review of Pharmacology and Toxicology* 42:437–467.
- Shi P, Zhang J (2007) Comparative genomic analysis identifies an evolutionary shift of vomeronasal receptor gene repertoires in the vertebrate transition from water to land. *Genome Research* 17:166–174.
- Shohayeb B, Diab M, Ahmed M, Ng DCH (2018) Factors that influence adult neurogenesis as potential therapy. *Translational Neurodegeneration* 7:4.
- Sholl DA (1953) Dendritic organization in the neurons of the visual and motor cortices of the cat. *Journal of Anatomy* 87:387–406.
- Silva L, Antunes A (2017) Vomeronasal Receptors in Vertebrates and the Evolution of Pheromone Detection. *Annual Review of Animal Biosciences* 5:353–370.
- Singer MS, Oliveira L, Vriend G, Shepherd GM (1995) Potential ligand-binding residues in rat olfactory receptors identified by correlated mutation analysis. *Receptors & Channels* 3:89–95.
- Smith CG (1951) Regeneration of sensory olfactory epithelium and nerves in adult frogs. *The Anatomical Record* 109:661–671.

- Sokpor G, Castro-Hernandez R, Rosenbusch J, Staiger JF, Tuoc T (2018) ATP-Dependent Chromatin Remodeling During Cortical Neurogenesis. *Frontiers in Neuroscience* 12:226.
- Sokpor G, Xie Y, Rosenbusch J, Tuoc T (2017) Chromatin Remodeling BAF (SWI/SNF) Complexes in Neural Development and Disorders. *Frontiers in Molecular Neuroscience* 10:243.
- Spehr M, Munger SD (2009) Olfactory receptors: G protein-coupled receptors and beyond. *Journal of Neurochemistry* 109:1570–1583.
- St John JA, Key B (2003) Axon Mis-targeting in the Olfactory Bulb During Regeneration of Olfactory Neuroepithelium. *Chemical Senses* 28:773–779.
- Steuer E, Schaefer ML, Belluscio L (2014) Using the Olfactory System as an *In Vivo* Model To Study Traumatic Brain Injury and Repair. *Journal of Neurotrauma* 31:1277–1291.
- Strotmann J, Conzelmann S, Beck A, Feinstein P, Breer H, Mombaerts P (2000) Local Permutations in the Glomerular Array of the Mouse Olfactory Bulb. *The Journal of Neuroscience* 20:6927–6938.
- Strotmann J, Wanner I, Helfrich T, Beck A, Meinken C, Kubick S, Breer H (1994) Olfactory neurones expressing distinct odorant receptor subtypes are spatially segregated in the nasal neuroepithelium. *Cell & Tissue Research* 276:429–438.
- Strotmann J, Wanner I, Krieger J, Raming K, Breer H (1992) Expression of odorant receptors in spatially restricted subsets of chemosensory neurones: *NeuroReport* 3:1053–1056.
- Supekar SC, Gramapurohit NP (2018) Larval skipper frogs recognise kairomones of certain predators innately. *Journal of Ethology* 36:143–149.
- Suzuki J, Yoshizaki K, Kobayashi T, Osumi N (2013) Neural crest-derived horizontal basal cells as tissue stem cells in the adult olfactory epithelium. *Neuroscience Research* 75:112–120.
- Suzuki Y, Kiyokage E, Sohn J, Hioki H, Toida K (2015) Structural basis for serotonergic regulation of neural circuits in the mouse olfactory bulb: Serotonergic circuits in the olfactory bulb. *Journal of Comparative Neurology* 523:262–280.
- Suzuki Y, Schafer J, Farbman AI (1995) Phagocytic Cells in the Rat Olfactory Epithelium after Bulbectomy. *Experimental Neurology* 136:225–233.
- Syed AS, Sansone A, Hassenklöver T, Manzini I, Korsching SI (2017) Coordinated shift of olfactory amino acid responses and V2R expression to an amphibian water nose during metamorphosis. *Cellular and Molecular Life Sciences* 74:1711–1719.
- Syed AS, Sansone A, Nadler W, Manzini I, Korsching SI (2013) Ancestral amphibian v2rs are expressed in the main olfactory epithelium. *Proceedings of the National Academy of Sciences* 110:7714–7719.

- Syed AS, Sansone A, Röner S, Bozorg Nia S, Manzini I, Korsching SI (2015) Different expression domains for two closely related amphibian TAARs generate a bimodal distribution similar to neuronal responses to amine odors. *Scientific Reports* 5:13935.
- Takahashi A, Flanigan ME, McEwen BS, Russo SJ (2018) Aggression, Social Stress, and the Immune System in Humans and Animal Models. *Frontiers in Behavioral Neuroscience* 12:56.
- Taniguchi K, Toshima Y, Saito TR, Taniguchi K (1996) Development of the Olfactory Epithelium and Vomeronasal Organ in the Japanese Reddish Frog, *Rana japonica*. *Journal of Veterinary Medical Science* 58:7–15.
- Taskinen HS, Røyttä M (1997) The dynamics of macrophage recruitment after nerve transection. *Acta Neuropathologica* 93:252–259.
- Tavosanis G (2012) Dendritic structural plasticity. *Developmental Neurobiology* 72:73–86.
- Terni B, Pacciolla P, Masanas H, Gorostiza P, Llobet A (2017) Tight temporal coupling between synaptic rewiring of olfactory glomeruli and the emergence of odor-guided behavior in *Xenopus* tadpoles. *Journal of Comparative Neurology* 525:3769–3783.
- Thompson CK, Brenowitz EA (2010) Neuroprotective effects of testosterone in a naturally occurring model of neurodegeneration in the adult avian song control system. *The Journal of Comparative Neurology* 518:4760–4770.
- Tirindelli R (2021) Coding of pheromones by vomeronasal receptors. *Cell and Tissue Research* 383:367–386.
- Valentinčič T, Caprio J (1997) Visual and Chemical Release of Feeding Behavior in Adult Rainbow Trout. *Chemical Senses* 22:375–382.
- Vassar R, Chao SK, Sitcheran R, Nunñez JM, Vosshall LB, Axel R (1994) Topographic organization of sensory projections to the olfactory bulb. *Cell* 79:981–991.
- Vassar R, Ngai J, Axel R (1993) Spatial segregation of odorant receptor expression in the mammalian olfactory epithelium. *Cell* 74:309–318.
- Vedin V, Slotnick B, Berghard A (2004) Zonal ablation of the olfactory sensory neuroepithelium of the mouse: effects on odorant detection. *European Journal of Neuroscience* 20:1858–1864.
- Veeranagoudar DheerajK, Shanbhag BhagyashriA, Saidapur SrinivasK (2004) Mechanism of food detection in the tadpoles of the bronze frog *Rana temporalis*. *acta ethologica* 7.
- Verhaagen J, Oestreicher A, Gispén W, Margolis F (1989) The expression of the growth associated protein B50/GAP43 in the olfactory system of neonatal and adult rats. *The Journal of Neuroscience* 9:683–691.

- Verhaagen J, Oestreicher AB, Grillo M, Khew-Goodall Y-S, Gispén WH, Margolis FL (1990) Neuroplasticity in the olfactory system: Differential effects of central and peripheral lesions of the primary olfactory pathway on the expression of B-50/GAP43 and the olfactory marker protein. *Journal of Neuroscience Research* 26:31–44.
- Virtanen P et al. (2020) SciPy 1.0: fundamental algorithms for scientific computing in Python. *Nature Methods* 17:261–272.
- Von Campenhausen H, Mori K (2000) Convergence of segregated pheromonal pathways from the accessory olfactory bulb to the cortex in the mouse: Accessory olfactory bulb mitral/tufted cell projections. *European Journal of Neuroscience* 12:33–46.
- von rekowski C, Zippel HP (1993) In goldfish the qualitative discriminative ability for odors rapidly returns after bilateral nerve axotomy and lateral olfactory tract transection. *Brain Research* 618:338–340.
- Waldman B (1986) Chemical Ecology of Kin Recognition in Anuran Amphibians. In: *Chemical Signals in Vertebrates 4* (Duvall D, Müller-Schwarze D, Silverstein RM, eds), pp 225–242. Boston, MA: Springer US.
- Wang F, Nemes A, Mendelsohn M, Axel R (1998) Odorant Receptors Govern the Formation of a Precise Topographic Map. *Cell* 93:47–60.
- Wassersug RJ, Hoff K (1979) A comparative study of the buccal pumping mechanism of tadpoles. *Biological Journal of the Linnean Society* 12:225–259.
- Weiss L, Jungblut LD, Pozzi AG, Zielinski BS, O’Connell LA, Hassenklöver T, Manzini I (2020) Multi-glomerular projection of single olfactory receptor neurons is conserved among amphibians. *Journal of Comparative Neurology* 528:2239–2253.
- Weiss L, Offner T, Hassenklöver T, Manzini I (2018) Dye Electroporation and Imaging of Calcium Signaling in *Xenopus* Nervous System. In: *Xenopus* (Vleminckx K, ed), pp 217–231 *Methods in Molecular Biology*. New York, NY: Springer New York.
- Weiss L, Segoviano Arias P, Offner T, Hawkins SJ, Hassenklöver T, Manzini I (2021) Distinct interhemispheric connectivity at the level of the olfactory bulb emerges during *Xenopus laevis* metamorphosis. *Cell and Tissue Research* 386:491–511.
- Weng P-L, Vinjamuri M, Ovitt CE (2016) *Ascl3* transcription factor marks a distinct progenitor lineage for non-neuronal support cells in the olfactory epithelium. *Scientific Reports* 6:38199.
- White EL (1972) Synaptic organization in the olfactory glomerulus of the mouse. *Brain Research* 37:69–80.

- Windus LCE, Chehrehasa F, Lineburg KE, Claxton C, Mackay-Sim A, Key B, St John JA (2011) Stimulation of olfactory ensheathing cell motility enhances olfactory axon growth. *Cellular and Molecular Life Sciences* 68:3233–3247.
- Windus LCE, Claxton C, Allen CL, Key B, St John JA (2007) Motile membrane protrusions regulate cell-cell adhesion and migration of olfactory ensheathing glia. *Glia* 55:1708–1719.
- Yang C, Delay RJ (2010) Calcium-activated chloride current amplifies the response to urine in mouse vomeronasal sensory neurons. *Journal of General Physiology* 135:3–13.
- Yee KK, Costanzo RM (1995) Restoration of olfactory mediated behavior after olfactory bulb deafferentation. *Physiology & Behavior* 58:959–968.
- Yee KK, Costanzo RM (1998) Changes in odor quality discrimination following recovery from olfactory nerve transection. *Chemical Senses* 23:513–519.
- Yoshino J, Tochikai S (2006) Functional regeneration of the olfactory bulb requires reconnection to the olfactory nerve in *Xenopus* larvae: Olfactory bulb regeneration in *Xenopus*. *Development, Growth & Differentiation* 48:15–24.
- Youngentob SL, Margolis FL, Youngentob LM (2001) OMP gene deletion results in an alteration in odorant quality perception. *Behavioral Neuroscience* 115:626–631.
- Youngentob SL, Schwob JE, Sheehe PR, Youngentob LM (1997) Odorant Threshold Following Methyl Bromide-Induced Lesions of the Olfactory Epithelium. *Physiology & Behavior* 62:1241–1252.
- Yu CR, Wu Y (2017) Regeneration and rewiring of rodent olfactory sensory neurons. *Experimental Neurology* 287:395–408.
- Zapiec B, Mombaerts P (2020) The Zonal Organization of Odorant Receptor Gene Choice in the Main Olfactory Epithelium of the Mouse. *Cell Reports* 30:4220-4234.e5.
- Zhang X, Firestein S (2002) The olfactory receptor gene superfamily of the mouse. *Nature Neuroscience* 5:124–133.
- Zhang X, Rogers M, Tian H, Zhang X, Zou D-J, Liu J, Ma M, Shepherd GM, Firestein SJ (2004) High-throughput microarray detection of olfactory receptor gene expression in the mouse. *Proceedings of the National Academy of Sciences* 101:14168–14173.
- Zippel HP (2000) In goldfish the discriminative ability for odours persists after reduction of the olfactory epithelium, and rapidly returns after olfactory nerve axotomy and crossing bulbs Collin SP, Marshall NJ, eds. *Philosophical Transactions of the Royal Society of London Series B: Biological Sciences* 355:1219–1223.